Intramolecular cyclization of β-nitroso-o-quinone methides

Tzeli, Demeter; Tsoungas, Petros G.; Petsalakis, Ioannis D.; Kozielewicz, Pawel; Zloh, Mire

DOI:
10.1016/j.tet.2014.11.020

Document Version
Peer reviewed version

Citation for published version (Harvard):
Tzeli, D, Tsoungas, PG, Petsalakis, ID, Kozielewicz, P & Zloh, M 2015, 'Intramolecular cyclization of β-nitroso-o-quinone methides: a theoretical endoscopy of a potentially useful innate 'reclusive' reaction', *Tetrahedron*, vol. 71, no. 2, pp. 359-369. https://doi.org/10.1016/j.tet.2014.11.020

Accepted Manuscript

Intramolecular Cyclization of β-Nitroso-*o*-Quinone Methides. A Theoretical Endoscopy of a Potentially Useful Innate "Reclusive" Reaction

Demeter Tzeli , Petros G. Tsoungas , Ioannis D. Petsalakis , Paweł Kozielewicz , Mire Zloh

PII: S0040-4020(14)01578-6

DOI: 10.1016/j.tet.2014.11.020

Reference: TET 26169

To appear in: *Tetrahedron*

Received Date: 10 September 2014

Revised Date: 24 October 2014

Accepted Date: 6 November 2014

Please cite this article as: Tzeli D, Tsoungas PG, Petsalakis ID, Kozielewicz P, Zloh M, Intramolecular Cyclization of β-Nitroso-*o*-Quinone Methides. A Theoretical Endoscopy of a Potentially Useful Innate "Reclusive" Reaction, *Tetrahedron* (2014), doi: 10.1016/j.tet.2014.11.020.

Intramolecular Cyclization of β-Nitroso-*o*-Quinone Methides. A Theoretical Endoscopy of a Potentially Useful Innate "Reclusive" Reaction.

Demeter Tzeli,[a] Petros G. Tsoungas,[b,*] Ioannis D. Petsalakis,[a] Paweł Kozielewicz,[c] Mire Zloh[d]

[a] *Theoretical and Physical Chemistry Institute, National Hellenic Research Foundation, 48 Vassileos Constantinou Ave., Athens 116 35, Greece.*

[b] *Department of Biochemistry, Hellenic Pasteur Institute, 127 Vas.Sofias Ave.,Athens, GR-11521, Greece*

[c] *School of Clinical and Experimental Medicine, University of Birmingham, Edgbaston, Birmingham B15 2TT, UK*

[d] *UCL School of Pharmacy, University College London, 29-39 Brunswick Square, London WC1 1AX, UK* and *Department of Pharmacy, University of Hertfordshire, College Lane, Hatfield, AL10 9AB, UK*

* To whom correspondence should be addressed:
P. G. Tsoungas: pgt@pasteur.gr, phone: ++3210-6478839, fax: ++3210-6478842

Abstract

Oxidatively generated *β*-nitroso-*o*-quinone methides undergo an *o*- and/or *peri*-intramolecular cyclization to arene-fused 1,2-oxazoles, 1,2-oxazines or indoles. The reaction, found to be an innate process, has been scrutinized by DFT/B3LYP and MP2 calculations. Due to its rapidity, the process has been termed a "reclusive" one. Competing *o*-(1,5)- and *peri*-(1,6)- or (1,5)-cyclizations advance *via* successive transition states. Activation barriers are drastically lowered in AcOH, probably through H hopping or tunneling whereas they are barely reduced in other solvents. Aromaticity indices, such as HOMA, I_A and ABO, have been used to assess the stability of the end-heterocycles and the preponderance of any one of them. Thus, the preferred cyclization mode, i.e., the prevalence or exclusive formation of one of the heterocycles, appears to be oxidant-directed rather than determined by the quinone methide geometry. The question of the *peri*-cyclization, being a primary or a secondary process, has been tackled.

Key words: β-nitroso-*o*-quinone methides, intramolecular *o*- and *peri*-cyclization, innate reclusive reaction, DFT and MP2 calculations.

1. Introduction

o-Quinone Methides (*o*-QM) **1** (Fig.1) have enjoyed considerable attention in organic and bioorganic synthesis as reactive intermediates. They have been invoked in biological processes, enzyme inhibition, natural product synthesis and polymer synthesis, such as melanin and lignin.[1-3] Lately, there has been a resurgence of interest in their chemistry[2-4] and biology.[5,6] They play a key role in the chemistry of several classes of antibiotics[7,8] and antitumour drugs.[9-11] As highly polarized species, they react with electrophiles[12] and nucleophiles.[13,14] The latter is the most commonly used and it is usually driven by the rearomatization of the structure. They are also known to act as DNA alkylating or cross-linking agents.[15] DFT calculations have been reported with sulfur, nitrogen and oxygen nucleophiles.[16] Consequently, many efforts have been directed towards understanding their properties and reaction mechanisms[17] while many approaches have been devised to generate their structure.[2-4, 18,19] **1** cannot be easily isolated, therefore, it is commonly trapped *in situ* by (Hetero) Diels-Alder reactions, where **1** acts as the (hetero) diene.[20,21] The reactions are exceptionally facile, compared with their traditional variants, owing to the transition state and product stabilization provided by the extended π-system.[22] Early computational studies on the parent structure **1**[2,3] as well as some recent DFT-based ones,[23,24] have focused on deciphering its reactivity as a Diels-Alder component or its biological activity as a Michael acceptor, in aqueous media.[13, 25-27]

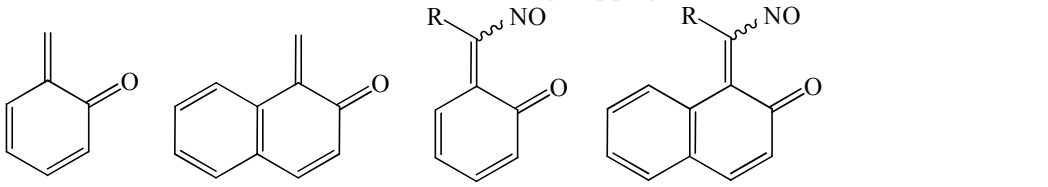

1 **2** **3** **4** R = H, Me, Et, Ph

Figure 1. Structures of *o*-quinone methides **1**, **2** and *β*-nitroso-*o*-quinone methides **3** and **4** (in the Z and E conformers, the NO group is towards and away from the carbonyl O atom, respectively. E is distinguished as E_1 or E_2 if the nitroso O atom is towards or away from the ring).

Conjugated β-nitrosoalkenes,[28-32] a class of reactive molecules, are of significant synthetic potential and are mainly known as 2π or 4π components in cycloaddition reactions. They have been identified by isolation (in some cases, at least),[33] spectroscopic characterization[34] or studies of their kinetics and stereo-chemistry.[35] In general, they are unstable but their stability increases markedly by halogen, aryl or t-alkyl substituents, strong intramolecular H-bonding[36] or formation of transition metal complexes.[37] These molecules are trapped by reactions similar to those of **1**.[28-32] A substantial part of their chemistry has been unveiled by Gilchrist[38,39] and Reissig.[40,41] The nitrosoalkene motif has been extensively studied in the N-oxide chemistry of furazans[42] and has also been invoked in the formation of N-oxides of 1,2-benzisoxazoles.[42,43]

β-Nitroso-*o*-quinone methides **3** or **4** (Fig. 1) encompass both **1** and **2** entities. In our earlier reports, they have been proposed as transiently generated during the oxidation of o-hydroxyaryl acyloximes.[42-45] A theoretical insight into the salient features of the structure of **3** and **4** (all its isomers) and the reflection upon

their reactivity profile has been recently reported.[46] Many useful heterocylic structures have been and can be prepared from these intermediates, fused 1,2-oxazoles **9** or **10** and 1,2-oxazines **12** among them (Scheme 1). 1,2-oxazoles, C-3 substituted with pharmacophores, is an area of intense research driven by diverse

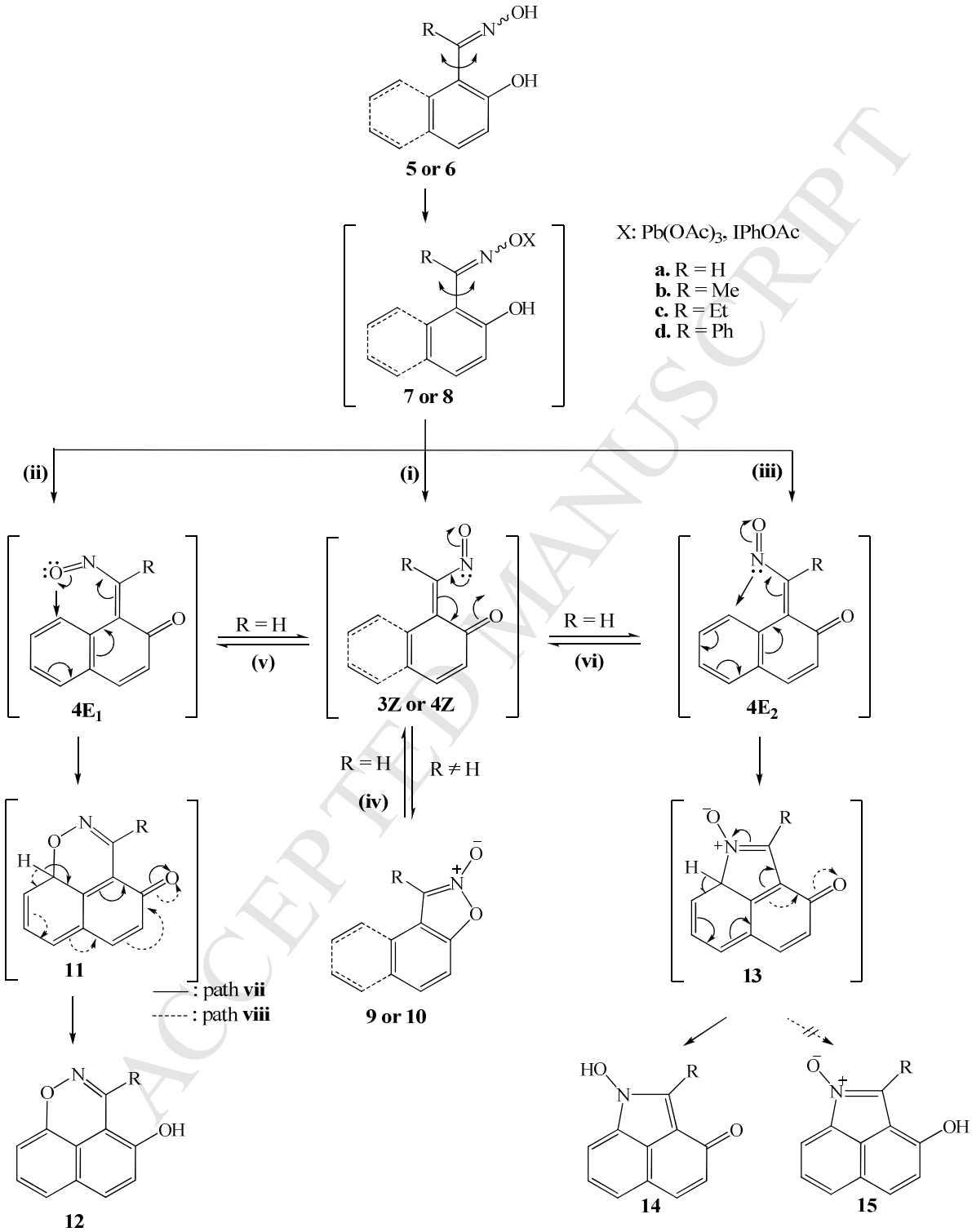

Scheme 1. *o*- and *peri*-Cyclization of oxime **5** or **6** Z/E isomers, through **7** or **8** and *β*-nitroso-*o*-quinone methides **3** or **4**.

pharmaceutical applications.[47] The 1,2-oxazole ring, for instance, occupies a prominent position in isoxazole-based marketed drugs, such as, penicillin antibiotics (cloxacillin, dicloxacillin, flucloxacillin), antipsychotics (risperidone, paliperidone), COX 2 inhibitors (parecoxib) to name a few.

It is known that heterocycles with a ring N-O bond are important core structures in many pharmaceuticals. Furthermore, ring opening of these heterocycles, asymmetric reduction in particular, provides access to optically active structures, core components in a variety of medicines.[48] Indeed, facile ring cleavage of 1,2-oxazine **12**[43,44] or 1,2-oxazole **9**[49] lead to chemically and biologically useful outcomes, for instance ring hydroxylation[43,44] or diaryl amines as perspective metal ion chelating ligands. It is, thus, the documented significance of **1 (**or **2)** and the potential of their nitroso analogues **3** (or **4)** as key intermediates or that of **9** and **12** in (bio)organic synthesis and biology, outlined above, along with some intriguing experimental data,[44,45] that sparked the present theoretical insight into the pathways of their innate intramolecular reactivity profile.

2. Methodology

The cyclization modes of **3** and **4** were studied in the gas phase and in solution (THF, CH_2Cl_2). AcOH is liberated from the oxidants during the reaction, thus, the latter was studied in the presence of AcOH; AcOH was included in the calculations of stable structures of all minima, intermediates and transition states (see Fig. 2). Minima of intermediates and transition states for tentative pathways were fully optimized using the hybrid B3LYP functional[50,51] coupled with the 6-311G+(d,p).[52] However, while the suitability of the B3LYP functional has been questioned, it has, in many cases, been found reliable for theoretical calculations[53-56] and prediction of organic reaction mechanisms.[57] Thus, for comparison, additional calculations were carried out for some minima and their intermediate transition states using the aug-cc-pVTZ[58] basis sets. The credibility of the B3LYP functional was tested using the M06-2X[59] functional (recommended for the study of non-covalent interactions) (Table 1). The second order Møller-Plesset perturbation theory (MP2) was also used. Relative energies, geometries and harmonic frequencies were also determined for C-3 substituted derivatives (R=H, Me, Et, Ph).

Our calculations show that all three B3LYP, M06-2X and MP2 methodologies give similar geometries. Moreover, they predict similar transition energies and comparable relative energy levels irrespective of the basis set used (Table 1). A larger energy barrier and a more stabilized product was calculated for **4E$_1$** $\rightarrow$ **11** reaction (Fig. 4) by the M06-2X functional compared to B3LYP and MP2 techniques; whereas all three techniques gave similar energy barriers and reaction energies for the **17**$\rightarrow$ **12** reaction (Fig. 4). Clearly, within the same method, both basis sets, 6-311G+(d,p) and aug-cc-pVTZ, give comparable results as do the B3LYP functional with the ab initio MP2 method. It is, thus, safe to consider B3LYP/6-311G+(d,p), as a good choice for our purpose.

For the calculations in THF and CH_2Cl_2 solvents, the polarizable continuum model was employed.[60] This model is divided into a solute part, lying inside a cavity, surrounded by the solvent part represented as a structureless material characterized by its macroscopic properties, i.e. dielectric constants and solvent radius.

This method reproduces solvent effects quite well.[60] For some minima and transition states, their fully optimized geometries in these solvents were found practically identical to those in the gas phase. Hence, single point calculations were carried out at the gas phase geometry for all minima and transition states.

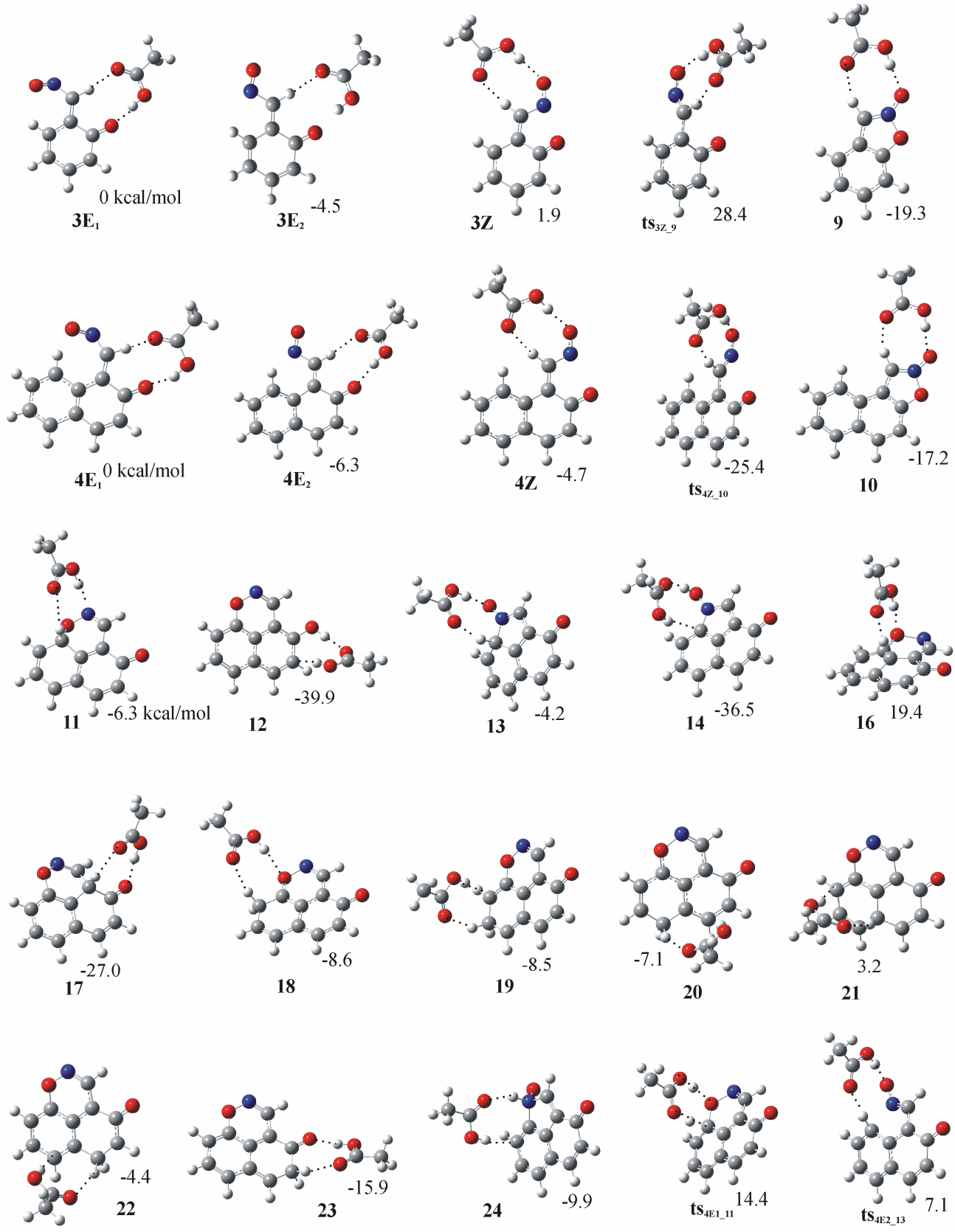

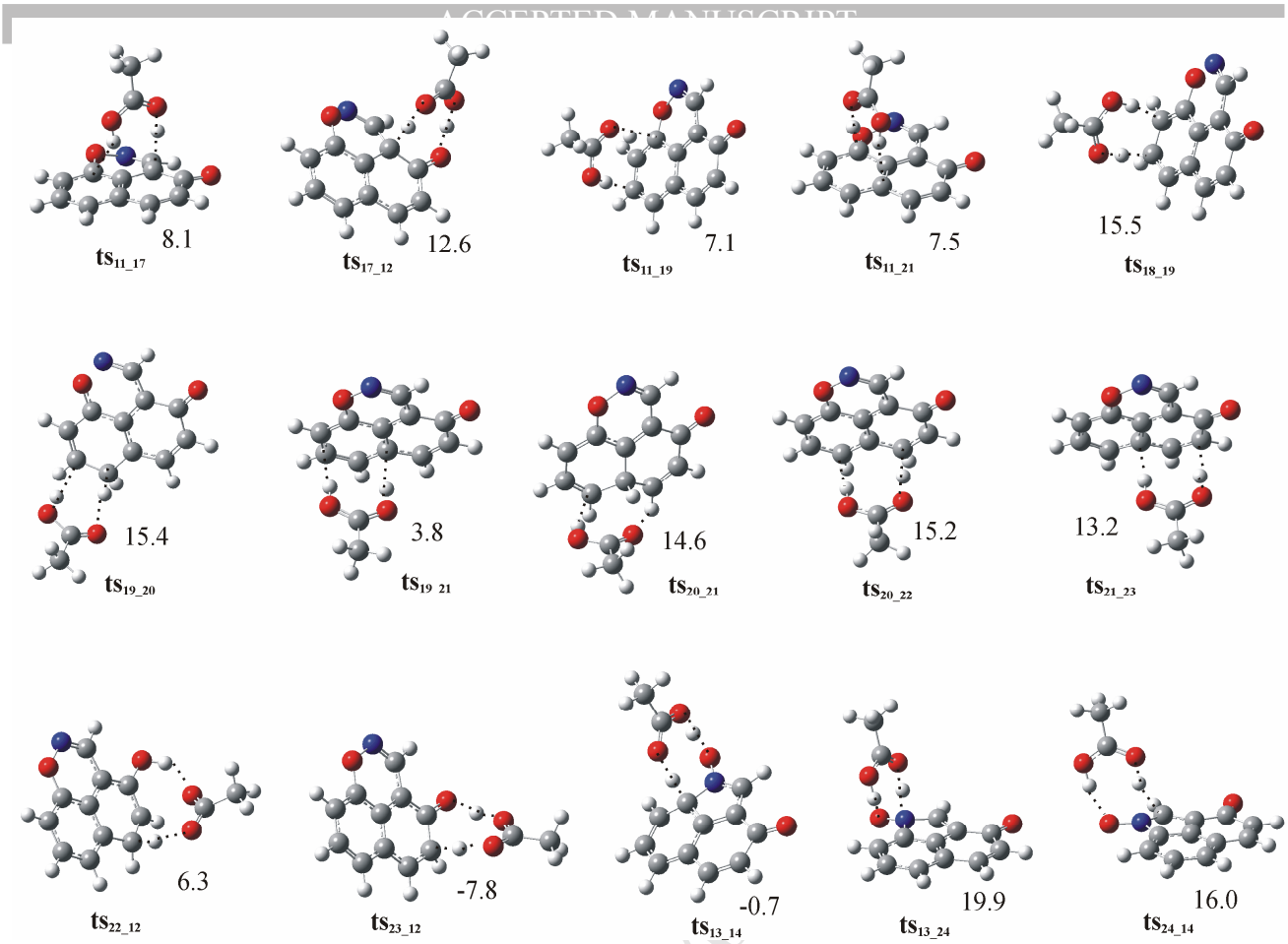

Fig. 2 Minima and transition structures in the *o*- and *peri*-cyclization modes of the *β*-nitroso-*o*-quinone methides **3** and **4** with AcOH; relative energies in kcal/mol with respect to the $\mathbf{3E_1}$ and $\mathbf{4E_2}$ minima structures, respectively.

Table 1. Relative energies (kcal/mol) of the calculated minima and transition states included in the $\mathbf{4E_1} \rightarrow \mathbf{11}$ and $\mathbf{17} \rightarrow \mathbf{12}$ reactions calculated at different levels of theory, for R = H.[a]

	$\mathbf{4E_1} \rightarrow \mathbf{11}$			$\mathbf{17} \rightarrow \mathbf{12}$		
	$\mathbf{4E_1}$	$\mathbf{ts_{4E1-11}}$	**11**	**17**	$\mathbf{ts_{17-12}}$	**12**
B3LYP/6-311+G(d,p)	0	8.3	-4.5	0	56.6	-14.4
B3LYP/aug-cc-pVTZ	0	8.1	-5.2	0	58.1	-16.0
M062X/6-311+G(d,p)	0	13.5	-8.2	0	58.9	-13.9
M062X/aug-cc-pVTZ	0	13.1	-9.0	0	57.2	-15.9
MP2/6-311+G(d,p)	0	7.3	-3.6	0	56.7	-12.9

[a] Minima **4**, **11**, **12**, and **17** are depicted in Fig.3 and Fig. 4.

For the calculations with AcOH, the basis set superposition error (BSSE) has been taken into account[61] assuming weak hydrogen bonds among the species formed during the various stages of the reaction.

Harmonic frequencies, performed using the Gaussian 09 program package,[62] confirmed that the structures are minima or transition states. All calculated minima and transition structures, for R = H, Me, Et,

and Ph, their absolute energies, relative energies and geometries in the gas phase, in THF and CH_2Cl_2 are given in the Supplementary material section, Fig. 1S. For R = H in the presence of AcOH, the calculated minima and transition structures are given in Fig. 2 and Fig. 2S, where some additional local minima are presented for some structures.

Reformulated HOMA (rHOMA), bond uniformity (I_A) and average bond order/bond order deviation (ABO/BOD) have been calculated as aromaticity indices, to assess relative stabilities of the heterocycles. Reformulated HOMA (rHOMA) index[63-65] has been calculated by the delineated equation.

$$\mathrm{rHOMA} = 1 - \frac{\alpha}{n}\sum_{i=1}^{n}\left(R_{opt} - R_i\right)^2$$

where *n* is the number of bonds in the aromatic system. R_{opt} is the optimum bond length, and R_i is the real bond length of the *i* bond taken into consideration. This equation necessitates the use of the normalization constant α for each type of bond. The used values are α_{CC} = 257.7 and R_{opt}=1.388 for CC, α_{CN} = 93.52 and R_{opt}= 1.334 for CN, α_{CO} = 157.38 and R_{opt}= 1.265 for CO, α_{NO} = 57.21 and R_{opt}= 1.248 for NO.[65]

Bond order Uniformity index I_A[66,67] and average bond order (ABO) and its deviation (BOD) from ABO index[68,69] are statistical estimates of bond order variations. I_A index is based upon a statistical evaluation of the extent of variation of ring bond order provided by the expression:

$I_A = 100F(1\text{-}V/V_K)$, where $V = \frac{100}{\overline{N}}\sqrt{\frac{\sum (N-\overline{N})^2}{n}}$

$\overline{N}$ is the arithmetic mean of the n various ring bond orders, N, is the bond order. V_K is the value of V for the corresponding non-delocalised form of the ring and F is a scaling factor.[66,67]

3. Results and Discussion

Features that dominate a structure invariably accompany or match those that dictate its reactivity. Pertinent to the reactivity of **3** or **4** are the exocyclic β-nitrosoalkene and o-quinone methide entities sharing the alkene moiety.

The NO group is a known participant in electrocyclizations[28-30,70] and hetero Diels-Alder cycloadditions.[28-30,71] In the case at hand it has a multiple engagement. As a substituent it gives rise to E- and Z-conformers of **3** and **4**. For the Z conformer only one minimum is stable. As an ambident nucleophile or electrophile[72,73] it may trigger intramolecular cyclization to **12** and **14** or **9** and **10** (Scheme 1). Its HOMO is a high energy antibonding combination of N and O lone pairs responsible for its nucleophilicity while orthogonal to those orbitals is a low-lying π* LUMO responsible for its electrophilicity.[72,73] This feature, as well as its powerful withdrawing ability, accounts for some polarization of the alkene in **3** and **4**. On the other hand, their propensity to aromatize, an inherent substantial driving force, in cooperation with the NO electronic effects, leads to the innate intramolecular cyclization.

Relative energies of Z- and E-conformers of **3** and **4** have been calculated (Fig. 3 and Table 3S). **3** or **4** for the **a**-**c** derivatives (Scheme 1) appear to have their lowest energy in the E_2 conformation. On the other

hand, it is **3d**, in its Z conformation, which is of lowest energy. The **3**$E_1 \rightarrow$**3**E_2 and **4**$E_1 \rightarrow$**4**E_2 interconversions have very low energy demands of *ca.* 1.4 – 4.2 and 0.8 – 3.1 kcal/mol, respectively (Fig. 3). On the contrary, the **3**$E_2 \rightarrow$Z and **4**$E_2 \rightarrow$Z interconversions have substantial energy barriers of ca. 28.1 – 34.8 and 18.1 – 35.2 kcal/mol, respectively.

The energy landscape for the intramolecular *o*- and *peri*- cyclizations of the **3** and **4** minima for R=H is depicted in Figs 3-6, with or without the AcOH-triggered interactions. That, on the other hand, for the other derivatives is depicted in Figs 3S-6S. The barriers of all transition states and intermediates are given with respect to **3**E_1 or **4**E_1 conformers, to allow for comparisons between competitive mechanisms.

3.1 o-(1,5)-Cyclization

o-(1,5)-Cyclization, with the NO group acting as an electrophile, takes place through the Z conformer (Scheme 1, path (iv), Fig. 3 and Fig. 3S).

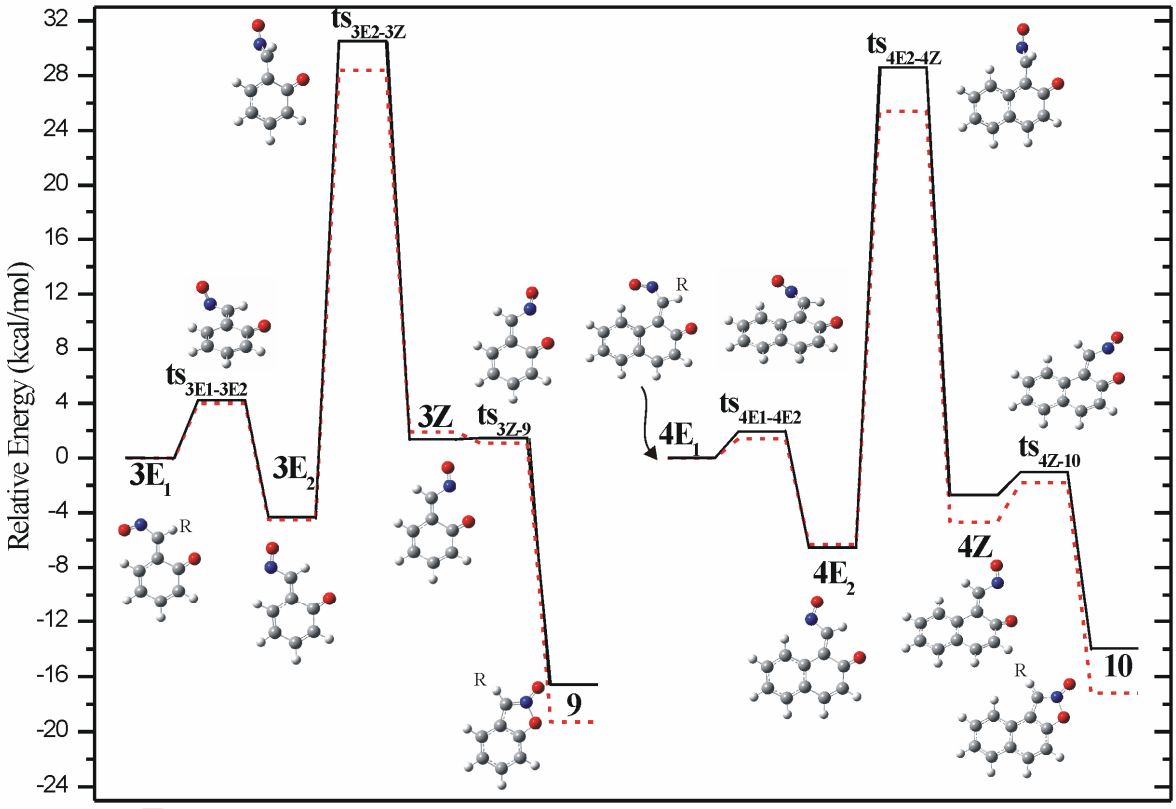

Fig 3 Relative energies corrected for ZPE of the *o*-(1,5)-cyclization of **3** and **4** minima to **9** and **10** (solid black line) in the presence of AcOH (dashed line) for R = H (C atoms = gray spheres, H = white, O = red, and N = blue). Note: C, H, and O atoms participating in the cyclizations in this and subsequent figures, are numbered only in a way to facilitate the presentation of results and relevant discussion.

Non zero but very low energy barriers were calculated for **3a** and **4a,b** of 0.1, 1.7 and 0.3 kcal/mol,

respectively. An insignificant elevation is observed in solution with the corresponding barriers being 0.5, 3.1 and 0.7 kcal/mol (Fig. 3S). *o*-cyclization of the other derivatives of **3** and **4** occurs instantaneously as the near zero energy barrier indicates (Scheme 1, path (iv), Fig. 3S). These observations reflect the stabilizing effect of (i) benzo-fusion, (ii) solvent and (iii) substitution on **3** or **4**. *o*-Cyclization of **3**→**9** has a higher energy demand of *ca.* 1.5-2.5 kcal/mol than its **4**→**10** counterpart. On the other hand, **9a-c** appears to be more stable than **10a-c** by *ca.* 1.5–3.0 kcal/mol and *ca.* 6.0 kcal/mol than the **10**d derivative. These variations may be attributed to a larger perturbation of the π density in **10**, induced by the 1,2-fusion of the isoxazole ring and its N-O dipole, onto the naphthalene core. The *o*-(1,5)-cyclization of **3** and **4** minima towards **9** and **10** in the presence of AcOH further stabilizes the transition states up to 3.5 kcal/mol while that for the overall reaction to **9** and **10** up to 3 kcal/mol (Fig. 3).

The N-O_2 bond in **10** or **9** falls within the range 1.202-1.242Å found in furoxans[74] and it remains as short as in the NO_2 group (Table 2), a feature common to heteroaromatic N-oxides.[75] The ring N-O_1 bond in **9** is quite stretched (*ca*. 1.492Å) and compares with the most strained bonds in fused furoxans. This bond is slightly shorter in **10**. The corresponding N-O_1 bond length of their deoxygenated congeners is shorter by 0.07 Å (Table 2). Interestingly, the C_1-O_1 bond appears within a range of 1.348-1.368Å, thus, implying some double bond character of this bond.

Table 2. Bond lengths (Å)[a] and angles (degrees)[a] of the N-oxides **9** and **10** compared to their deoxygenated analogues.

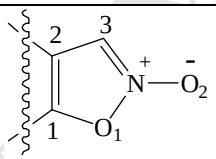

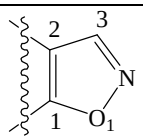

	Expt[b]	9	10	
N-O_2	1.247	1.215	1.217	
N-O_1	1.468	1.492	1.485	1.416(1.412)[c]
C_3-N	1.319	1.323	1.325	1.302(1.306)
C_1-O_1	1.368	1.356	1.354	1.356(1.351)
C_1-O_1-N	103.9	105.1	105.1	108.1(108.2)

[a] B3LYP/6-311G+(d,p) level of theory. [b] Experimental values from X-ray analysis, ref. 76.[c] Values refer to the deoxygenated derivatives of **9** and in parenthesis of **10**.

3.2 Peri-cyclization

Peri-cyclization (Scheme 1) to either **12** or **14** may take place through the O- (Scheme 1, path (v)) or N-site (Scheme 1, path (vi)) of the NO group, respectively. The latter may act as either an electrophile or a nucleophile. The first and key step in either path is the formation of the ring (**11** or **13** in Scheme 1).

1,6-Cyclization to **12** occurs through the E_1 conformer and may be envisaged to proceed by way of two alternative reaction paths (Scheme 1, **11**). Energy requirements for their minima and transition states are depicted in Figs. 4 (via path vii) and 5 (via path viii) and in Figs. 4S (via path vii) and 5S (via path viii).

Energy barriers (reflecting the distortion of the transition state geometry) for some intermediates are quite high, e.g **17**→**12**, having an energy barrier in the range of 56.6-58.9 kcal/mol (Fig. 4S). Slightly lower energy demands, in the range of 1-2 kcal/mol, are observed in CH_2Cl_2 and THF compared with those in the gas phase. A marked drop for the energy barriers in the presence of AcOH is generally observed. For example for the **17**→**12** conversion, the energy barrier is reduced by about 20 kcal/mol. The largest one, however, of ca.39 kcal/mol is observed for the **23**→**12** conversion (Fig. 5). Apparently, AcOH facilitates a H transfer, taking place not only contiguously but more interestingly through hopping[77] or tunnelling,[78] perhaps, as shown by the additional transition states corresponding to H transfer between non adjacent C positions (see Figs. 2, 4 and 5). This may well account for the 20 kcal/mol drop (Fig. 4) while the lower still energy demand of 39 kcal/mol transition (Fig.5) may be regarded as the preferred one. It is to be noted that AcOH facilitates H transfers between C atoms, which are not adjacent. As a result, AcOH intervenes in the process (Fig. 4, path vii and Fig. 5, path viii). For instance, **11** is converted to **17** in two steps, via **16** (path vii), without AcOH while in the presence of AcOH, the same conversion can occur as a one-step process, via the $\mathbf{ts_{11\text{-}17}}$ transition state with an overall activation energy drop of 23 kcal./mol.

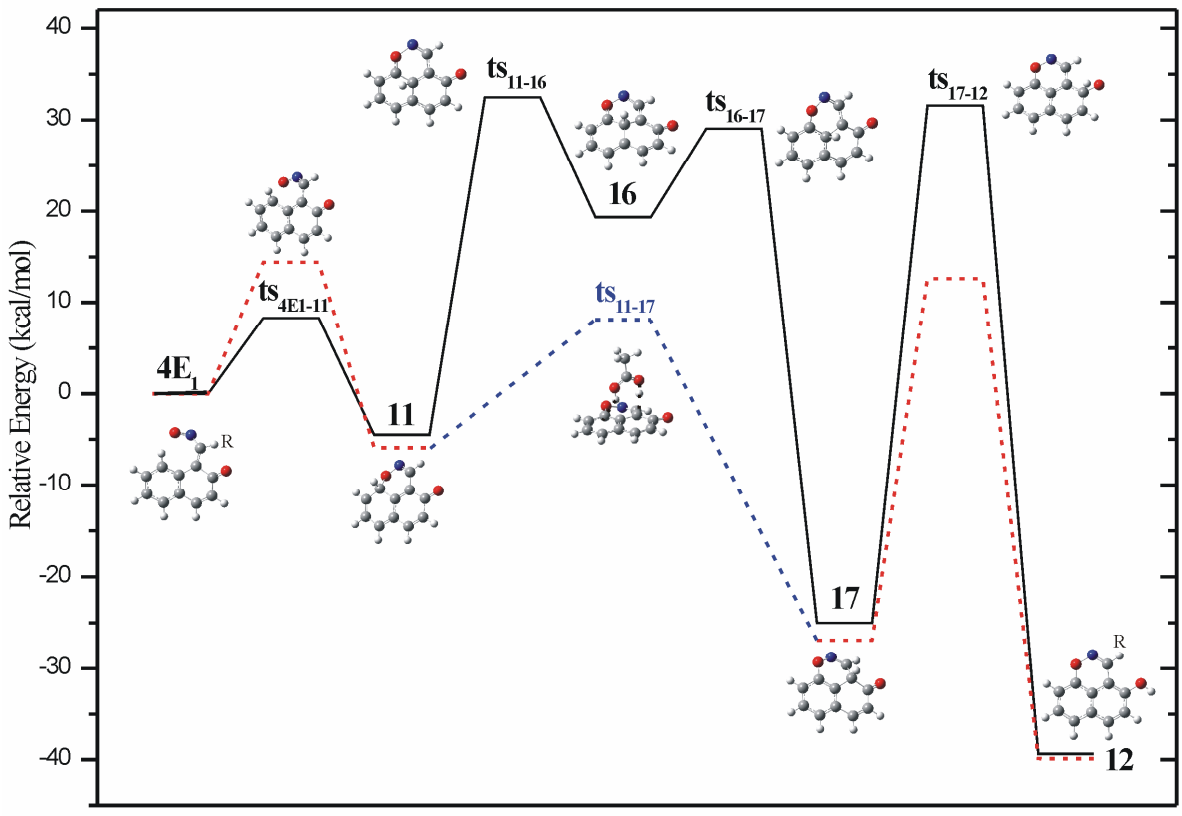

Fig 4 Relative energies corrected for ZPE of the *peri*-(1,6)-cyclization (via path vii, Scheme 1) of **4** minimum to **12** (solid black line) and in the presence of AcOH (dashed lines) for R = H (C atoms = gray spheres, H = white, O = red, and N = blue). ($\mathbf{ts_{11\text{-}17}}$ only in AcOH)

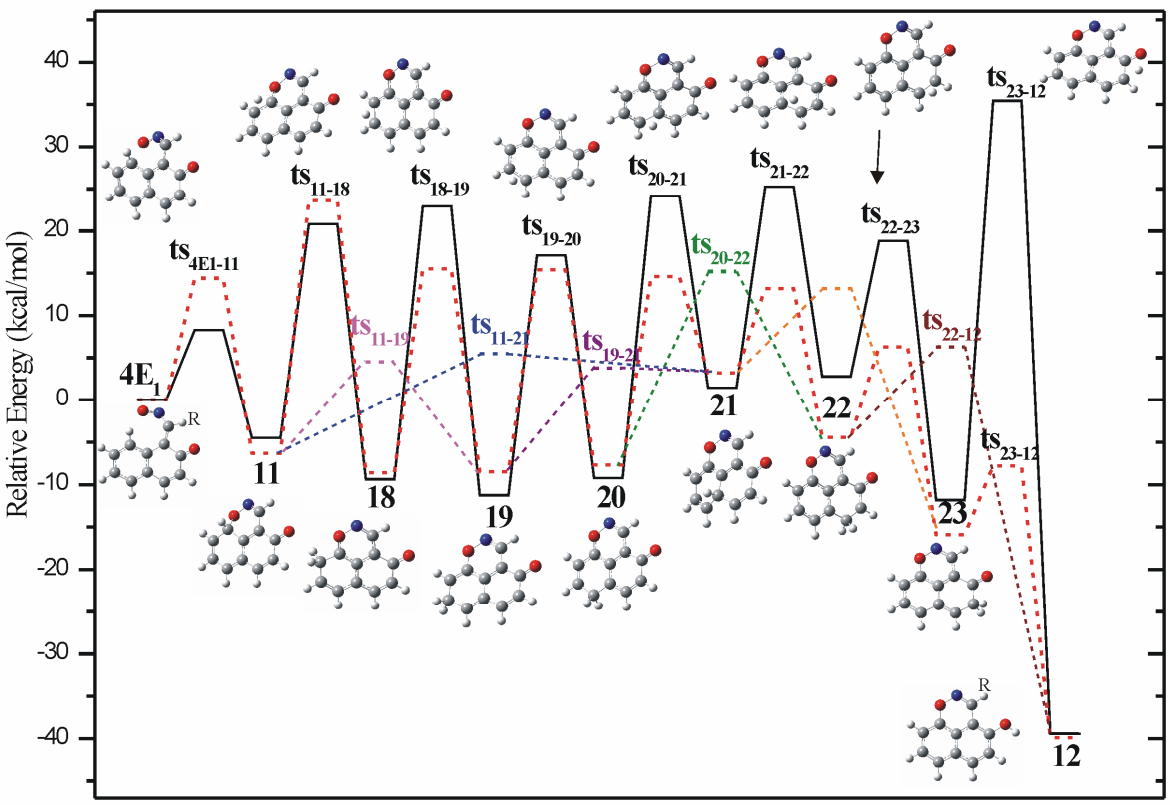

Fig 5 Relative energies corrected for ZPE of the *peri*-(1,6)-cyclization (via path viii, Scheme 1) of **4** minimum to **12** (solid black line), in the presence of AcOH (dashed lines) for R = H (C atoms = gray spheres, H = white, O = red, and N = blue).

3.2.2. 1,5-Cyclization

1,5-Cyclization occurs through the E_2 conformer (Scheme 1, path (vi)). Energy demands for minima and transition state structures are given in Fig. 6 and Fig. 6S. The formation of the final quinonoid structure **14** may be explained on the same grounds as in **12.** This is in evidence by the notably lower energy barrier to cyclization of **4b-d,** in the range of *ca.* 5.1–6.3 kcal/mol compared with that of its parent structure **4a** of *ca.* 15 kcal/mol, in the gas phase. The inherent ring strain in **15**, a result of accumulated π-density (see earlier arguments on **9** and **10**), discourages its formation, in favour of **14**. It is of interest to note that substitution, once again, confers stability on **14**. The reaction (total) energy for the conversion **4E$_2$→14** is 26.8, 32.7, 33.4 and 35.6 kcal/mol for the **a-c** derivatives in the gas phase. A lower energy demand of 1-3 kcal/mol is observed in CH_2Cl_2 and THF. Again, the presence of AcOH results in a significant decrease of the energy demand by about 30 kcal/mol (see Fig. 6). As shown in Fig. 6, in the absence of AcOH, **13** is converted to **14** via **24,** in a two-step process while the presence of AcOH, effects the same conversion in one-step, via the **ts$_{13\text{-}14}$** transition state, with an overall activation energy drop from 35 to 5 kcal/mol.

It should be noted that the diagrams for the relative energies, relative enthalpies and free Gibbs energies for the *o*-(1,5)-, *peri*- (1,6)- and (1,5)-cyclizations of **3** or **4** minima to **9**, **10**, **12** or **14** are similar to the relative energies corrected for ZPE depicted in Figs. 3-6.

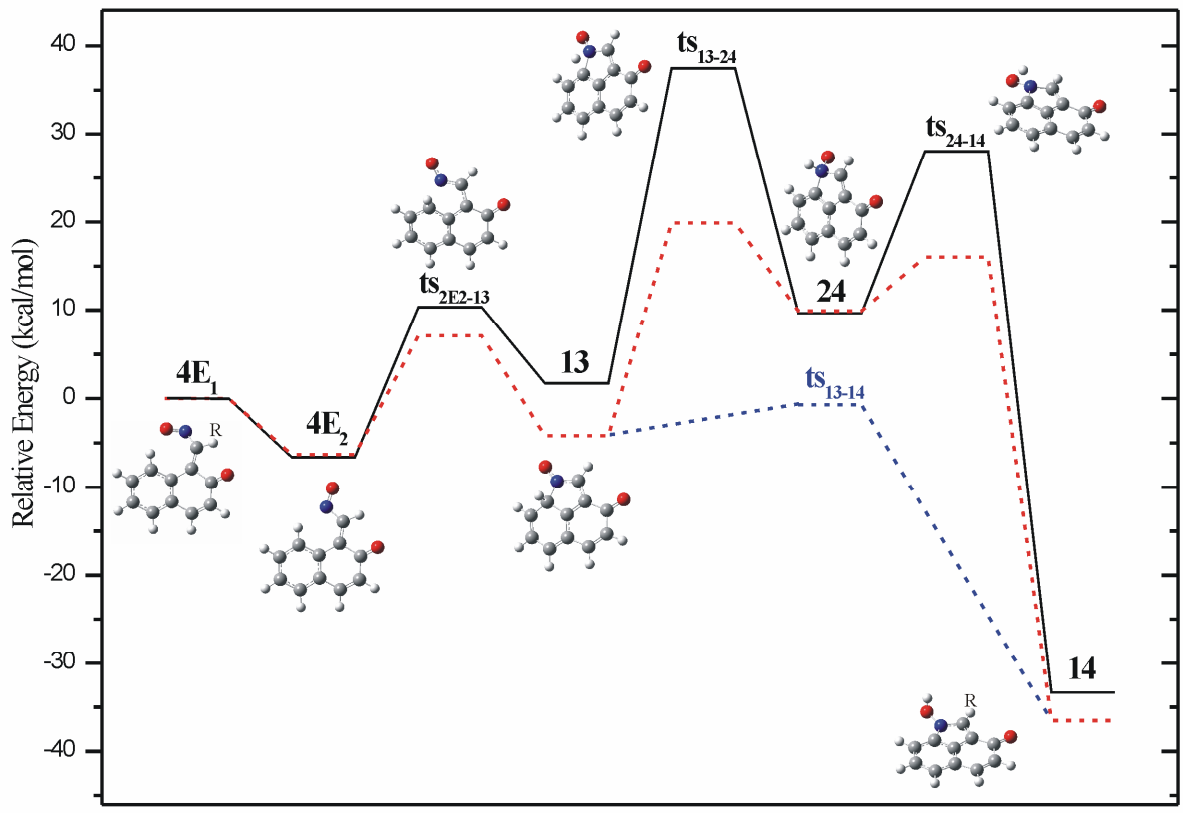

Fig 6 Relative energies corrected for ZPE of the *peri*-(1,5)-cyclization of **4** minimum to **14** (solid black line) and in the presence of AcOH (dashed lines) for R = H (C atoms = gray spheres, H = white, O = red, and N = blue).

3.3. Reflections on the Cyclization Profile of 3 and 4

Experimental findings on the cyclization of **3** or **4,** oxidatively generated from the oximes **5** or **6,** have been quite intriguing, with regard to the varying reaction outcomes.[43-45] Accordingly, **3b**,**c** and **4a-d** give the corresponding **9** and **10,** respectively (Scheme 1, path (iv)) while **3a** is quite tempermental, furnishing mainly hydrolysis and polymerization products.[42,43] The latter is a hardly surprising result, taking note of (a) the propensity of **3a** to rapid re-aromatization and (b) the C-3 unsubstituted reactive position of **9**, as soon as it is formed, giving rise to other, alternative to cyclization, competing reactions. An analogous primary *o*-cyclization is shown by **4a.** In that case, however, benzo-fusion (a) confers stabilization and (b) offers alternative *peri*-cyclization routes (Scheme 1, paths (v) and (vi)).[43,44,46]

Lead (IV) acetate (LTA) oxidation of oximes **5** or **6** produces both **12** and **14**[78] while the use of phenyliododiacetate (PIDA) as oxidant, under similar conditions, directs the reaction selectively to **12**.[43-45,79] Worth noting is that the reaction proceeds equally well in solvents of varying polarity, e.g. THF, CH_2Cl_2 mainly but also in MeCN.

This oxidant-selective outcome may be correlated to the O-X bond dissociation enthalpy in the transient complexes **7** or **8** (Scheme 1).[80] The easier the O-X rupture, the faster will be the cyclization of the resulting intermediates **3** or **4** to the corresponding N-oxides **9**, **10** or 1,2-oxazine **12**. Indeed, bond

dissociation enthalpies of *ca*. 91.17 and *ca*. 55.60 kcal/mol have been reported for Pb-O and I-O in various compounds.[80] The notably stronger former bond, of an estimated length of ca. 2.25-2.30Å, probably attributed to a multiple back-bonding from Pb lone pairs[81] is apparently the toughest to cleave. Accordingly, of the corresponding complexes **7** or **8,** the Pb-based ones have the highest energy demands for cyclization. An energy demanding 6-membered pseudo chelate ring structure for these complexes may also be regarded as a viable possibility. The experimental outcomes are, indeed, consistent with these arguments.

Both oxidants release acetic acid during the reaction, regardless of the solvent used, unless it is trapped. Thus, the overall process is, in effect, dominantly acid-catalyzed by way of a 1,5-electrocyclization of **3** or **4** to **9** or **10** [43,44] or a 1,6 (5)-electrocyclization and sequential H shifts to **14** and/or **12**[82] (Scheme 1). The latter may be effected by hydrogen scrambling (a) *intra*molecularly, via a trajectory of successive shifts or (b) *inter*molecularly, via either acid-or solvent-assisted proton shuttling.[83-84] It is the trajectory mode of the successive H shifts that differentiates between the two paths.

H transfer (polar or radical in nature), an arguably important process in chemistry and biology, is usually fast but it can become rate determining if catalyzed. This is especially true when the transfer is to and from C atoms or concerted bond cleavage and formation among heavy atoms (i.e non H atoms).

H transfer, in our case, does not necessarily impart a kinetic advantage towards stabilizing the transition states, it rather complements the thermodynamic driving force, through re-aromatization, to the end-products. The latter, perhaps, may sidestep the formation of charged intermediates.

Given that the activation energy is inversely related to the solvent dielectric constant,[85] the insignificant drop of the activation barriers, in the range of 1-3 kcal/mol, in other solvents, may be indicative of a rather negligible sensitivity of the reaction path to solvent polarity. Yet, this observation cannot still firmly point to the identity of the engaged species (be that dipolar, diradical or neutral).

HOMA, I_A and ABO/BOD indices have been chosen as the most responsive to the observed outcomes. Calculated HOMA values (Table 3) are consistent with a massive revert-to-type process to the extent of 81-95%. Comparing, however, the overall aromaticity change in the reaction sequences (Scheme 1), a substantial decrease is evident in the fused heterocycles **9**, **10, 12** and **14.** A drop in the range of 23-51% is estimated in going from the oximes **5** and **6** to **9, 10, 12** or **14**. Certain features are of particular interest (a) the generation of *o*-quinone methide intermediates **3** and **4** is accompanied by a rise of 23% and 7%, respectively, followed by a *ca*. 28% drop towards the products, (b) the reaction coordinate encompasses successive transition states,[86] activation barriers being due to their geometry distortion, (c) the aromatic character of **9** and **10** compares well with that of **12**, (d) **10** shows a markedly lower aromatic character against **15**. (e) *peri* (1,8)- fusion appears to increase the diene geometry of the tricycles **12** and **14**, (f) a naphthalene–based *peri*-fused tricycle **12** appears to have an aromatic character of comparable magnitude to a quinonoid tricycle, like **14**, of distinct diene geometry, (g) **15**, with a higher aromatic "arrangement" than the rest, cannot survive due to the severe strain inherent in the 5-membered *peri* (1,8)-fused ring exacerbated by the N-O dipole-induced accumulated ring π-density.

Table 3. Calculated rHOMA, I_A and ABO/BOD values for heterocycles **9**, **10**, **12**, **14**, **15** and their precursors *o*-quinone methides **3**, **4** and oximes **5**,**6** (a:R=H).[a]

	rHOMA			I_A	ABO/BOD
	Z	**E_1**	**E_2**		
3	0.971[b]	[c]			
4	0.818[b]	0.026	0.101		
5	0.787[b]	0.923	0.951		
6	0.764[b]		0.778		
9		0.476[d]		90.20[d]	1.607/0.229[d]
10		0.550[d]			1.638/0.163[d]
12		0.585		109.10	1.296/0.077
14		0.528		112.43	1.281/0.078
15		0.740		164.25	1.306/0.042

[a] B3LYP/6-311G+(d,p). [b] Ref. 46. [c] insignificantly low value. [d] Ref 82.

Compounds **3** and **4**, in their Z conformation, show higher HOMA values than their precursor oximes **5** and **6**, respectively (Table 3). Geometry optimization has demonstrated the development of an extended π delocalization into a 5-membered N-oxide ring, through *o*-(1,5)-cyclization.[46] The end-products N-oxides **9** and **10**, on the other hand, indicate markedly lower HOMA values. The extent of delocalization, gradually building up along the reaction path, reaching the successive transition states, subsequently descends towards the end product. It is the N-O dipole, in the latter, that has been incriminated for this change.[87] The issues of stabilization through resonance or extended conjugation are in effect, herein. Indeed, **12** and **14** have HOMA values of comparable magnitude (Table 3). Apparently both have an inherent extended diene character, as their common stabilizing factor, of different origin, nonetheless, i.e. localized π frames due to *peri*-fusion in **12**, and benzo-fused quinone type in **14**.

Bond uniformity I_A and bond order ABO/BOD variations (Table 3) follow, in general, the HOMA portrait. Accordingly, the aromatic character increases in going from the N-oxides **9** and **10** to the *peri*-fused **12, 14** and the fictitious **15,** in concert with a corresponding increase of their diene character. The only discordance is the reverse order of magnitude among the HOMA and I_A of **12** and **14.**

In as much as aromaticity reflects stability one expects that the former lags behind bonding changes at the transition states (in other words, its loss or drop should be ahead of these changes) leading to an increase of $\Delta G°$ along the reaction path. Interestingly, a benzo-fused quinone stabilization in **14** (an optimal orbital alignment, perhaps?) could be similarly accounted for a comparable $\Delta G°$ increase in the corresponding reaction path. In both cases, aromaticity changes of transition structures, as the reaction progresses, are confirmed from the bond length changes of the quinone and the nitrosoalkene entities (Tables 4S-7S).

Substitution also introduces selectivity in the reaction outcome (Tables 4 and 5). What is more interesting is that substitution follows the pattern observed for oxidant selectivity. Indeed, oxidation of oximes

6b-d with PIDA leads selectively to **12d** or **10b,c** , i.e., alkyl substitution favours *o*-cyclization whereas aryl substitution prefers exclusively *peri*-(1,6)-cyclization. Oxidation with LTA, on the other hand, appears to be substituent- insensitive and leads to both **12** and **10** in a 3:2 ratio.

It is, therefore, clear that 1,6-cyclization competes with its 1,5-rivals, in terms of geometry and energy constraints of the process. Relative energies of both *o*- and *peri*-cyclization modes suggest that **12** and **14** have comparable stabilities (Tables 4 and 5), indicating a stability order **12≥14>9>10**. We observe an overall stabilazion of the reaction, up to 3 kcal/mol, in AcOH (see Tables 4 and 5) while this catalyst has a marked stabilizing effect on the minima or transition states (Fig. 5, $\mathbf{ts_{23\text{-}12}}$ or Fig. 6, $\mathbf{ts_{24\text{-}14}}$) (see also sections **3.2.1** and **3.2.2** earlier).

Table 4. Reaction energies[a] (kcal/mol) for *o*- and *peri*-cyclization structures of **4** to **10**, **12** and **14**.[b]

Reaction	H	H[c]	Me	Et	Ph
$\mathbf{4E_1 \rightarrow 10}$	-14.0(-13.9)[-13.9]	-17.2(-17.0)[-17.0]	-18.1(-18.6)[-18.7]	-18.1(-18.6)[-18.7]	-17.3(-17.1)[-17.0]
$\mathbf{4E_1 \rightarrow 12}$	-39.4(-40.1)[-40.1]	-39.9(-40.2)[-40.3]	-41.1(-42.1)[-42.2]	-40.5(-41.6)[-41.7]	-38.2(-39.4)[-39.4]
$\mathbf{4E_1 \rightarrow 14}$	-33.3(-35.4)[-35.5]	-36.5(-38.4)[-38.5]	-39.2(-42.2)[-42.3]	-39.1(-42.1)[-42.3]	-39.1(-40.9)[-40.9]
$\mathbf{4E_2 \rightarrow 14}$	-26.8(-28.4)[-28.5]	-30.2(-32.1)[-32.2]	-32.7(-35.1)[-35.2]	-33.4(-35.8)[-35.9]	-35.6(-36.4)[-36.4]

[a] At the B3LYP/6-311G+(d,p) level of theory; data in the gas phase(in THF solvent)[in CH_2Cl_2 solvent]. [b]a: R=H, b: R=Me, c: R=Et, d: R=Ph. [c] Structures interacting with AcOH.

Table 5. Reaction zero point energies corrected ΔE_0 (kcal/mol), enthalpies ΔH (kcal/mol) and free energies ΔG(kcal/mol) for *o*- and *peri*-cyclization structures of **3** to **9**, and **4** to **10**, **12** and **14**.[a].

Reaction	H			H[b]			Me			Et			Ph		
	ΔE_0	ΔH	ΔG	ΔE_0	ΔH	ΔG	ΔE_0	ΔH	ΔG	ΔE_0	ΔH	ΔG	ΔE_0	ΔH	ΔG
$\mathbf{3E_1 \rightarrow 9}$	14.8	15.6	13.4	17.6	18.3	16.5	18.3	19.4	16.6	19.1	19.8	18.2	20.8	21.7	19.0
$\mathbf{4E_1 \rightarrow 10}$	12.6	13.3	11.3	15.8	16.4	14.6	16.5	17.1	15.5	16.4	17.0	15.2	15.4	16.1	14.4
$\mathbf{4E_1 \rightarrow 12}$	38.1	38.6	36.9	38.4	39.1	37.1	39.6	40.0	38.6	38.8	39.4	37.6	36.6	37.1	35.7
$\mathbf{4E_1 \rightarrow 14}$	31.8	32.2	30.8	34.8	35.4	33.5	37.5	37.7	36.7	37.4	37.7	36.8	37.2	37.5	36.2

[a] At the B3LYP/6-311G+(d,p) level of theory; data in the gas phase; a R=H, b R=Me, c R=Et, d R=Ph. [b] Structures interacting with AcOH.

From the data at hand and their analysis the following question is inevitably raised: "is *peri*-annelation to **12** or **14** a primary or a secondary process?" That is, does **4** assume the E conformation directly, as soon as it is generated (primary process) or does it do it through its Z variant, *o*-cyclization to **10**, re-opening of the latter and isomerization (secondary process)? A primary process should require that the precursor oxime

(Scheme 1) takes up its *E*- conformation, followed by its oxidation through the complex **7** or **8** and its eventual collapse directly to **4**E (E_1 or E_2). The Z-conformation of oxime **6a** is more stable than its E-variant by 7.7 kcal/mol. The energy cost for their E- to Z-conversion is 4.2 kcal/mol. In a secondary process, on the other hand, the required Z→E conversion should go through the intermediacy of a form of **4.**[46]

Indeed, **4** cyclizes to **10** readily, via its Z conformer, with a very low or no energy barrier and this has been experimentally observed.[43] Unsubstituted **10** (i.e., **10a**) re-opens equally readily and assumes the E conformation[88] (Scheme 2), ultimately cyclizing to **12** or **14.**

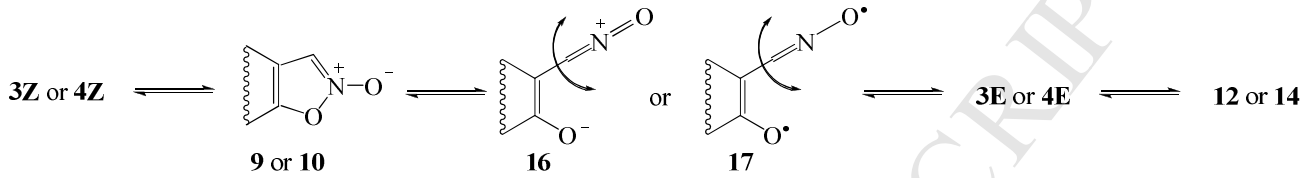

Scheme 2. Isomerization rearrangement of *β*-nitroso-*o*-quinone methides **3** and **4.**

The N-O_1 bond compressed among accumulated π-density of a distorted ring[46, 74] is seriously weakened[86] and suffers facile rupture, when triggered. It is the lability of H-3 in **9** or **10** that provides that trigger. The isoxazole ring, once opened, may revert to its Z precursor or change into its E counterpart (Scheme 2), eventually undergoing a *peri*-cyclisation. Thus, it is reasonable to assume an equilibrium among the proposed *o*-quinone methide forms[46] prior to final cyclization. It is worth noting that the Z→E conversion can be envisaged through a dipolar (zwitterionic) species, such as **16** (Scheme 2). A biradical species, such as **17** (Scheme 2), on the other hand, would be consistent with some of the calculated high energy barriers (Fig.3-6). However, the comparable barrier magnitudes calculated in solution (see earlier comments), cannot safely favour one of the possible arrangements of the intermediate species. The estimated rise in HOMA values (Table 3), during the generation of **3** and **4**, lends support to an "aromatic" arrangement like **16** without ruling out that of **17**.

The energy barriers of these successive changes range from 12-16 kcal/mol, 16-32 kcal/mol and 6-9 kcal/mol, respectively. These energy costs can be supplied by the total reaction energy of ca.38-42 kcal/mol for the most favoured reaction **4**E_1**→12**.

The reaction **4a→12** is favoured over its competitor **4a→14** by *ca*. 6 kcal/mol (i.e., the former has a higher total reaction energy of 39.3(40.1) kcal/mol over the latter of 33.3(35.4) kcal/mol, in the gas phase (or in solution). Interestingly, the reactions **4b-d→12** and **4b-d→14** of the other derivatives have comparable reaction energies. However, the largest barrier in the sequence of the most favoured route of **4→12** exceeds that of **4→14** by ~10 kcal/mol. This indicates a larger distortion of the relevant transition state and is consistent with the observed much longer time taken for the cyclization reaction to be completed.[88]

Overall, it appears that the 1,6-sequence is the preferred *peri*–cyclization mode. However, it is of interest that whether this is the prevalent or the sole reaction path will depend primarily on the oxidant-

directed conformation and subsequent collapse of **7** or **8** and not that of *o*-quinone methides **3** or **4.** The reaction is so fast that takes precedence over any other that could compete through the presence of a nucleophile.[44] The term "reclusive" is, therefore, coined to identify its uniqueness.

4. Conclusions

The intramolecular cyclization of **3** and **4** is a reclusive process in that it takes precedence over any other from external stimuli. It follows an oxidant-dependent 1,6- or a competing 1,5-electrocyclization. This selectivity appears to be correlated to the dissociation enthalpy of the O-Pb or I-O bond of the Pb-or I-based intermediate complexes **7** or **8.**

Regardless of the solvent used, it appears that the dominant reaction medium, unless trapped, is AcOH, liberated by both oxidants. Intramolecular or intermolecular solvent-assisted, contiguous or not, H shift trajectories, probably through hopping or tunneling, account for the successive transition states involved and the substantial drop of activation barriers. Rather insignificant changes have been observed in other solvents, in the absence of AcOH, compared to those in the gas phase though stabilization, in all cases, was larger in solution. Thus, the proposed reaction paths, apparently, do not favour charged species.

Substitution follows the oxidant selectivity pattern. Accordingly, in PIDA, alkyl substitution prefers the *o*-(1,5)-cyclization to N-oxides **9** or **10** and aryl substitution favours the peri -(1,6)-cyclization to 1,2-oxazine 12. LTA, on the other hand, proves to be substituent-insensitive, giving rise to all cyclization products.

Aromaticity indices, as stability indicators of the end structures, cannot discriminate between competing paths, as their values are of comparable magnitude. They do, however, suggest a markedly lower aromaticity of the heterocycles compared to their precursors, attributed to the *peri*-triggered enhanced diene geometry of their π-frame.

The available evidence cannot irrefutably clarify whether the *peri*-cyclization is a primary or a secondary process. It appears that the preferred path is oxidant-directed.

The reaction takes precedence over any other that could compete through the presence of a nucleophile and has been termed "reclusive" to identify its uniqueness.

References and Notes

1. R. W. Van de Water and T. R. R. Pettus, Tetrahedron, 2002, **58**, 5367.
2. T. P. Pathek and M. S. Singman, *J. Org. Chem.*, 2011, **76**, 9210.
3. M.W. Chen, L. L. Cao, Z. S. Ye, G. F. Jiang, and Y. G. Zhou, *Chem. Commun.*, 2013, **49**, 1660.
4. N. J. Willis and C. D. Bray, *Chem. Eur. J*., 2012, **18**, 9160.
5. H. Wang, M. S. Wahl, and S. E. Rokita, *Angew. Chem. Int. Ed.*, 2008, **47**, 1291.
6. A. Sharma, I. O. Santos, P. Gaur, V. E. Ferreira, C. R. S. Garcia, and D. R. da Rocha, *Eur. J. Med. Chem.*, 2013, **59**, 48.
7. I. Han, D. J. Russell, and H. Kohn, *J. Org. Chem*., 1992**, 57**, 1799.
8. M. Tomasz, A. Das, K. S. Tang, M. G. J. Ford, A. Minnock, S.M. Musser, and M.J. Waring, *J. Am. Chem. Soc*., 1992, **120**, 11581.
9. S. R. Angle, J. D. Rainier, and C. Woytowicz, *J. Org. Chem.*, 1997, **62**, 5884.
10. S. R.Angle and W. J.Yang, *J. Org. Chem.*, 1992, **57**, 1092.
11. G. Gaudiano, M. Frigerio, P. Bravo, and T. H. Koch, *J. Am. Chem. Soc*., 1990**, 112**, 6704.
12. H. Amouri and J. Le Bras, *Acc. Chem. Res*., 2002, **35**, 501.
13. Y. Chiang, A. J. Kresge, and Y. Zhu, *J. Am. Chem. Soc.*, 2000**, 122**, 9854.
14. A. K. Shaikh, A. J. A. Cobb, and G. Varvounis, *Org. Lett.*, 2012**, 14**, 584.
15. M. Freccero, *Mini-Rev. Org. Chem*., 2004**, 1**, 403.
16. C. Di Valentin, M. Freccero, R. Zanaletti, and M. Sarzi-Amade, *J. Am. Chem. Soc.*, 2001, **123**, 8366.
17. E. E. Weinert, R. Dondi, S. Colloredo-Melz, K. N. Frankenfield, C. H. Mitchell, M. Freccero, and C. E. Rokita, *J. Am. Chem. Soc.*, 2006, **128**, 11940.
18. H. Sugimoto, S. Nakamura, and T. Ohwada, *Adv. Synth. Catal.*, 2007, **349**, 669.
19. A. F. Barrero, J. F. Quilez del Moral, M. Mar Herrador, P. Arteaga, M. Cortes, J. Benites, and A. Rosellon, *Tetrahedron*, 2006, **62**, 6012.
20. C. P. Dell, *J. Chem. Soc. Perkin* Trans., 1998, **1**, 3873 and references cited therein.
21. L. Tietze and G. Kettschau, *Top Curr. Chem*., 1997, ed. P. Metz, Springer Berlin Heidelberg, pp. 1-120.
22. P. Wan, B. Barker, L. Diana, M. Fischer, Y. Shi, and C. Yang, *Can. J. Chem.*, 1996, **74**, 465.
23. N. Basaric, N. Doslic, J. Ivkovic, Y. H. Wang, M. Malis, and P. Wan, *Chem. Eur. J.*, 2012, **18**, 10617.
24. T. W. Bentley, *Org. Biomol. Chem.*, 2011, **9**, 6685.
25. Y. Chiang, A. J. Kresge, and Y. Zhu, *J. Am. Chem. Soc.*, 2001, **123**, 8089.
26. Y. Chiang, A. J. Kresge, and Y. Zhu, *J. Am. Chem. Soc.*, 2002, **124**, 717.
27. E. Modica, R. Zanaletti, M. Freccero, and M. Mella, *J. Org. Chem*., 2001, **66**, 41.
28. P. G. Tsoungas, *Heterocycles*, 2002, **57**, 915 and references cited therein.
29. P. G. Tsoungas, *Heterocycles*, 2002, **57**, 1149 and references cited therein.
30. A. Marwaha, P. Singh, and M. P. Mahajan, *Tetrahedron*, 2006, **62**, 5474 and references cited therein.
31. B. Y. Yang, T. Zollner, P. Gebhardt, U. Mollmann, M.J. Miller, *Org. Biomol. Chem.*, 2010, **8**, 691.
32. B. S. Bodnar, M. J. Miller, *Angew. Chem. Int. Ed. Engl.*, 2011, **50**, 5629.

33. K. Wieser and A. Berndt, *Angew. Chem. Int. Ed. Engl.*, 1975, **14**, 70.
34. E. Francotte, R. Merenyi, B. Vandelbulcke-Coyette, and H. G. Viehe, *Helv. Chim. Acta*, 1981, **64**, 1208.
35. J. H. Smith, J. H. Heidema, and E. T. Kaiser, *J. Am. Chem. Soc.*, 1972, **94**, 9276.
36. A. C. Veronese, G. Vecchiati, S. Sferra, and P. Orlandini, *Synthesis*, 1985, 300.
37. M. Kwiatkowski, E. Kwiatkowski, A. Olechnowicz, D. M. Ho, E. Deutsch, *J. Chem. Soc. Dalton Trans.*, 1990, 2497.
38. D. E. Davies, T. L. Gilchrist, and T. G. Roberts, *J. Chem. Soc. Perkin Trans.* 1, 1983, 1275.
39. T. L. Gilchrist and T. G. Roberts, *J. Chem. Soc. Perkin Trans. 1*, 1983, 1283.
40. R. Zimmer and H. U. Reissig, *J. Org. Chem.*, 1992, **57**, 339.
41. H. U. Reissig, C. Hippeli, and T. Arnold, *Chem. Ber.*, 1990, **123**, 2403.
42. A. J. Boulton, P. G. Tsoungas, and C. Tsiamis, *J. Chem. Soc. Perkin Trans. 1*, 1986, 1665.
43. P. Supsana, P. G. Tsoungas, A. Aubry, S. Skoulika, and G. Varvounis, *Tetrahedron*, 2001, **57**, 3445.
44. C. Dolka, K. Van Hecke, L. Van Meervelt, P. G. Tsoungas, E. V. Van der Eycken, and G. Varvounis, *Org. Lett.*, 2009, **11**, 2964.
45. T. Liaskopoulos, S. Skoulika, P. G. Tsoungas, and G. Varvounis, unpublished results.
46. P. Kozielewicz, P. G. Tsoungas, D. Tzeli, I. D.; Petsalakis, and M. Zloh, *Struct. Chem.*, 2014, doi:10.1007/S11224-014-0454-y.
47. J. A. Smith, Q. Le, E. D. Jones, and J. Deadman, *Future Med. Chem.*, 2010, **2**, 215.
48. R. Ikeda and R. Kuwano, *Molecules*, 2012, **17**, 6901.
49. M. Searcey, S.S.Grewal, F.Madeo, P.G. Tsoungas *Tetrahedron Lett*., **2003** *44*, 6745-6747.
50. A. D. Becke, *J. Chem. Phys*., 1993, **98**, 1372.
51. C. Lee, W. Yang, and R. G. Parr, *Phys. Rev.* B, 1988, **37**, 785.
52. L. A. Curtiss, M. P. McGrath, J.-P. Blandeau, N. E. Davis, R. C. Binning, Jr, and L. Radom, *J. Chem. Phys*,. 1995, **103**, 6104.
53. J.-P. Zhang, X. Zhou, F. Q. Bai, H. X. Zhang, and A. C.Tang, *Theor. Chem. Acc*., 2009, **122**, 31.
54. H. Wang and F. Meng, *Theor. Chem. Acc*., 2010, **127**, 561.
55. A. Irfan, J.-P. Zhang, and Y. F. Chang, *Theor. Chem. Acc*., 2010, **127**, 587.
56. D. Tzeli, I. D.; Petsalakis, G. Theodorakopoulos, *Phys. Chem. Chem. Phys*., 2011, **13**, 954.
57. L. Simón and J. M. Goodman, *Org. Biomol. Chem.*, 2011, **9**, 689.
58. T. H. Dunning, Jr., *J. Chem. Phys*., 1989, **90**, 1007; D. Woon, and T. H. Dunning, Jr., *J. Chem. Phys*., 1995, **103**, 4572.
59. Y. Zhao and D. Truhlar, *Theor. Chem. Acc*., 2008, **120**, 215.
60. J. Tomasi, B. Mennucci, and R. Cammi, *Chem. Rev.*, 2005, **105**, 2999; A. Pedone, J. Bloino, S. Monti, G. Prampolini, and V. Barone, *Phys. Chem. Chem. Phys.*, 2010, **12**, 1000.
61. S. F. Boys and F. Bernardi, *Mol. Phys.*, **1970,** *19*:553-566; S. S. Xantheas, *J. Chem. Phys.*, 1994, **104**, 8821.
62. Gaussian 09, Revision **A.1**, M. J. Frisch, G. W. Trucks, H. B. Schlegel, G. E. Scuseria, M. A. Robb, J.

R. Cheeseman, G. Scalmani, V. Barone, B. Mennucci, G. A. Petersson, H. Nakatsuji, M. Caricato, X. Li, H. P. Hratchian, A. F. Izmaylov, J. Bloino, G. Zheng, J. L. Sonnenberg, M. Hada, M. Ehara, K. Toyota, R. Fukuda, J. Hasegawa, M. Ishida, T. Nakajima, Y. Honda, O. Kitao, H. Nakai, T. Vreven, J. A. Montgomery, Jr., J. E. Peralta, F. Ogliaro, M. Bearpark, J. J. Heyd, E. Brothers, K. N. Kudin, V. N. Staroverov, R. Kobayashi, J. Normand, K. Raghavachari, A. Rendell, J. C. Burant, S. S. Iyengar, J. Tomasi, M. Cossi, N. Rega, J. M. Millam, M. Klene, J. E. Knox, J. B. Cross, V. Bakken, C. Adamo, J. Jaramillo, R. Gomperts, R. E. Stratmann, O. Yazyev, A. J. Austin, R. Cammi, C. Pomelli, J. W. Ochterski, R. L. Martin, K. Morokuma, V. G. Zakrzewski, G. A. Voth, P. Salvador, J. J. Dannenberg, S. Dapprich, A. D. Daniels, Ö. Farkas, J. B. Foresman, J. V. Ortiz, J. Cioslowski, and D. J. Fox, Gaussian, Inc., Wallingford CT, 2009

63. J. Poater, M. Duran, M. Sola, and B. Silvi, *Chem.* Rev., 2005, **105**, 3911.
64. E. D. Raczyńska, M. Hallman, K. Kolczyńska, and T. M. Stępniewski, *Symmetry*, 2010, **2**, 1485.
65. C. P. Frizzo-Marcos and A. P. Martins, *Struct. Chem.*, 2012, **23**, 375.
66. C. W. Bird, *Tetrahedron*, 1997, **53**, 3319.
67. C. W. Bird, *Tetrahedron*, 1996, **52**, 9945.
68. E. Matito, P. Salvador, M. Duran, and M. Solà, *J. Phys. Chem.*, 2006, **110**, 5108.
69. B. S. Jursic, *Tetrahedron*, 1997, **53**, 13285.
70. G. Rauhut, *J. Org. Chem.*, 2001, **66**, 5444 and references cited therein.
71. I. W. Davies, V. A. Guner, and K. N. Houk, *Org. Lett.*, 2004, **6**, 743 and references cited therein
72. V. Pilepic and S. Ursic, *J. Mol. Struct. THEOCHEM*, 2001, **538**, 41 and references cited therein
73. A. G. Leach and K. N. Houk, *Org. Biomolec. Chem.*, 2003, **1**, 1389.
74. T. Pasinszki, B. Havasi, B. Hajgato, and N. P. C. Westwood, *J. Phys. Chem. A*, 2009, **113**, 170.
75. G. Sivasubramanian, and V. R. Parameswaran, *J. Heterocycl. Chem.*, 2007, **44**, 1223 and references cited therein.
76. G. Chiari and D.Viterbo, *Acta Cryst B*, 1982, **38**, 323.
77. G. A. Voth, *Acc.Chem.Res*., 2006, **39**, 143 and references cited therein
78. D. Marx, M. E. Tuckerman, J. Hutter, and M. Parrinello, *Nature*, 1999, **397**, 601.
79. Lead(IV)acetate oxidation of **4** gives **12** and **14** in moderate yields and a spiro dimer as the major product (see ref 43). Phenyliododiacetate (PIDA) oxidation, furnishes **12** selectively (see ref 47). On the other hand, the oxidation can be selectively driven to the dimer, if run in AcOH/TFA or to **12** (as with PIDA) in the presence of N-morpholine oxide (NMO) (see T. Rosenau, K. Mereiter, C. Jäger, P. Schmidt, and P. Kosma, *Tetrahedron*, 2004, **60**, 5719) and ref 43. Same reaction outcome is obtained with Ag_2O oxidant.
80. Y.-R. Luo in "*Handbook of Bond Dissociation Energies in Organic Compounds*", CRC Press LLC, Boca Raton, 2003.
81. O. I. Siidra, S. V. Krivovichev, and S. K. Filatov, *Z. Kristallogr*., 2008, **223**, 114.
82. A. T. Balaban, *Chem. Rev.*, 2004, **104**, 2777.
83. Many experimental and theoretical reports, as well as book chapters and reviews, have been devoted to

Proton Transfer (PT) phenomena. Tunneling (a quantum effect of going *through* and not *over* an energy reaction barrier) (see ref 76) or hopping (or "hop-turn" or Grötthuss mechanism) are the currently accepted proton relay modes (see also I. Alkorta and J. Elguero, *Org. Biomol. Chem.*, 2006, **4**, 3096 and references cited therein).

84. Proton relay is a concept of growing interest and importance in deciphering mechanisms of many Processes see J. Bonin, C. Costentin, M. Robert, J.-M. Saveánt, and C. Tard, *Acc. Chem. Res.*, 2012, **45**, 372 and references cited therein.
85. H. Wang, Y. Wang, K.-L. Han, and X.-J. Peng *J. Org. Chem.*, 2005, **70**, 4910 and references cited therein.
86. (a) P. von Ragué Schleyer, J. I. Wu, F. P. Cossio, and I. Fernandez, *Chem. Soc. Rev.*, 2014, **43**, 4909. (b) D. M. Birney, *Curr. Org. Chem.*, 2010, **14**, 1658.
87. P. Kozielevicz, D. Tzeli, P. G. Tsoungas, and M. Zloh, *Struct. Chem.*, doi:10.1007/S11224-014-0459-6.
88. (a)Unsubstituted **9** or **10** are not isolable, see also ref.79. (b) Aryl substituted **10**, upon prolonged reaction, leads to **12** whereas its alkyl substituted analogues give **14** ; Supsana, P.; Tsoungas, P. G.; Tzeli D.,Varvounis, G., unpublished results.

Graphical abstract

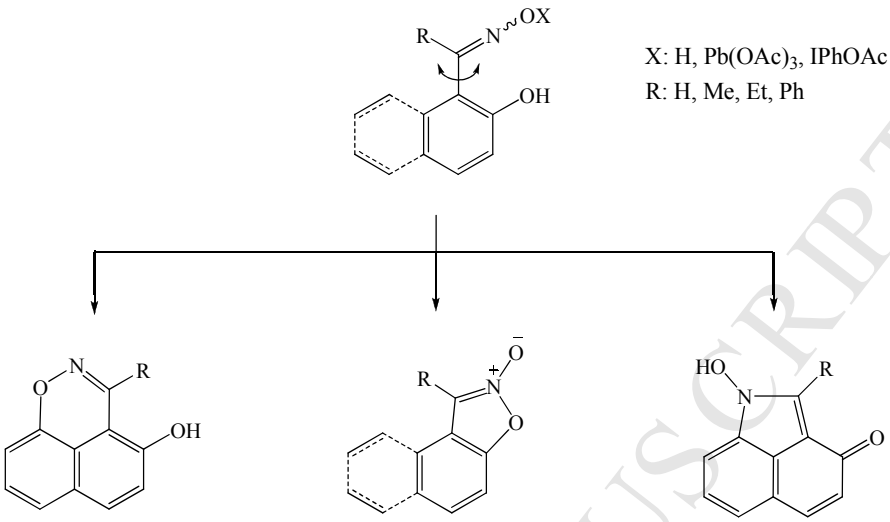

Intramolecular Cyclization of β-Nitroso-*o*-Quinone Methides. A Theoretical Endoscopy of a Potentially Useful Innate "Reclusive" Reaction.

Demeter Tzeli,[a] Petros G. Tsoungas,[b,*] Ioannis D. Petsalakis,[a] Paweł Kozielewicz,[c] Mire Zloh[d]

[a] *Theoretical and Physical Chemistry Institute, National Hellenic Research Foundation, 48 Vassileos Constantinou Ave., Athens 116 35, Greece.*

[b] *Department of Biochemistry, Hellenic Pasteur Institute, 127 Vas.Sofias Ave.,Athens, GR-11510, Greece*

[c] *School of Clinical and Experimental Medicine, University of Birmingham, Edgbaston, Birmingham B15 2TT, UK*

[d] *UCL School of Pharmacy, University College London, 29-39 Brunswick Square, London WC1 1AX, UK* and *Department of Pharmacy, University of Hertfordshire, College Lane, Hatfield, AL10 9AB, UK*

Supplementary material

Table 1S Absolute energies E(hartree) of the calculated minima and transition states including in the **$4E_1 \rightarrow 11$** and **$17 \rightarrow 12$** reactions calculated at the different level of Theory, for R = H.

	B3LYP/6-311+G(d,p)	M062X/6-311+G(d,p)	B3LYP/aug-cc-pVTZ	M062X/aug-cc-pVTZ	MP2/6-311+G(d,p)
$4E_1$	-628.6336672	-628.3755581	-628.6940221	-628.4426685	-626.8808669
ts_{4E1-11}	-628.6204659	-628.3540327	-628.6811214	-628.4217762	-626.8692873
11	-628.6408267	-628.3885758	-628.7023249	-628.4570791	-626.8866461
17	-628.6735007	-628.4260921	-628.7353191	-628.4946151	-626.9245853
ts_{17-12}	-628.5833857	-628.3322955	-628.6427488	-628.4033982	-626.8342524
12	-628.6964032	-628.4482470	-628.7608848	-628.5199157	-626.9451728

Table 2S Absolute energies E(hartree) of the calculated minima and transition states (ts) at B3LYP/6-311+G(d,p) level of theory in the gas phase and in THF and CH_2Cl_2 solvents.

R	**-H**			**-Me**			**-Et**			**-Ph**		
-E	**Gas phase**	**THF**	**CH_2Cl_2**	**Gas phase**	**THF**	**CH_2Cl_2**	**Gas phase**	**THF**	**CH_2Cl_2**	**Gas phase**	**THF**	**CH_2Cl_2**
	Fig. 2:	**3→9**										
$3E_1$	474.9506962	474.9579536	474.9582475	514.2790486	514.2853570	514.2856169	553.6019143	553.6079219	553.6081726	706.0548490	706.0628668	706.0632247
$ts_{3E1-3E2}$	474.9439574	474.9513783	474.9516774	514.2754487	514.2820820	514.2823539	553.5994658	553.6056581	553.6059173	706.0505064	706.0583147	706.0586536
$3E_2$	474.9575672	474.9654561	474.9657753	514.2871233	514.2934606	514.2937213	553.6098440	553.6159450	553.6162000	706.0588100	706.0678553	706.0682732
ts_{3Z-3E2}	474.9020528	474.9112037	474.9115902	514.2350507	514.2439206	514.2443047	553.5599202	553.5682407	553.5686136	706.0140700	706.0236574	706.0240881
3Z	474.9484999	474.9592437	474.9597105	514.2829390[a]	514.2917589[a]	514.2921378[a]	553.606600[a]	553.6150987[a]	553.6154695[a]	706.0614480[a]	706.0711740[a]	706.0716020[a]
ts_{3Z-9}	474.9483638	474.9584321	474.9588720	[b]	[b]	[b]	[b]	[b]	[b]	[b]	[b]	[b]
9	474.9771083	474.9843307	474.9846314	514.3108880	514.3184057	514.3187216	553.6350983	553.6421981	553.6425047	706.0916436	706.0989217	706.0992400
	Fig. 2:	**4→10**										
$4E_1$	628.6336672	628.6418541	628.6421915	667.9590967	667.9665427	667.9668563	707.2827697	707.2898389	707.2901407	859.7385026	859.7474627	859.7478670
$ts_{4E1-4E2}$	628.6305954	628.6383250	628.6386419	667.9571040	667.9643168	667.9646150	707.2815649	707.2882557	707.2885376	859.7343008	859.7425466	859.7429062
$4E_2$	628.6441212	628.6529377	628.6532994	667.9695513	667.9778502	667.9782004	707.2918544	707.2999762	707.3003217	859.7441669	859.7546339	859.7551091
ts_{4Z-4E2}	628.5880761	628.5989566	628.5994286	667.9212489	667.9318464	667.9323180	707.2463983	707.2564137	707.2568725	859.7154207	859.7273319	859.7278581
4Z	628.6379789	628.6498244	628.650331	667.9635983	667.9749553	667.9754452	707.2870940	707.2970574	707.2974913	859.742627	859.7529273	859.7533751
ts_{4Z-10}	628.6353218	628.6449581	628.6453769	667.9630908	667.9738853	667.9743514	[b]	[b]	[b]	[b]	[b]	[b]
10	628.6559149	628.6640721	628.6644155	667.9880029	667.9962599	667.9966100	707.3116056	707.3195361	707.3198751	859.7660683	859.7746488	859.7750243
	Fig. 3:	**4→12**										
$4E_1$	628.6336672	628.6418541	628.6421915	667.9590967	667.9665427	667.9668563	707.2827697	707.2898389	707.2901407	859.7385026	859.7474627	859.7478670
ts_{4E1-11}	628.6204659	628.6297728	628.6301673	667.9478227	667.9561990	667.9565599	707.2717030	707.2797663	707.2801207	859.7266688	859.7371585	859.7376508
11	628.6408267	628.6527581	628.6532694	667.9704931	667.9816727	667.9821628	707.2941900	707.3051373	707.3056208	859.746601	859.7599215	859.7605451
ts_{11-16}	628.5819469	628.5985602	628.5992622	667.9122276	667.9274468	667.9281007	707.2355005	707.2500482	707.2506808	859.6847042	859.7024513	859.7032720
16	628.6028577	628.6176865	628.6183314	667.9325229	667.9462774	667.9468835	707.2552377	707.2689163	707.2695205	859.7064438	859.7231903	859.7239750
ts_{16-17}	628.5873955	628.6015743	628.602172	667.9181958	667.9311615	667.9317174	707.2417193	707.2539571	707.2544899	859.6904880	859.7049177	859.7055766
17	628.6735007	628.6830375	628.6834325	668.0036167	668.0128146	668.0132035	707.3259775	707.3346710	707.3350457	859.7775442	859.7876498	859.7880974
ts_{17-12}	628.5833857	628.5902224	628.5906886	667.9157640	667.9248943	667.9252821	707.2373589	707.2461600	707.2465377	859.682589	859.6944856	859.6950381
12	628.6964032	628.7057692	628.7061703	668.0245771	668.0336790	668.0340766	707.3472664	707.3561440	707.3565358	859.7993516	859.8102085	859.8107086

	Fig. 4:	**4→12**										
$4E_1$	628.6336672	628.6418541	628.6421915	667.9590967	667.9665427	667.9668563	707.2827697	707.2898389	707.2901407	859.7385026	859.7474627	859.747867
ts_{4E1-11}	628.6204659	628.6297728	628.6301673	667.9478227	667.956199	667.9565599	707.271703	707.2797663	707.2801207	859.7266688	859.7371585	859.7376508
11	628.6408267	628.6527581	628.6532694	667.9704931	667.9816727	667.9821628	707.2941900	707.3051370	707.3056208	859.7466010	859.7599215	859.7605451
ts_{11-18}	628.6004883	628.6165972	628.6172892	667.9308854	667.9455419	667.9461843	707.2543708	707.2686660	707.2693009	859.7048729	859.7222045	858.7230121
18	628.6485905	628.6634126	628.6640324	667.9790913	667.9922589	667.9928259	707.3025619	707.3151471	707.3156934	859.7509426	859.7668346	859.7675682
ts_{18-19}	628.5971445	628.6152071	628.6159887	667.9265872	667.9431492	667.9438782	707.2499175	707.2660303	707.2667466	859.6986611	859.7181934	859.7191060
19	628.6515645	628.6636255	628.6641452	667.9797162	667.9908214	667.9913097	707.3028184	707.3137760	707.3142613	859.7539706	859.7678381	859.7684876
ts_{19-20}	628.6063952	628.6255729	628.6264111	667.9355294	667.9530793	667.9538601	707.2587598	707.2758194	707.2765849	859.7080428	859.7285079	859.7294683
20	628.6483354	628.6653222	628.666035	667.9785760	667.9937624	667.9944161	707.3020719	707.3166296	707.3172626	859.7504033	859.7683825	859.7692106
ts_{20-21}	628.5951333	628.6122996	628.6130472	667.9247382	667.9403369	667.9410309	707.2481135	707.2632739	707.2639558	859.6980088	859.7165257	859.7174031
21	628.6313363	628.6417989	628.642246	667.9601455	667.9697762	667.9701969	707.2831302	707.2925408	707.2929565	859.7340990	859.7464335	859.7470172
ts_{21-22}	628.5934285	628.608428	628.6090726	667.9214979	667.9351767	667.9357797	707.2447308	707.2579075	707.2584969	859.6947704	859.7112353	859.7120018
22	628.6292351	628.6446323	628.6452764	667.9567349	667.9702789	667.9708626	707.2808556	707.2938035	707.2943653	859.7309989	859.7469489	859.7476847
ts_{22-23}	628.6036526	628.6202666	628.6209737	667.9318677	667.9473006	667.9479713	707.2553099	707.2702719	707.2709309	859.7048796	859.7232125	859.7240596
23	628.6525108	628.6630061	628.6634529	667.9807005	667.9903975	667.9908202	707.3037828	707.3132212	707.3136371	859.7553514	859.7676035	859.7681821
ts_{23-12}	628.5771736	628.5869533	628.5873653	667.9092009	667.9182643	667.9186558	707.2320974	707.2408449	707.2412276	859.6851737	859.6960981	859.6966096
12	628.6964032	628.7057692	628.7061703	668.0245771	668.033679	668.0340766	707.3472664	707.356144	707.3565358	859.7993516	859.8102085	859.8107086
	Fig. 5:	**4→14**										
$4E_1$	628.6336672	628.6418541	628.6421915	667.9590967	667.9665427	667.9668563	707.2827697	707.2898389	707.2901407	859.7385026	859.7474627	859.7478670
$4E_2$	628.6441212	628.6529377	628.6532994	667.9695513	667.9778502	667.9782004	707.2918544	707.2999762	707.3003217	859.7441669	859.7546339	859.7551091
ts_{4E2-13}	628.6171982	628.6281712	628.6286212	667.9571043	667.9643199	667.9646182	707.2815648	707.2882553	707.2885372	859.7343008	859.7425467	859.7429063
13	628.6309337	628.6442693	628.6448244	667.9662119	667.9787891	667.9793237	707.2897969	707.3020235	707.3025516	859.7440391	859.7569872	859.7575686
ts_{13-24}	628.5739896	628.5879251	628.5884941	667.9111402	667.9238133	667.9243434	707.2350032	707.2471834	707.2477035	859.6889988	859.7012518	859.7017932
24	628.6182587	628.6377776	628.63859703	667.9577040	667.9752283	667.9759803	707.2815612	707.2984955	707.2992240	859.7393424	859.7555071	859.7562364
ts_{24-14}	628.5889780	628.60219996	628.6027423	667.9266598	667.9385075	667.9390091	707.2503012	707.2616775	707.2621600	859.7053227	859.7159023	859.7163678
14	628.6867541	628.6982498	628.69877998	668.0216119	668.033784	668.0343068	707.3451583	707.3569925	707.3575093	859.8008493	859.8125613	859.8130799

[a] The structure is not very stable because there is no gap which has to overcome and it end up to lowest **9** or **10** minimum. [b] There is no transition state, the gap is 0.

Table 3S Relative energy levels (kcal/mol) of the calculated minima and transition states (ts) involving in the *intra*molecular cyclization of β-nitroso-*o*-benzo(naphtho)quinone methide, **3**(**4**) at B3LYP/6-311+G(d,p) level of theory in gas phase and in THF and CH_2Cl_2 solvent.

R	**-H**			**-Me**			**-Et**			**-Ph**		
	Gas ph.	**THF**	**CH_2Cl_2**	**Gas ph.**	**THF**	**CH_2Cl_2**	**Gas ph.**	**THF**	**CH_2Cl_2**	**Gas ph.**	**THF**	**CH_2Cl_2**
	Fig. 2:	**3→9**										
$3E_1$	0	0	0	0	0	0	0	0	0	0	0	0
$ts_{3E1\text{-}3E2}$	4.2	4.1	4.1	2.3	2.1	2.0	1.5	1.4	1.4	2.7	2.9	2.9
$3E_2$	-4.3	-4.7	-4.7	-5.1	-5.1	-5.1	-5.0	-5.0	-5.0	-2.5	-3.1	-3.2
$ts_{3Z\text{-}3E2}$	30.5	29.3	29.3	27.6	26.0	25.9	26.4	24.9	24.8	25.6	24.6	24.6
3Z	1.4	-0.8	-0.9	-2.4	-4.0	-4.1	-2.9	-4.5	-4.6	-4.1	-5.2	-5.3
$ts_{3Z\text{-}9}$	1.5	-0.3	-0.4									
9	-16.6	-16.6	-16.6	-20.0	-20.7	-20.8	-20.8	-21.5	-21.5	-23.1	-22.6	-22.6
	Fig. 2:	**4→10**										
$4E_1$	0	0	0	0	0	0	0	0	0	0	0	0
$ts_{4E1\text{-}4E2}$	1.9	2.2	2.2	1.3	1.4	1.4	0.8	1.0	1.0	2.6	3.1	3.1
$4E_2$	-6.6	-7.0	-7.0	-6.6	-7.1	-7.1	-5.7	-6.4	-6.4	-3.6	-4.5	-4.5
$ts_{4Z\text{-}4E2}$	28.6	26.9	26.8	23.7	21.8	21.7	22.8	21.0	20.9	14.5	12.6	12.6
4Z	-2.7	-5.0	-5.1	-2.8	-5.3	-5.4	-2.7	-4.5	-4.6	-2.6	-3.4	-3.5
$ts_{4Z\text{-}10}$	-1.0	-1.9	-2.0	-2.5	-4.6	-4.7						
10	-14.0	-13.9	-13.9	-18.1	-18.6	-18.7	-18.1	-18.6	-18.7	-17.3	-17.1	-17.0
	Fig. 3:	**4→12**										
$4E_1$	0	0	0	0	0	0	0	0	0	0	0	0
$ts_{4E1\text{-}11}$	8.3	7.6	7.5	7.1	6.5	6.5	6.9	6.3	6.3	7.4	6.5	6.4
11	-4.5	-6.8	-7.0	-7.2	-9.5	-9.6	-7.2	-9.6	-9.7	-5.1	-7.8	-8.0
$ts_{11\text{-}16}$	32.5	27.2	26.9	29.4	24.5	24.3	29.7	25.0	24.8	33.8	28.2	28.0
16	19.3	15.2	15.0	16.7	12.7	12.5	17.3	13.1	12.9	20.1	15.2	15.0
$ts_{16\text{-}17}$	29.0	25.3	25.1	25.7	22.2	22.1	25.8	22.5	22.4	30.1	26.7	26.5
17	-25.0	-25.8	-25.9	-27.9	-29.0	-29.1	-27.1	-28.1	-28.2	-24.5	-25.2	-25.2
$ts_{17\text{-}12}$	31.6	32.4	32.3	27.2	26.1	26.1	28.5	27.4	27.4	35.1	33.2	33.2
12	-39.4	-40.1	-40.1	-41.1	-42.1	-42.2	-40.5	-41.6	-41.7	-38.2	-39.4	-39.4
	Fig. 4:	**4→12**										
$4E_1$	0	0	0	0	0	0	0	0	0	0	0	0
$ts_{4E1\text{-}11}$	8.3	7.6	7.5	7.1	6.5	6.5	6.9	6.3	6.3	7.4	6.5	6.4
11	-4.5	-6.8	-7.0	-7.2	-9.5	-9.6	-7.2	-9.6	-9.7	-5.1	-7.8	-8.0
$ts_{11\text{-}18}$	20.8	15.8	15.6	17.7	13.2	13.0	17.8	13.3	13.1	21.1	15.8	15.6
18	-9.4	-13.5	-13.7	-12.5	-16.1	-16.3	-12.4	-15.9	-16.0	-7.8	-12.2	-12.4
$ts_{18\text{-}19}$	22.9	16.7	16.4	20.4	14.7	14.4	20.6	14.9	14.7	25.0	18.4	18.0
19	-11.2	-13.7	-13.8	-12.9	-15.2	-15.3	-12.6	-15.0	-15.1	-9.7	-12.8	-12.9
$ts_{19\text{-}20}$	17.1	10.2	9.9	14.8	8.4	8.2	15.1	8.8	8.5	19.1	11.9	11.5
20	-9.2	-14.7	-15.0	-12.2	-17.1	-17.3	-12.1	-16.8	-17.0	-7.5	-13.1	-13.4
$ts_{20\text{-}21}$	24.2	18.5	18.3	21.6	16.4	16.2	21.7	16.7	16.4	25.4	19.4	19.1
21	1.5	0.03	-0.03	-0.7	-2.0	-2.1	-0.2	-1.7	-1.8	2.8	0.6	0.5
$ts_{21\text{-}22}$	25.3	21.0	20.8	23.6	19.7	19.5	23.9	20.0	19.9	27.4	22.7	22.5
22	2.8	-1.7	-1.9	1.5	-2.3	-2.5	1.2	-2.5	-2.7	4.7	0.3	0.1
$ts_{22\text{-}23}$	18.8	13.5	13.3	17.1	12.1	11.9	17.2	12.3	12.1	21.1	15.2	14.9
23	-11.8	-13.3	-13.3	-13.6	-15.0	-15.0	-13.2	-14.7	-14.7	-10.6	-12.6	-12.7
$ts_{23\text{-}12}$	35.5	34.5	34.4	31.3	30.3	30.2	31.8	30.7	30.7	33.5	32.2	32.2
12	-39.4	-40.1	-40.1	-41.1	-42.1	-42.2	-40.5	-41.6	-41.7	-38.2	-39.4	-39.4
	Fig. 5:	**4→14**										
$4E_1$	0	0	0	0	0	0	0	0	0	0	0	0
$4E_2$	-6.6	-7.0	-7.0	-6.6	-7.1	-7.1	-5.7	-6.4	-6.4	-3.6	-4.5	-4.5
$ts_{4E2\text{-}13}$	10.3	8.6	8.5	1.3	1.4	1.4	0.8	1.0	1.0	2.6	3.1	3.1
13	1.7	-1.5	-1.7	-4.5	-7.7	-7.8	-4.4	-7.6	-7.8	-3.5	-6.0	-6.1
$ts_{13\text{-}24}$	37.4	33.8	33.7	30.1	26.8	26.7	30.0	26.8	26.6	31.1	29.0	28.9
24	9.7	2.6	2.3	0.9	-5.5	-5.7	0.8	-5.4	-5.7	-0.5	-5.0	-5.3
$ts_{24\text{-}14}$	28.0	24.9	24.8	20.4	17.6	17.5	20.4	17.7	17.6	20.8	19.8	19.8
14	-33.3	-35.4	-35.5	-39.2	-42.2	-42.3	-39.1	-42.1	-42.3	-39.1	-40.9	-40.9

Table 4S Bond distances (Å), angles and dihedral angles (degrees) of the structures (minima and transition states (ts)) of Fig. 3S.

R = H	**$3E_1$**	**$ts_{3E1-3E2}$**	**$3E_2$**	**3Z**	**ts_{3Z-9}**	**9**
O1-C1	1.223	1.224	1.222	1.221	1.229	1.356
C1-C2	1.520	1.513	1.520	1.508	1.493	1.404
C2-C3	1.366	1.349	1.361	1.361	1.364	1.426
C3-N	1.404	1.090	1.412	1.416	1.408	1.323
N-O2	1.216	2.128	1.222	1.218	1.211	1.215
C3-R	1.085	2.255	1.087	1.090	1.088	1.077
N-O1	4.145	2.422	4.199	2.716	2.511	1.492
O1-C1-C2	121.6	121.7	121.3	121.6	120.2	111.1
C1-C2-C3	115.7	116.4	117.5	120.5	117.1	105.6
R-C3-N	113.4	111.3	118.1	115.7	115.3	118.3
C3-N-O2	119.0	37.7	113.5	114.2	118.5	135.5
O1-C1-C2-C3	8.1	2.0	0.0	21.8	15.6	0.0
C1-C2-C3-N	170.6	2.9	180.0	12.0	13.2	0.0
C3-N-O1-O2	24.8	5.5	0.2	120.3	122.5	180.0
R-C3-N-O2	152.3	30.6	0.0	22.0	39.3	0.0
R = Me	**$3E_1$**	**$ts_{3E1-3E2}$**	**$3E_2$**	**3Z**	**ts_{3Z-9}**	**9**
O1-C1	1.229	1.230	1.227	1.249	1.259	1.355
C1-C2	1.514	1.504	1.515	1.460	1.451	1.404
C2-C3	1.378	1.362	1.198	1.378	1.384	1.431
C3-N	1.435	1.458	1.449	1.422	1.396	1.325
N-O2	1.210	1.204	3.692	1.204	1.203	1.221
C3-R	1.496	1.495	3.408	1.492	1.493	1.490
N-O1	4.271	4.300	4.496	2.129	2.016	1.486
O1-C1-C2	122.2	122.4	122.0	118.0	117.1	111.1
C1-C2-C3	119.0	119.9	141.2	112.2	111.4	106.2
R-C3-N	110.3	111.9	114.7	113.5	114.1	119.6
C3-N-O2	118.9	115.9	64.9	121.7	127.8	134.0
O1-C1-C2-C3	0.2	0.4	170.8	8.2	3.6	0.0
C1-C2-C3-N	172.4	176.1	95.9	13.3	8.6	0.0
C3-N-O1-O2	53.8	46.7	68.6	125.5	134.1	180.0
R-C3-N-O2	139.1	87.5	43.0	51.7	54.5	0.0
R = Et	**$3E_1$**	**$ts_{3E1-3E2}$**	**$3E_2$**	**3Z**	**ts_{3Z-9}**	**9**
O1-C1	1.229	1.230	1.227	1.240		1.354
C1-C2	1.515	1.506	1.517	1.476		1.404
C2-C3	1.376	1.362	1.379	1.377		1.432
C3-N	1.438	1.457	1.449	1.418		1.326
N-O2	1.211	1.206	1.215	1.209		1.221
C3-R	1.502	1.502	1.493	1.500		1.496
N-O1	4.300	4.326	4.320	2.248		1.489
O1-C1-C2	122.3	122.7	122.2	119.1		111.1
C1-C2-C3	119.7	120.8	120.9	114.4		106.2
R-C3-N	109.7	110.7	118.4	115.2		119.9
C3-N-O2	118.3	115.7	114.9	120.8		134.3
O1-C1-C2-C3	9.8	6.6	12.1	11.2		0.2
C1-C2-C3-N	172.3	175.7	179.3	11.8		0.4
C3-N-O1-O2	74.7	66.8	25.4	126.9		179.7
R-C3-N-O2	133.7	84.6	1.3	43.5		1.2
R = Ph	**$3E_1$**	**$ts_{3E1-3E2}$**	**$3E_2$**	**3Z**	**ts_{3Z-9}**	**9**
O1-C1	1.225	1.226	1.222	1.244		1.355
C1-C2	1.518	1.509	1.523	1.477		1.402
C2-C3	1.383	1.367	1.379	1.388		1.441
C3-N	1.432	1.485	1.456	1.443		1.335
N-O2	1.208	1.201	1.213	1.206		1.220
C3-R	1.472	1.469	1.475	1.464		1.467
N-O1	4.243	4.385	4.322	2.213		1.478
O1-C1-C2	122.9	123.2	122.4	119.1		111.2
C1-C2-C3	120.0	122.1	121.2	113.4		106.2
R-C3-N	109.0	110.6	118.7	116.0		121.5
C3-N-O2	120.9	115.0	115.5	121.5		134.8
O1-C1-C2-C3	7.5	9.8	3.0	7.5		0.4
C1-C2-C3-N	156.8	169.4	170.0	15.6		0.9
C3-N-O1-O2	60.3	45.6	44.6	126.7		179.6
R-C3-N-O2	136.5	79.8	2.0	43.9		0.5
R = H	**$4E_1$**	**$ts_{4E1-4E2}$**	**$4E_2$**	**4Z**	**ts_{4Z-10}**	**10**
O1-C1	1.221	1.223	1.221	1.217	1.249	1.354
C1-C2	1.526	1.532	1.526	1.512	1.459	1.389

C2-C3	1.369	1.362	1.362	1.356	1.374	1.423
C3-N	1.407	1.409	1.408	1.418	1.380	1.325
N-O2	1.216	1.214	1.224	2.121	2.073	2.062
C3-R	2.962	2.906	2.838	2.204	2.310	2.353
N-O1	4.116	4.024	4.137	2.771	2.154	1.485
C2-C4	1.463	1.477	1.469	1.469	1.450	1.424
O1-C1-C2	121.4	121.5	121.2	122.2	117.9	111.5
C1-C2-C3	112.3	110.9	113.5	120.1	111.5	105.6
R-C3-N	72.3	61.7	53.4	30.6	24.7	21.3
C3-N-O2	121.0	119.8	113.3	27.7	28.6	27.5
O1-C1-C2-C3	27.1	3.3	18.5	33.9	9.8	0.0
C1-C2-C3-N	154.8	171.0	172.9	5.6	10.1	0.0
C3-N-O1-O2	3.7	32.4	174.1	5.2	1.6	0.0
R-C3-N-O2	8.5	49.9	155.2	15.1	50.0	0.0
R = Me	**$4E_1$**	**$ts_{4E1-4E2}$**	**$4E_2$**	**4Z**	**ts_{4Z-10}**	**10**
O1-C1	1.224	1.225	1.223	1.215	1.229	1.352
C1-C2	1.511	1.508	1.510	1.514	1.491	1.389
C2-C3	1.382	1.358	1.376	1.366	1.370	1.433
C3-N	1.426	1.460	1.442	1.450	1.445	1.331
N-O2	1.210	1.204	1.218	1.215	1.210	1.224
C3-R	1.501	1.501	1.497	1.499	1.501	1.493
N-O1	4.258	4.328	4.316	2.696	2.363	1.473
C2-C4	1.463	1.481	1.468	1.471	1.467	1.044
O1-C1-C2	122.8	122.9	122.7	123.0	120.7	111.6
C1-C2-C3	116.4	117.0	118.4	119.0	114.5	105.9
R-C3-N	109.5	107.5	118.3	117.3	114.1	119.1
C3-N-O2	123.3	117.3	115.6	114.4	117.1	134.5
O1-C1-C2-C3	35.7	34.4	30.3	44.8	25.4	0.0
C1-C2-C3-N	144.0	161.1	162.5	4.0	6.5	0.0
C3-N-O1-O2	57.2	17.4	16.3	128.2	122.3	180.0
R-C3-N-O2	144.2	98.8	13.0	16.7	42.7	0.0
R = Et	**$4E_1$**	**$ts_{4E1-4E2}$**	**$4E_2$**	**4Z**	**ts_{4Z-10}**	**10**
O1-C1	1.224	1.225	1.222	1.231		1.352
C1-C2	1.512	1.507	1.514	1.494		1.390
C2-C3	1.381	1.359	1.375	1.374		1.435
C3-N	1.428	1.455	1.444	1.462		1.331
N-O2	1.210	1.205	1.218	1.207		1.225
C3-R	1.507	1.509	1.502	1.500		1.498
N-O1	4.289	4.323	4.355	2.307		1.470
C2-C4	1.467	1.481	1.467	1.472		1.430
O1-C1-C2	123.0	122.8	123.5	119.9		111.6
C1-C2-C3	116.6	116.9	119.7	113.0		105.8
R-C3-N	109.4	107.3	117.1	112.1		118.3
C3-N-O2	122.7	117.7	115.5	117.9		134.2
O1-C1-C2-C3	38.2	34.7	30.8	19.3		0.6
C1-C2-C3-N	145.5	160.4	159.3	16.9		0.9
C3-N-O1-O2	56.0	14.6	25.5	121.9		179.5
R-C3-N-O2	139.4	100.5	14.7	36.6		0.7
R = Ph	**$4E_1$**	**$ts_{4E1-4E2}$**	**$4E_2$**	**4Z**	**ts_{4Z-10}**	**10**
O1-C1	1.222	1.221	1.220	1.236		1.353
C1-C2	1.512	1.509	1.511	1.482		1.389
C2-C3	1.393	1.359	1.379	1.371		1.438
C3-N	1.421	1.480	1.453	1.445		1.337
N-O2	1.208	1.201	1.214	1.204		1.221
C3-R	1.471	1.478	1.475	1.484		1.476
N-O1	4.210	4.391	4.369	2.240		1.469
C2-C4	1.454	1.479	1.464	1.467		1.432
O1-C1-C2	123.8	123.5	123.8	119.7		111.7
C1-C2-C3	117.6	117.9	119.6	113.1		105.7
R-C3-N	110.2	107.5	118.3	112.6		118.9
C3-N-O2	124.8	116.8	115.8	120.8		134.7
O1-C1-C2-C3	33.2	38.6	34.5	17.4		1.0
C1-C2-C3-N	131.6	158.0	154.3	6.2		1.3
C3-N-O1-O2	74.2	30.5	34.6	124.8		179.3
R-C3-N-O2	148.3	92.8	12.5	55.6		1.9

Table 5S Bond distances (Å), angles and dihedral angles (degrees) of the structures (minima and transition states (ts)) of Fig. 4S.

R = H	**$4E_1$**	**ts_{4E1-11}**	**11**	**ts_{11-16}**	**16**	**ts_{16-17}**	**17**	**ts_{17-12}**	**12**
C5-O2	2.813	1.954	1.443	1.337	1.288	1.354	1.374	1.369	1.378
O2-N	1.216	1.260	1.406	1.539	1.475	1.502	1.437	1.403	1.412
N-C3	1.407	1.327	1.289	1.283	1.322	1.283	1.272	1.290	1.284
C2-C3	1.369	1.428	1.454	1.435	1.384	1.438	1.506	1.438	1.449
C3-R	1.084	1.081	1.084	1.089	1.088	1.088	1.086	1.085	1.085
C2-C4	1.463	1.390	1.356	1.415	1.513	1.492	1.497	1.408	1.417
C4-C5	1.405	1.441	1.500	1.462	1.496	1.444	1.384	1.412	1.411
C2-C1	1.526	1.495	1.479	1.440	1.440	1.449	1.535	1.443	1.384
C1-O1	1.221	1.225	1.227	1.236	1.233	1.235	1.217	1.363	1.368
H1-C5	1.078	1.083	1.108	1.369	2.088	2.068	2.924	4.177	5.579
H1-C4	2.150	2.163	2.131	1.319	1.116	1.176	2.125	3.030	4.343
H1-C2	2.763	2.728	2.822	2.310	2.182	1.572	1.105	2.006	3.171
H1-C1	4.213	4.159	4.170	3.405	3.086	2.492	2.090	1.170	1.924
H1-O1	5.010	4.986	5.067	4.498	4.182	3.539	2.786	1.530	0.963
C5-O2-N	104.0	111.9	115.4	118.3	123.9	116.3	117.0	121.6	121.2
O2-N-C3	121.0	124.5	116.6	112.5	111.3	113.3	116.1	117.3	117.6
N-C3-C2	129.5	119.5	124.2	128.8	128.5	128.0	125.2	125.8	126.1
C5-C4-C2	123.8	118.5	116.0	118.1	107.4	116.7	117.4	118.1	118.5
O2-C5-H1	41.3	84.2	107.0	110.4	111.6	95.8	84.0	95.4	95.7
C4-H1-C5	34.7	36.3	41.9	65.9	43.7	42.7	26.2	13.3	7.9
C9-C4-H1	143.8	139.5	123.1	99.3	105.8	108.1	120.3	97.4	93.2
C4-H1-C2	31.6	30.3	27.5	33.6	40.3	63.9	41.9	22.6	12.3
C3-C2-H1	84.4	77.5	78.8	105.4	108.4	114.5	106.9	106.6	105.1
C1-H1-O1	11.5	11.4	10.4	8.4	9.0	12.7	23.9	58.8	41.9
H1-O1-C1	43.7	42.1	38.0	23.8	23.1	26.2	44.0	47.3	110.1
C5-C4-C9-C2	178.2	173.3	179.0	172.2	122.9	162.9	179.6	177.9	180.0
N-O2-C5-C4	3.9	39.8	52.1	28.9	16.6	43.8	30.3	3.2	0.0
C2-C3-N-O2	48.4	32.8	6.0	8.6	12.6	11.8	0.1	0.6	0.0
C5-C4-C9-C8	5.1	5.3	9.3	0.2	19.4	6.0	4.2	1.5	0.0
C4-C9-C8-C7	2.1	0.0	2.4	1.7	7.7	5.3	1.7	0.8	0.0
C2-C4-C9-C10	6.8	11.1	4.6	7.7	37.7	11.9	5.7	0.3	0.0
C4-C9-C10-C11	5.5	2.9	2.4	3.6	22.7	5.6	5.5	1.2	0.0
C10-C11-C1-C2	9.9	2.6	1.7	4.9	10.5	5.2	13.6	7.8	0.0
R = Me	**$4E_1$**	**ts_{4E1-11}**	**11**	**ts_{11-16}**	**16**	**ts_{16-17}**	**17**	**ts_{17-12}**	**12**
C5-O2	2.674	1.940	1.433	1.334	1.284	1.349	1.369	1.369	1.370
O2-N	1.210	1.260	1.411	1.525	1.471	1.495	1.442	1.455	1.409
N-C3	1.426	1.334	1.295	1.291	1.331	1.290	1.278	1.283	1.290
C2-C3	1.382	1.442	1.474	1.455	1.400	1.456	1.530	1.492	1.470
C3-R	1.501	1.502	1.504	1.508	1.509	1.509	1.501	1.503	1.507
C2-C4	1.463	1.396	1.361	1.420	1.521	1.499	1.501	1.450	1.426
C4-C5	1.404	1.438	1.500	1.462	1.491	1.443	1.384	1.393	1.411
C2-C1	1.511	1.497	1.486	1.444	1.436	1.453	1.537	1.451	1.389
C1-O1	1.224	1.227	1.228	1.238	1.238	1.237	1.219	1.288	1.370
H1-C5	1.078	1.084	1.109	1.367	2.072	2.052	2.830	3.597	5.594
H1-C4	2.151	2.160	2.133	1.315	1.118	1.173	2.120	2.728	4.332
H1-C2	2.753	2.711	2.816	2.312	2.182	1.582	1.104	1.444	3.187
H1-C1	4.153	4.141	4.183	3.362	3.074	2.460	2.092	1.605	1.918
H1-O1	4.942	4.975	5.107	4.457	4.190	3.506	2.699	1.370	0.963
C5-O2-N	105.6	110.6	113.4	117.8	123.9	115.8	115.6	115.3	121.1
O2-N-C3	123.3	126.3	117.4	114.2	113.0	114.8	116.6	116.0	119.3
N-C3-C2	121.5	116.7	122.0	126.3	126.1	125.6	121.5	122.0	124.1
C5-C4-C2	123.2	118.4	116.1	118.4	108.5	117.0	116.5	117.7	119.0
O2-C5-H1	56.6	85.0	107.2	109.9	110.9	94.9	79.1	78.1	97.6
C4-H1-C5	34.6	36.4	41.8	66.0	44.2	43.3	28.1	20.0	7.3
C9-C4-H1	143.6	140.1	123.7	98.2	104.9	108.2	125.8	120.1	91.8
C4-H1-C2	31.8	30.8	27.8	33.7	40.7	63.9	42.3	19.5	13.1
C3-C2-H1	84.1	76.1	76.9	106.4	107.0	115.1	104.9	94.8	108.0
C1-H1-O1	11.9	11.4	10.0	8.5	8.5	12.9	25.7	50.6	42.4
H1-O1-C1	44.2	41.7	36.4	23.8	21.7	26.4	48.1	74.2	109.4
C5-C4-C9-C2	176.9	173.4	179.8	173.2	125.4	163.9	179.9	171.8	180.0
N-O2-C5-C4	19.7	43.8	57.5	31.5	13.5	45.6	36.7	38.3	0.0
C2-C3-N-O2	53.0	33.9	4.7	9.3	13.6	11.4	1.3	1.7	0.0
C5-C4-C9-C8	5.9	3.9	7.7	1.3	18.5	4.8	3.5	7.4	0.0
C4-C9-C8-C7	2.6	0.0	2.6	1.2	8.2	4.7	1.1	2.8	0.0
C2-C4-C9-C10	6.6	9.6	4.0	8.4	36.6	12.7	4.2	2.4	0.0
C4-C9-C10-C11	7.6	1.4	2.9	2.3	22.1	4.5	2.0	3.4	0.0
C10-C11-C1-C2	15.0	1.2	2.8	2.5	11.2	2.9	4.7	16.0	0.0

R = Et	$4E_1$	ts_{4E1-11}	11	ts_{11-16}	16	ts_{16-17}	17	ts_{17-12}	12
C5-O2	2.688	1.942	1.434	1.334	1.282	1.348	1.368	1.368	1.369
O2-N	1.210	1.259	1.410	1.525	1.484	1.497	1.440	1.455	1.409
N-C3	1.428	1.334	1.295	1.291	1.327	1.290	1.279	1.283	1.290
C2-C3	1.381	1.444	1.476	1.457	1.404	1.458	1.534	1.494	1.472
C3-R	1.507	1.508	1.509	1.519	1.519	1.519	1.512	1.517	1.516
C2-C4	1.467	1.397	1.361	1.422	1.523	1.503	1.504	1.451	1.428
C4-C5	1.404	1.438	1.500	1.462	1.492	1.443	1.384	1.393	1.411
C2-C1	1.512	1.498	1.486	1.444	1.435	1.454	1.539	1.451	1.390
C1-O1	1.224	1.228	1.228	1.238	1.239	1.238	1.219	1.288	1.371
H1-C5	1.078	1.084	1.109	1.363	2.064	2.057	2.853	3.601	5.596
H1-C4	2.151	2.160	2.134	1.317	1.119	1.174	2.120	2.726	4.331
H1-C2	2.756	2.709	2.812	2.314	2.180	1.578	1.105	1.441	3.189
H1-C1	4.148	4.141	4.184	3.369	3.078	2.460	2.088	1.601	1.919
H1-O1	4.931	4.976	5.109	4.470	4.200	3.512	2.720	1.372	0.963
C5-O2-N	104.8	110.4	113.3	117.4	123.9	115.4	115.9	115.2	121.0
O2-N-C3	122.7	126.5	117.5	114.3	113.3	114.9	117.3	116.4	119.6
N-C3-C2	121.4	116.6	121.9	126.1	126.4	125.4	121.6	121.9	123.9
C5-C4-C2	123.3	118.4	116.0	118.5	109.3	117.1	116.9	117.9	119.1
O2-C5-H1	55.6	85.0	107.2	109.9	111.6	95.0	80.4	78.4	97.9
C4-H1-C5	34.6	36.4	41.7	66.1	44.6	43.1	27.6	19.9	7.3
C9-C4-H1	143.6	140.2	124.2	98.2	104.1	108.3	124.4	120.0	91.6
C4-H1-C2	31.8	30.8	27.9	33.8	40.9	64.2	42.5	19.6	13.3
C3-C2-H1	85.0	75.9	76.7	106.2	107.4	115.3	105.2	94.7	108.5
C1-H1-O1	11.9	11.4	10.0	8.4	8.4	12.8	25.3	50.6	42.4
H1-O1-C1	44.5	41.7	36.4	23.4	21.3	26.0	47.0	73.9	109.4
C5-C4-C9-C2	176.9	173.3	179.7	173.5	127.1	163.9	179.5	171.6	179.6
N-O2-C5-C4	15.3	44.1	57.7	31.9	13.4	46.0	35.1	38.1	3.9
C2-C3-N-O2	56.0	34.0	5.4	10.7	11.8	12.7	0.1	3.2	0.4
C5-C4-C9-C8	5.9	3.7	7.1	1.3	18.8	4.9	3.3	7.5	0.7
C4-C9-C8-C7	2.7	0.0	2.7	1.2	8.5	4.8	1.1	2.8	0.3
C2-C4-C9-C10	6.7	9.6	3.8	8.1	34.8	12.7	4.5	2.4	0.7
C4-C9-C10-C11	8.0	1.4	2.9	2.5	21.5	4.7	2.5	3.4	0.4
C10-C11-C1-C2	16.3	1.3	2.7	3.1	10.5	3.7	6.6	15.9	0.4
R = Ph	**$4E_1$**	**ts_{4E1-11}**	**11**	**ts_{11-16}**	**16**	**ts_{16-17}**	**17**	**ts_{17-12}**	**12**
C5-O2	2.655	1.922	1.438	1.330	1.283	1.350	1.371	1.365	1.372
O2-N	1.208	1.260	1.404	1.513	1.471	1.491	1.441	1.396	1.408
N-C3	1.421	1.333	1.298	1.300	1.334	1.292	1.282	1.300	1.292
C2-C3	1.393	1.449	1.476	1.448	1.401	1.460	1.541	1.461	1.470
C3-R	1.471	1.478	1.487	1.494	1.495	1.501	1.490	1.489	1.495
C2-C4	1.454	1.393	1.361	1.428	1.523	1.504	1.503	1.419	1.427
C4-C5	1.406	1.440	1.499	1.451	1.493	1.442	1.383	1.409	1.410
C2-C1	1.512	1.501	1.488	1.445	1.442	1.460	1.537	1.452	1.390
C1-O1	1.222	1.224	1.225	1.235	1.234	1.234	1.219	1.356	1.364
H1-C5	1.080	1.085	1.108	1.414	2.074	2.044	2.780	4.056	5.584
H1-C4	2.153	2.160	2.138	1.330	1.118	1.173	2.120	2.943	4.329
H1-C2	2.722	2.698	2.810	2.282	2.185	1.587	1.102	1.991	3.186
H1-C1	4.162	4.162	4.215	3.431	3.136	2.437	2.100	1.172	1.916
H1-O1	4.980	5.024	5.150	4.532	4.275	3.454	2.635	1.530	0.963
C5-O2-N	104.8	109.6	112.7	117.7	123.7	114.5	114.7	120.9	120.5
O2-N-C3	124.8	125.9	117.3	114.5	112.7	114.5	116.3	118.9	118.9
N-C3-C2	120.5	116.1	121.5	125.7	125.9	125.4	120.2	123.4	124.1
C5-C4-C2	122.0	117.9	115.9	118.5	108.3	117.1	116.0	118.7	119.0
O2-C5-H1	63.1	85.6	106.8	116.0	110.9	94.3	76.7	94.7	96.9
C4-H1-C5	34.7	36.5	41.4	63.7	44.2	43.6	29.0	14.4	7.5
C9-C4-H1	143.9	140.3	125.4	102.0	105.0	108.8	129.5	97.5	92.0
C4-H1-C2	32.1	30.9	27.9	35.6	40.7	64.0	42.4	25.1	13.2
C3-C2-H1	79.4	73.4	75.5	91.8	105.1	116.3	104.8	110.8	108.6
C1-H1-O1	11.5	10.9	9.7	8.1	7.4	13.8	26.9	58.5	42.1
H1-O1-C1	42.5	40.1	35.6	23.2	19.2	28.2	51.3	47.5	109.6
C5-C4-C9-C2	177.1	172.5	178.2	170.4	125.1	163.8	178.7	180.0	178.4
N-O2-C5-C4	36.9	48.6	59.7	28.0	9.3	48.9	39.6	14.0	14.3
C2-C3-N-O2	48.0	33.6	5.9	11.5	15.1	11.5	2.5	0.6	1.0
C5-C4-C9-C8	4.1	2.3	5.7	3.6	19.4	4.8	4.5	0.9	2.4
C4-C9-C8-C7	1.9	0.7	3.3	1.3	9.1	4.6	1.2	0.4	0.8
C2-C4-C9-C10	3.8	9.1	4.0	3.1	35.2	12.5	4.2	1.8	2.3
C4-C9-C10-C11	6.5	4.0	4.9	4.9	24.2	3.2	0.4	4.0	1.4
C10-C11-C1-C2	14.1	5.3	7.5	5.0	15.1	1.4	3.6	10.9	1.2

Table 6S Bond distances (Å), angles and dihedral angles (degrees) of the structures (minima and transition states (ts)) of Fig. 5S.

R = H	$4E_1$	ts_{4E1-11}	11	ts_{11-18}	18	ts_{18-19}	19	ts_{19-20}	20	ts_{20-21}	21	ts_{21-22}	22	ts_{22-23}	23	ts_{23-12}	12
C5-O2	2.813	1.954	1.443	1.344	1.304	1.341	1.381	1.337	1.304	1.343	1.375	1.369	1.365	1.370	1.375	1.376	1.378
O2-N	1.216	1.260	1.406	1.486	1.464	1.477	1.420	1.465	1.464	1.470	1.420	1.415	1.393	1.417	1.418	1.425	1.412
N-C3	1.407	1.327	1.289	1.286	1.301	1.284	1.281	1.285	1.302	1.284	1.282	1.285	1.295	1.286	1.283	1.283	1.284
C2-C3	1.369	1.428	1.454	1.440	1.411	1.436	1.451	1.435	1.410	1.438	1.451	1.446	1.433	1.442	1.445	1.446	1.449
C3-R	1.084	1.081	1.084	1.087	1.088	1.087	1.085	1.087	1.088	1.087	1.085	1.085	1.085	1.085	1.085	1.085	1.085
C2-C4	1.463	1.390	1.356	1.383	1.423	1.394	1.362	1.390	1.422	1.392	1.359	1.383	1.409	1.404	1.376	1.413	1.417
C4-C5	1.405	1.441	1.500	1.440	1.396	1.415	1.446	1.432	1.410	1.418	1.436	1.430	1.414	1.423	1.436	1.418	1.411
C2-C1	1.526	1.495	1.479	1.459	1.459	1.453	1.474	1.460	1.458	1.452	1.476	1.471	1.470	1.449	1.463	1.401	1.384
C1-O1	1.221	1.225	1.227	1.235	1.239	1.237	1.227	1.237	1.240	1.237	1.225	1.238	1.248	1.241	1.223	1.292	1.368
C5-C6	1.396	1.434	1.495	1.445	1.494	1.401	1.346	1.388	1.443	1.396	1.361	1.370	1.388	1.376	1.363	1.374	1.378
C6-C7	1.390	1.368	1.347	1.408	1.502	1.490	1.496	1.412	1.345	1.398	1.449	1.424	1.393	1.413	1.437	1.421	1.411
C7-C8	1.394	1.426	1.449	1.391	1.345	1.400	1.489	1.446	1.492	1.396	1.345	1.368	1.400	1.377	1.356	1.368	1.378
C8-C9	1.396	1.377	1.368	1.403	1.447	1.396	1.355	1.415	1.501	1.490	1.509	1.435	1.388	1.414	1.448	1.431	1.417
C4-C9	1.425	1.437	1.441	1.430	1.414	1.443	1.457	1.430	1.400	1.442	1.500	1.445	1.416	1.428	1.466	1.444	1.422
C9-C10	1.454	1.450	1.449	1.434	1.413	1.433	1.453	1.425	1.411	1.440	1.501	1.476	1.497	1.429	1.360	1.399	1.421
C10-C11	1.346	1.349	1.351	1.361	1.377	1.361	1.348	1.364	1.378	1.359	1.340	1.396	1.483	1.456	1.490	1.416	1.376
C11-C1	1.464	1.472	1.476	1.471	1.460	1.470	1.475	1.465	1.459	1.472	1.479	1.446	1.418	1.460	1.525	1.458	1.414
H1-C5	1.078	1.083	1.108	1.318	2.110	2.242	3.216	2.961	3.653	2.829	2.912	3.377	4.439	4.120	5.053	5.068	5.579
H1-C6	2.143	2.164	2.124	1.410	1.099	1.321	2.148	2.317	3.207	2.818	3.239	3.805	4.825	4.779	5.866	6.037	6.765
H1-C7	3.389	3.334	3.081	2.304	2.154	1.292	1.103	1.341	2.109	2.201	2.902	3.351	4.155	4.433	5.613	5.966	6.949
H1-C8	3.860	3.810	3.484	2.862	3.221	2.206	2.114	1.335	1.101	1.309	2.072	2.285	2.834	3.299	4.492	4.923	6.052
H1-C9	3.405	3.387	3.157	2.842	3.679	2.834	3.218	2.309	2.154	1.307	1.114	1.347	2.131	2.189	3.233	3.584	4.644
H1-C10	4.633	4.578	4.360	4.150	5.061	4.175	4.470	3.417	2.874	2.253	2.068	1.299	1.103	1.247	2.131	2.627	3.835
H1-C11	4.946	4.862	4.735	4.759	5.859	5.117	5.609	4.573	4.181	3.339	2.990	2.228	2.112	1.399	1.099	1.375	2.467
H1-C1	4.213	4.159	4.170	4.461	5.684	5.196	5.922	5.020	4.957	3.873	3.404	2.948	3.299	2.377	2.128	1.646	1.924
H1-O1	5.010	4.986	5.067	5.485	6.744	6.344	7.114	6.228	6.174	5.071	4.553	4.099	4.370	3.357	2.667	1.441	0.963
C5-O2-N	104.0	111.9	115.4	118.3	123.1	121.3	122.1	122.6	123.3	121.9	121.7	121.8	121.7	121.6	122.0	121.3	121.2
O2-N-C3	121.0	124.5	116.6	113.6	113.2	114.2	117.0	114.5	113.0	114.8	116.8	116.9	117.2	116.8	116.5	116.6	117.6
N-C3-C2	129.5	119.5	124.2	127.5	127.5	127.7	125.7	127.3	127.9	127.4	125.7	126.2	126.3	126.6	126.0	126.0	126.1
C5-C4-C2	123.8	118.5	116.0	117.4	117.0	118.0	119.2	118.3	116.6	119.2	118.9	119.2	118.1	118.2	118.0	117.5	118.5
C5-C6-C7	120.4	120.0	120.6	119.8	114.1	119.0	121.2	119.1	119.3	120.6	119.9	119.3	118.3	119.6	119.9	120.0	119.1
C6-C7-C8	119.5	121.4	121.8	119.6	121.7	119.0	115.0	120.5	123.4	121.3	122.5	122.6	121.5	121.5	122.0	121.2	121.6
C7-C8-C9	121.0	120.9	121.8	122.7	122.1	121.3	123.2	120.1	114.9	119.2	119.6	119.0	120.5	119.6	120.3	120.2	119.9
C8-C9-C10	119.7	123.0	124.4	124.7	124.4	123.5	123.4	124.1	123.3	124.5	118.2	125.7	124.2	124.2	123.9	123.1	124.5
C9-C10-C11	122.7	121.8	121.2	121.6	122.5	121.9	121.8	121.6	122.5	120.9	122.8	122.0	117.3	120.9	123.0	119.8	121.4
C10-C11-C1	120.9	121.9	122.4	123.7	124.2	123.7	122.2	123.3	123.9	124.0	122.6	123.4	126.1	123.3	117.8	119.5	121.1
C11-C1-O1	122.1	122.1	122.3	122.6	123.7	122.4	122.2	122.9	123.5	122.1	122.4	124.3	126.0	122.0	121.1	108.2	122.1
O2-C5-H1	41.3	84.2	107.0	112.5	96.9	130.9	141.7	153.4	165.6	155.4	140.4	138.7	142.8	128.5	119.5	111.4	95.7
C5-H1-C6	34.5	35.8	41.9	63.9	42.3	35.7	17.9	27.2	23.1	28.6	24.8	20.9	16.6	15.6	11.5	10.1	6.6
C6-H1-C7	13.1	15.1	21.3	35.2	40.7	69.5	40.7	33.6	17.2	29.2	26.6	21.8	15.7	17.1	14.2	13.6	11.7
C7-H1-C8	20.9	21.7	24.5	28.7	17.9	36.6	42.0	65.4	42.3	36.9	24.9	17.8	7.8	11.7	8.7	9.4	9.3
C8-H1-C9	21.0	21.0	23.1	28.5	23.0	28.9	17.3	34.0	40.6	69.5	45.1	36.0	28.2	18.8	10.8	6.9	1.8
C9-H1-C10	11.3	12.1	12.5	9.8	3.9	8.4	11.2	18.4	28.2	36.9	44.9	67.8	41.6	37.9	17.5	19.1	15.9
C10-H1-C11	15.7	16.1	16.4	15.7	11.8	12.2	8.3	10.5	7.2	17.1	22.6	35.7	41.7	66.5	41.1	20.0	2.8
C11-H1-C1	16.0	16.5	17.6	18.0	14.4	16.4	14.4	16.7	15.6	22.0	25.7	28.3	16.9	34.6	43.2	56.9	34.9

C1-H1-O1	11.5	11.4	10.4	8.0	5.9	4.6	2.6	2.8	2.4	4.0	6.2	7.5	9.7	15.5	26.6	49.0	41.9
C1-O1-H1	43.7	42.1	38.0	30.2	28.3	19.8	12.6	11.3	9.7	12.6	17.4	18.0	26.4	30.8	51.3	73.8	110.1
C5-C4-C9-C2	178.2	173.3	179.0	179.4	180.0	179.9	180.0	179.4	180.0	178.8	179.1	178.5	180.0	179.6	180.0	176.1	180.0
N-O2-C5-C4	3.9	39.8	52.1	30.0	0.0	8.6	0.0	0.9	0.0	1.8	7.4	3.5	0.0	1.5	0.1	11.4	0.0
C2-C3-N-O2	48.4	32.8	6.0	5.3	0.0	1.4	0.0	0.1	0.0	1.1	3.1	0.9	0.0	0.5	0.0	0.3	0.0
C5-C4-C9-C8	5.1	5.3	9.3	1.6	0.0	0.4	0.0	1.1	0.0	2.4	26.4	5.0	0.0	0.5	0.0	1.2	0.0
C4-C9-C8-C7	2.1	0.0	2.4	2.4	0.0	1.6	0.0	1.4	0.0	1.3	21.9	3.8	0.0	0.0	0.0	0.9	0.0
C2-C4-C9-C10	6.8	11.1	4.6	0.7	0.0	0.4	0.0	0.1	0.0	2.7	16.8	0.7	0.0	1.2	0.0	6.2	0.0
C4-C9-C10-C11	5.5	2.9	2.4	0.9	0.0	0.1	0.0	0.4	0.0	1.8	13.7	1.5	0.0	3.2	0.0	2.8	0.0
C10-C11-C1-C2	9.9	2.6	1.7	1.3	0.0	0.9	0.0	0.4	0.0	1.8	6.2	1.4	0.0	1.2	0.2	19.0	0.0
R =Me	**$4E_1$**	**ts_{4E1-11}**	**11**	**ts_{11-18}**	**18**	**ts_{18-19}**	**19**	**ts_{19-20}**	**20**	**ts_{20-21}**	**21**	**ts_{21-22}**	**22**	**ts_{22-23}**	**23**	**ts_{23-12}**	**12**
C5-O2	2.674	1.940	1.433	1.338	1.300	1.335	1.373	1.331	1.300	1.337	1.366	1.360	1.356	1.362	1.367	1.370	1.370
O2-N	1.210	1.260	1.411	1.479	1.452	1.467	1.416	1.455	1.452	1.461	1.417	1.412	1.390	1.414	1.414	1.424	1.409
N-C3	1.426	1.334	1.295	1.294	1.311	1.293	1.288	1.294	1.313	1.292	1.289	1.293	1.305	1.294	1.291	1.288	1.290
C2-C3	1.382	1.442	1.474	1.461	1.431	1.458	1.473	1.457	1.430	1.460	1.473	1.469	1.455	1.463	1.467	1.459	1.470
C3-R	1.501	1.502	1.504	1.506	1.504	1.506	1.506	1.506	1.505	1.506	1.506	1.506	1.507	1.507	1.506	1.504	1.507
C2-C4	1.463	1.396	1.361	1.388	1.430	1.401	1.369	1.397	1.430	1.400	1.366	1.392	1.420	1.414	1.384	1.416	1.426
C4-C5	1.404	1.438	1.500	1.440	1.396	1.416	1.446	1.432	1.410	1.418	1.435	1.430	1.414	1.422	1.435	1.417	1.411
C2-C1	1.511	1.497	1.486	1.465	1.464	1.459	1.483	1.467	1.463	1.458	1.484	1.480	1.480	1.455	1.470	1.403	1.389
C1-O1	1.224	1.227	1.228	1.237	1.242	1.239	1.228	1.238	1.243	1.239	1.225	1.239	1.249	1.243	1.223	1.295	1.370
C5-C6	1.396	1.432	1.495	1.445	1.495	1.401	1.347	1.389	1.444	1.397	1.363	1.372	1.390	1.378	1.365	1.376	1.380
C6-C7	1.390	1.368	1.346	1.406	1.499	1.487	1.493	1.410	1.344	1.396	1.445	1.420	1.390	1.410	1.433	1.419	1.408
C7-C8	1.394	1.423	1.448	1.391	1.343	1.399	1.486	1.444	1.490	1.394	1.345	1.367	1.399	1.377	1.355	1.368	1.378
C8-C9	1.396	1.378	1.368	1.403	1.447	1.396	1.355	1.414	1.502	1.490	1.508	1.434	1.388	1.413	1.448	1.431	1.417
C4-C9	1.424	1.437	1.444	1.432	1.416	1.446	1.461	1.433	1.402	1.445	1.505	1.449	1.420	1.431	1.470	1.446	1.424
C9-C10	1.452	1.447	1.446	1.432	1.410	1.431	1.450	1.423	1.408	1.438	1.497	1.473	1.493	1.427	1.358	1.398	1.419
C10-C11	1.346	1.348	1.349	1.358	1.374	1.357	1.345	1.360	1.374	1.355	1.337	1.391	1.476	1.450	1.483	1.414	1.371
C11-C1	1.468	1.472	1.476	1.471	1.459	1.470	1.475	1.465	1.458	1.472	1.479	1.446	1.418	1.459	1.526	1.460	1.416
H1-C5	1.078	1.084	1.109	1.318	2.110	2.249	3.219	2.958	3.644	2.818	2.886	3.368	4.430	4.107	5.046	5.066	5.594
H1-C6	2.141	2.164	2.123	1.410	1.099	1.324	2.147	2.310	3.200	2.810	3.213	3.796	4.807	4.764	5.855	6.031	6.766
H1-C7	3.387	3.342	3.091	2.308	2.153	1.289	1.103	1.336	2.108	2.204	2.893	3.350	4.136	4.423	5.601	5.955	6.927
H1-C8	3.859	3.817	3.497	2.867	3.214	2.202	2.113	1.340	1.101	1.312	2.070	2.279	2.812	3.285	4.473	4.906	6.004
H1-C9	3.404	3.390	3.170	2.850	3.672	2.834	3.220	2.315	2.153	1.304	1.114	1.348	2.130	2.181	3.222	3.572	4.603
H1-C10	4.620	4.585	4.380	4.165	5.052	4.173	4.457	3.409	2.852	2.246	2.069	1.295	1.103	1.244	2.127	2.617	3.777
H1-C11	4.907	4.858	4.750	4.773	5.848	5.116	5.595	4.563	4.155	3.329	2.981	2.212	2.108	1.402	1.099	1.370	2.410
H1-C1	4.153	4.141	4.183	4.482	5.685	5.210	5.924	5.024	4.941	3.869	3.388	2.931	3.300	2.388	2.124	1.652	1.918
H1-O1	4.942	4.975	5.107	5.536	6.771	6.381	7.126	6.238	6.155	5.071	4.534	4.066	4.345	3.363	2.629	1.437	0.963
C5-O2-N	105.6	110.6	113.4	117.3	123.2	120.8	122.1	122.6	123.3	121.8	121.7	121.7	121.6	121.5	122.0	121.7	121.1
O2-N-C3	123.3	126.3	117.4	115.0	115.1	115.9	118.7	116.4	115.0	116.5	118.5	118.8	119.1	118.5	118.3	118.0	119.3
N-C3-C2	121.5	116.7	122.0	125.1	125.2	125.3	123.5	125.0	125.5	125.1	123.5	124.0	123.9	124.4	123.8	124.1	124.1
C5-C4-C2	123.2	118.4	116.1	117.7	117.7	118.6	119.8	118.9	117.3	119.7	119.6	119.9	118.8	118.9	118.7	117.7	119.0
C5-C6-C7	120.4	120.1	120.7	119.8	114.1	119.1	121.4	119.3	119.4	120.8	120.2	119.6	118.6	119.8	120.1	120.1	119.3
C6-C7-C8	119.5	121.1	121.5	119.2	121.2	118.5	114.4	119.9	122.8	120.8	122.0	122.0	120.9	121.0	121.5	121.0	121.1
C7-C8-C9	120.9	121.0	122.1	123.0	122.4	121.5	123.4	120.3	115.1	119.4	119.6	119.2	120.8	119.7	120.4	120.2	120.0
C8-C9-C10	120.3	122.4	123.7	123.9	123.4	122.6	122.3	123.0	122.3	123.4	117.2	124.4	122.8	123.1	122.8	122.7	123.6
C9-C10-C11	122.0	121.3	120.7	121.0	121.8	121.2	121.2	121.0	121.8	120.3	122.1	121.3	116.6	120.3	122.5	119.5	120.8
C10-C11-C1	121.2	122.3	122.8	124.1	124.6	124.1	122.7	123.8	124.4	124.5	123.0	123.9	126.8	123.8	118.2	119.6	121.6
C11-C1-O1	121.3	120.7	120.6	120.9	121.7	120.3	120.2	120.8	121.6	120.0	120.3	122.0	123.4	119.7	119.0	107.5	119.6

O2-C5-H1	56.6	85.0	107.2	112.7	96.4	131.4	141.1	152.9	165.5	156.2	140.9	138.8	143.9	129.4	120.4	111.9	97.6
C5-H1-C6	34.6	35.8	42.0	63.9	42.4	35.5	17.9	27.2	23.2	28.7	25.1	21.0	16.7	15.7	11.6	10.2	6.8
C6-H1-C7	13.2	14.8	21.0	34.9	40.6	69.4	40.6	33.8	17.3	29.3	26.7	21.8	15.7	17.1	14.2	13.6	11.7
C7-H1-C8	20.9	21.6	24.4	28.7	18.0	36.7	41.9	65.3	42.2	36.7	25.1	17.7	7.6	11.7	8.6	9.3	9.1
C8-H1-C9	21.0	21.0	23.0	28.4	23.1	28.8	17.2	33.8	40.8	69.4	45.2	36.3	28.6	19.0	11.0	7.1	2.3
C9-H1-C10	11.5	11.9	12.2	9.4	3.9	8.4	11.5	18.6	28.5	37.0	44.6	67.7	41.4	38.1	17.7	19.2	15.9
C10-H1-C11	15.9	16.1	16.3	15.7	11.8	12.1	8.2	10.5	7.2	17.1	22.7	36.0	41.5	66.1	40.9	20.2	2.0
C11-H1-C1	16.0	16.5	17.6	17.9	14.4	16.3	14.3	16.7	15.6	22.0	25.9	28.5	16.7	34.2	43.4	56.9	36.0
C1-H1-O1	11.9	11.4	10.0	7.4	5.6	4.0	2.2	2.5	2.7	3.9	6.4	8.2	10.4	15.6	27.3	49.0	42.4
C1-O1-H1	44.2	41.7	36.4	28.0	26.4	17.1	10.8	10.2	10.9	12.2	17.9	19.8	28.4	31.2	52.7	74.2	109.4
C5-C4-C9-C2	176.9	173.4	179.8	178.4	180.0	179.3	180.0	179.4	180.0	178.8	178.0	178.4	180.0	179.7	180.0	176.6	180.0
N-O2-C5-C4	19.7	43.8	57.5	34.4	0.0	14.6	0.0	1.1	0.0	5.9	3.9	7.2	0.0	2.6	0.1	6.8	0.0
C2-C3-N-O2	53.0	33.9	4.7	5.9	0.0	2.4	0.0	0.2	0.0	1.9	3.4	0.6	0.0	1.0	0.0	0.8	0.0
C5-C4-C9-C8	5.9	3.9	7.7	0.1	0.0	1.2	0.0	1.3	0.0	2.4	26.5	5.1	0.0	0.7	0.0	1.0	0.0
C4-C9-C8-C7	2.6	0.0	2.6	1.7	0.0	1.4	0.0	1.7	0.0	1.5	22.3	3.7	0.0	0.1	0.0	0.6	0.0
C2-C4-C9-C10	6.6	9.6	4.0	1.2	0.0	1.0	0.0	0.1	0.0	3.5	17.9	1.1	0.0	1.4	0.0	6.1	0.0
C4-C9-C10-C11	7.6	1.4	2.9	0.0	0.0	0.4	0.0	0.5	0.0	1.5	13.4	1.5	0.0	4.2	0.0	3.3	0.0
C10-C11-C1-C2	15.0	1.2	2.8	0.6	0.0	0.7	0.0	0.0	0.0	1.1	7.1	3.4	0.0	1.5	0.2	19.8	0.0
R = Et	**$4E_1$**	**ts_{4E1-11}**	**11**	**ts_{11-18}**	**18**	**ts_{18-19}**	**19**	**ts_{19-20}**	**20**	**ts_{20-21}**	**21**	**ts_{21-22}**	**22**	**ts_{22-23}**	**23**	**ts_{23-12}**	**12**
C5-O2	2.688	1.942	1.434	1.338	1.299	1.335	1.371	1.331	1.300	1.337	1.366	1.360	1.357	1.362	1.367	1.369	1.369
O2-N	1.210	1.259	1.410	1.480	1.452	1.468	1.421	1.455	1.452	1.461	1.418	1.411	1.391	1.413	1.414	1.425	1.409
N-C3	1.428	1.334	1.295	1.293	1.310	1.292	1.288	1.293	1.312	1.291	1.289	1.293	1.303	1.294	1.290	1.288	1.290
C2-C3	1.381	1.444	1.476	1.463	1.433	1.460	1.474	1.459	1.432	1.462	1.474	1.471	1.455	1.465	1.468	1.461	1.472
C3-R	1.507	1.508	1.509	1.514	1.514	1.515	1.514	1.515	1.514	1.515	1.514	1.514	1.513	1.514	1.514	1.513	1.516
C2-C4	1.467	1.397	1.361	1.388	1.432	1.402	1.369	1.399	1.432	1.401	1.368	1.394	1.420	1.415	1.385	1.418	1.428
C4-C5	1.404	1.438	1.500	1.441	1.397	1.416	1.446	1.432	1.410	1.418	1.434	1.429	1.413	1.422	1.435	1.417	1.411
C2-C1	1.512	1.498	1.486	1.466	1.465	1.460	1.483	1.468	1.464	1.459	1.484	1.481	1.477	1.456	1.471	1.403	1.390
C1-O1	1.224	1.228	1.228	1.237	1.242	1.240	1.228	1.239	1.243	1.239	1.226	1.239	1.250	1.244	1.223	1.296	1.371
C5-C6	1.396	1.432	1.495	1.445	1.496	1.401	1.347	1.389	1.445	1.397	1.364	1.372	1.390	1.378	1.365	1.376	1.380
C6-C7	1.390	1.368	1.346	1.406	1.499	1.486	1.494	1.410	1.343	1.395	1.444	1.420	1.390	1.410	1.433	1.418	1.407
C7-C8	1.394	1.422	1.447	1.390	1.343	1.399	1.487	1.444	1.489	1.394	1.345	1.367	1.399	1.377	1.356	1.368	1.378
C8-C9	1.397	1.378	1.368	1.403	1.448	1.396	1.355	1.414	1.502	1.490	1.507	1.434	1.388	1.413	1.448	1.431	1.417
C4-C9	1.424	1.437	1.444	1.432	1.417	1.446	1.460	1.433	1.403	1.446	1.506	1.450	1.420	1.432	1.471	1.447	1.425
C9-C10	1.452	1.447	1.445	1.431	1.409	1.430	1.450	1.422	1.407	1.437	1.497	1.472	1.495	1.426	1.359	1.398	1.419
C10-C11	1.346	1.348	1.349	1.358	1.373	1.357	1.345	1.360	1.374	1.354	1.336	1.391	1.478	1.449	1.483	1.413	1.370
C11-C1	1.468	1.471	1.476	1.470	1.458	1.469	1.475	1.464	1.457	1.472	1.480	1.445	1.416	1.458	1.523	1.460	1.416
H1-C5	1.078	1.084	1.109	1.318	2.109	2.249	3.212	2.957	3.644	2.823	2.893	3.357	4.385	4.111	4.875	5.078	5.596
H1-C6	2.142	2.164	2.123	1.410	1.099	1.325	2.147	2.308	3.200	2.814	3.213	3.787	4.788	4.769	5.696	6.043	6.767
H1-C7	3.388	3.344	3.098	2.311	2.152	1.288	1.103	1.335	2.109	2.208	2.890	3.347	4.150	4.428	5.479	5.964	6.925
H1-C8	3.859	3.819	3.507	2.874	3.210	2.202	2.112	1.341	1.101	1.314	2.067	2.283	2.848	3.289	4.388	4.910	5.999
H1-C9	3.403	3.391	3.179	2.859	3.666	2.834	3.208	2.314	2.152	1.303	1.114	1.347	2.128	2.183	3.126	3.576	4.598
H1-C10	4.619	4.587	4.390	4.178	5.047	4.176	4.447	3.411	2.849	2.246	2.071	1.295	1.103	1.245	2.109	2.616	3.771
H1-C11	4.904	4.859	4.757	4.786	5.844	5.119	5.576	4.566	4.153	3.330	2.982	2.217	2.109	1.399	1.103	1.368	2.404
H1-C1	4.148	4.141	4.184	4.492	5.684	5.212	5.895	5.027	4.939	3.871	3.389	2.951	3.310	2.386	2.105	1.654	1.919
H1-O1	4.931	4.976	5.109	5.550	6.776	6.387	7.100	6.246	6.154	5.076	4.546	4.111	4.396	3.361	2.737	1.437	0.963
C5-O2-N	104.8	110.4	113.3	117.2	123.1	120.6	121.0	122.4	123.2	121.6	121.5	121.7	121.3	121.4	121.7	121.4	121.0
O2-N-C3	122.7	126.5	117.5	115.2	115.3	116.1	118.3	116.6	115.2	116.7	118.4	118.9	119.1	118.7	118.4	118.2	119.6
N-C3-C2	121.4	116.6	121.9	125.0	125.1	125.2	123.3	124.9	125.5	125.0	123.4	123.9	123.7	124.3	123.6	124.0	123.9

C5-C4-C2	123.3	118.4	116.0	117.7	117.8	118.6	119.6	119.0	117.4	119.8	119.7	120.0	118.7	118.9	118.6	117.8	119.1
C5-C6-C7	120.4	120.1	120.8	119.8	114.2	119.1	121.3	119.3	119.5	120.8	120.3	119.6	118.5	119.8	120.1	120.1	119.4
C6-C7-C8	119.5	121.1	121.4	119.1	121.2	118.4	114.5	119.9	122.7	120.8	121.9	121.9	121.0	120.9	121.5	121.0	121.1
C7-C8-C9	120.9	121.0	122.1	123.0	122.4	121.5	123.4	120.4	115.1	119.4	119.6	119.2	120.7	119.7	120.4	120.2	120.1
C8-C9-C10	120.3	122.4	123.6	123.8	123.2	122.5	122.5	122.8	122.1	123.2	117.2	124.3	123.2	123.0	122.8	122.6	123.4
C9-C10-C11	122.0	121.3	120.7	121.0	121.7	121.1	121.1	120.9	121.7	120.2	122.1	121.3	116.4	120.2	122.2	119.4	120.8
C10-C11-C1	121.2	122.4	122.9	124.1	124.7	124.2	122.8	123.9	124.4	124.5	123.1	124.0	126.1	123.8	117.8	119.7	121.7
C11-C1-O1	121.3	120.6	120.4	120.6	121.3	120.1	120.0	120.4	121.2	119.8	120.1	121.7	123.8	119.4	119.4	107.3	119.2
O2-C5-H1	55.6	85.0	107.2	112.8	96.6	131.8	143.9	153.7	166.0	157.1	143.3	140.1	142.3	129.7	119.7	112.2	97.9
C5-H1-C6	34.6	35.8	41.9	63.9	42.5	35.5	18.1	27.2	23.2	28.7	25.1	21.1	16.7	15.7	11.9	10.2	6.8
C6-H1-C7	13.1	14.8	20.8	34.8	40.6	69.3	40.6	33.8	17.3	29.2	26.7	21.9	15.9	17.1	14.6	13.5	11.7
C7-H1-C8	20.9	21.6	24.3	28.6	18.1	36.7	41.9	65.3	42.2	36.6	25.2	17.9	8.6	11.6	9.4	9.2	9.1
C8-H1-C9	21.0	21.0	22.9	28.3	23.1	28.9	17.6	33.8	40.8	69.4	45.2	36.1	27.9	18.9	11.0	7.1	2.3
C9-H1-C10	11.5	11.9	12.1	9.2	3.8	8.3	11.4	18.5	28.6	37.0	44.5	67.7	41.6	38.0	20.2	19.1	15.9
C10-H1-C11	15.9	16.1	16.3	15.6	11.8	12.1	8.4	10.4	7.2	17.1	22.7	35.8	41.6	66.2	41.9	20.2	2.0
C11-H1-C1	16.0	16.5	17.5	17.9	14.4	16.3	14.4	16.7	15.6	22.0	25.9	28.2	16.3	34.2	44.3	56.8	36.1
C1-H1-O1	11.9	11.4	10.0	7.4	5.5	3.9	2.1	2.3	2.8	3.7	5.9	7.1	9.3	15.7	25.2	49.0	42.4
C1-O1-H1	44.5	41.7	36.4	27.7	25.9	16.7	10.3	9.3	11.1	11.7	16.6	17.2	25.3	31.2	47.1	74.3	109.4
C5-C4-C9-C2	176.9	173.3	179.7	177.9	179.5	178.8	179.6	180.0	179.6	178.3	177.8	179.0	179.7	179.5	179.1	176.8	179.6
N-O2-C5-C4	15.3	44.1	57.7	35.0	0.3	16.2	19.2	3.7	0.0	8.1	5.9	3.0	7.3	4.3	7.2	9.8	3.9
C2-C3-N-O2	56.0	34.0	5.4	4.9	1.0	1.6	1.4	0.5	1.0	1.2	3.5	0.7	0.3	0.3	1.3	1.7	0.4
C5-C4-C9-C8	5.9	3.7	7.1	0.9	0.6	2.1	3.2	0.4	0.6	1.6	24.8	4.6	1.5	0.2	0.2	0.0	0.7
C4-C9-C8-C7	2.7	0.0	2.7	1.2	0.1	1.1	0.0	1.4	0.2	1.2	21.9	3.8	0.7	0.0	0.5	0.3	0.3
C2-C4-C9-C10	6.7	9.6	3.8	1.7	0.4	1.5	3.1	0.6	0.4	3.9	19.4	0.4	3.0	0.8	1.5	7.2	0.7
C4-C9-C10-C11	8.0	1.4	2.9	0.3	0.1	0.7	0.3	0.9	0.1	1.1	12.8	3.0	6.1	4.4	0.5	3.1	0.4
C10-C11-C1-C2	16.3	1.3	2.7	0.9	0.2	1.2	1.5	1.0	0.1	0.4	5.6	3.2	15.0	2.3	15.8	19.7	0.4
R = Ph	**$4E_1$**	**ts_{4E1-11}**	**11**	**ts_{11-18}**	**18**	**ts_{18-19}**	**19**	**ts_{19-20}**	**20**	**ts_{20-21}**	**21**	**ts_{21-22}**	**22**	**ts_{22-23}**	**23**	**ts_{23-12}**	**12**
C5-O2	2.655	1.922	1.438	1.339	1.301	1.338	1.373	1.334	1.301	1.340	1.367	1.363	1.361	1.365	1.369	1.373	1.372
O2-N	1.208	1.260	1.404	1.476	1.449	1.462	1.421	1.452	1.448	1.458	1.418	1.412	1.387	1.412	1.414	1.414	1.408
N-C3	1.421	1.333	1.298	1.298	1.314	1.295	1.291	1.296	1.315	1.295	1.292	1.295	1.306	1.296	1.293	1.292	1.292
C2-C3	1.393	1.449	1.476	1.461	1.432	1.459	1.473	1.458	1.431	1.461	1.473	1.468	1.454	1.464	1.465	1.461	1.470
C3-R	1.471	1.478	1.487	1.492	1.494	1.494	1.491	1.494	1.494	1.492	1.491	1.491	1.489	1.493	1.491	1.489	1.495
C2-C4	1.454	1.393	1.361	1.388	1.433	1.402	1.368	1.397	1.433	1.400	1.367	1.390	1.419	1.413	1.381	1.417	1.427
C4-C5	1.406	1.440	1.499	1.439	1.395	1.414	1.445	1.432	1.409	1.416	1.432	1.429	1.410	1.422	1.435	1.418	1.410
C2-C1	1.512	1.501	1.488	1.468	1.468	1.461	1.483	1.469	1.468	1.460	1.484	1.479	1.473	1.456	1.474	1.407	1.390
C1-O1	1.222	1.224	1.225	1.233	1.237	1.236	1.225	1.235	1.238	1.235	1.223	1.235	1.245	1.239	1.218	1.290	1.364
C5-C6	1.394	1.434	1.494	1.445	1.495	1.402	1.346	1.388	1.444	1.396	1.364	1.370	1.389	1.377	1.363	1.374	1.379
C6-C7	1.392	1.367	1.345	1.407	1.499	1.485	1.495	1.410	1.344	1.396	1.444	1.422	1.391	1.411	1.435	1.419	1.409
C7-C8	1.394	1.424	1.448	1.391	1.343	1.399	1.489	1.445	1.489	1.396	1.346	1.367	1.399	1.377	1.356	1.367	1.378
C8-C9	1.396	1.377	1.368	1.403	1.447	1.397	1.355	1.415	1.502	1.488	1.506	1.435	1.388	1.413	1.449	1.431	1.417
C4-C9	1.424	1.439	1.444	1.432	1.417	1.446	1.459	1.432	1.403	1.446	1.506	1.447	1.418	1.430	1.469	1.447	1.423
C9-C10	1.451	1.447	1.446	1.432	1.410	1.430	1.451	1.423	1.408	1.438	1.498	1.475	1.496	1.427	1.360	1.397	1.419
C10-C11	1.346	1.347	1.348	1.358	1.373	1.357	1.345	1.360	1.373	1.355	1.337	1.391	1.481	1.447	1.486	1.412	1.371
C11-C1	1.471	1.474	1.477	1.473	1.461	1.471	1.477	1.467	1.460	1.475	1.482	1.448	1.418	1.465	1.523	1.462	1.417
H1-C5	1.080	1.085	1.108	1.321	2.116	2.234	3.224	2.947	3.649	2.837	2.910	3.375	4.478	4.124	5.180	5.039	5.584
H1-C6	2.142	2.165	2.125	1.401	1.098	1.318	2.145	2.309	3.202	2.824	3.228	3.800	4.834	4.765	5.987	6.004	6.759
H1-C7	3.388	3.341	3.109	2.307	2.156	1.296	1.102	1.341	2.108	2.207	2.893	3.345	4.129	4.409	5.710	5.931	6.925

H1-C8	3.862	3.818	3.528	2.880	3.227	2.205	2.117	1.334	1.101	1.308	2.066	2.268	2.783	3.263	4.558	4.885	6.005
H1-C9	3.408	3.394	3.199	2.874	3.690	2.842	3.239	2.310	2.152	1.311	1.114	1.348	2.134	2.186	3.309	3.556	4.604
H1-C10	4.623	4.591	4.414	4.198	5.066	4.164	4.481	3.392	2.832	2.261	2.075	1.294	1.102	1.247	2.152	2.612	3.781
H1-C11	4.906	4.868	4.784	4.813	5.853	5.092	5.619	4.532	4.128	3.358	3.001	2.200	2.114	1.399	1.094	1.372	2.414
H1-C1	4.162	4.162	4.215	4.526	5.678	5.179	5.945	4.981	4.914	3.909	3.427	2.894	3.273	2.373	2.140	1.652	1.916
H1-O1	4.980	5.024	5.150	5.591	6.737	6.308	7.118	6.155	6.099	5.128	4.611	3.974	4.260	3.276	2.547	1.433	0.963
C5-O2-N	104.8	109.6	112.7	116.4	123.0	120.6	120.0	121.8	123.2	120.6	120.9	120.5	121.1	120.5	121.0	121.7	120.5
O2-N-C3	124.8	125.9	117.3	114.6	115.1	115.9	117.5	116.2	115.0	116.0	117.5	118.2	118.9	118.1	117.6	118.3	118.9
N-C3-C2	120.5	116.1	121.5	124.8	125.2	125.2	123.3	124.8	125.5	124.7	123.3	123.7	123.5	124.2	123.7	123.9	124.1
C5-C4-C2	122.0	117.9	115.9	117.5	117.8	118.6	119.3	118.9	117.4	119.6	119.5	119.6	118.6	118.7	118.4	117.8	119.0
C5-C6-C7	120.2	120.0	120.7	119.6	114.1	119.1	121.0	119.1	119.5	120.7	120.2	119.4	118.4	119.7	119.9	120.0	119.2
C6-C7-C8	119.7	121.2	121.6	119.2	121.1	118.5	114.6	119.9	122.7	120.8	122.1	122.0	121.1	120.9	121.6	120.9	121.1
C7-C8-C9	120.9	121.0	122.1	123.0	122.4	121.5	123.4	120.4	115.2	119.5	119.6	119.3	120.6	119.8	120.5	120.4	120.1
C8-C9-C10	120.7	122.5	123.7	124.0	123.2	122.6	123.0	123.1	122.1	123.5	117.4	124.9	123.6	123.4	123.3	122.6	123.7
C9-C10-C11	122.0	121.2	120.7	121.0	121.7	121.2	121.1	120.9	121.7	120.2	122.3	121.3	116.3	120.2	122.1	119.4	120.8
C10-C11-C1	121.9	122.5	122.8	124.1	124.6	124.2	122.7	123.8	124.4	124.5	123.2	123.6	125.4	123.8	117.2	119.6	121.7
C11-C1-O1	120.7	120.5	120.8	121.0	121.5	120.4	120.7	120.9	121.3	120.2	120.7	122.6	124.8	120.1	120.6	107.4	119.8
O2-C5-H1	63.1	85.6	106.8	113.0	95.2	126.4	138.6	149.6	164.8	159.3	145.3	136.6	144.2	127.7	119.1	111.2	96.9
C5-H1-C6	34.5	35.8	41.8	64.1	42.1	36.0	17.6	27.3	23.2	28.6	25.0	21.0	16.6	15.8	11.3	10.2	6.8
C6-H1-C7	13.2	14.9	20.6	34.8	40.4	69.2	40.8	33.9	17.3	29.0	26.6	21.8	15.4	17.1	13.8	13.6	11.7
C7-H1-C8	20.9	21.7	24.2	28.5	17.7	36.6	41.8	65.4	42.2	36.6	25.1	17.6	6.5	11.6	8.0	9.4	9.1
C8-H1-C9	21.0	21.0	22.8	28.2	22.9	28.8	16.7	33.9	40.8	69.3	45.2	36.7	29.2	19.7	10.8	7.3	2.3
C9-H1-C10	11.5	11.8	12.0	9.0	4.1	9.1	11.3	19.0	28.9	36.6	44.4	67.8	41.4	38.0	15.4	19.5	15.9
C10-H1-C11	15.9	16.0	16.2	15.5	11.9	12.3	8.2	10.9	7.6	16.6	22.3	36.5	41.5	66.0	39.7	20.6	2.1
C11-H1-C1	16.1	16.5	17.5	17.8	14.5	16.4	14.3	16.9	15.7	21.8	25.6	29.2	17.9	34.9	42.4	56.9	35.9
C1-H1-O1	11.5	10.9	9.7	7.1	5.9	5.0	3.1	3.9	3.8	2.6	4.4	10.1	11.7	17.5	28.5	48.8	42.1
C1-O1-H1	42.5	40.1	35.6	26.9	28.4	21.5	15.2	16.1	15.0	8.2	12.3	24.3	32.1	35.2	56.9	74.5	109.6
C5-C4-C9-C2	177.1	172.5	178.2	176.4	177.3	177.5	179.5	177.1	177.4	176.4	178.9	179.0	178.5	179.6	178.5	176.1	178.4
N-O2-C5-C4	36.9	48.6	59.7	38.1	6.8	16.0	27.4	15.0	5.9	19.6	17.1	21.4	11.9	18.9	18.8	7.3	14.3
C2-C3-N-O2	48.0	33.6	5.9	7.0	0.8	3.4	2.9	2.4	0.9	4.5	5.3	0.5	0.4	1.3	3.1	3.0	1.0
C5-C4-C9-C8	4.1	2.3	5.7	2.0	1.3	2.7	5.1	3.4	2.0	0.4	22.9	6.6	1.0	2.4	2.3	2.9	2.4
C4-C9-C8-C7	1.9	0.7	3.3	0.5	0.6	1.9	0.6	2.1	1.7	0.4	21.2	4.1	0.4	0.5	0.2	1.1	0.8
C2-C4-C9-C10	3.8	9.1	4.0	1.5	0.1	1.5	3.7	1.0	0.2	4.1	20.2	1.6	3.6	2.2	0.3	4.0	2.3
C4-C9-C10-C11	6.5	4.0	4.9	1.8	2.2	1.9	1.3	1.7	1.9	0.8	11.0	1.7	8.7	0.1	0.3	4.1	1.4
C10-C11-C1-C2	14.1	5.3	7.5	4.9	6.7	6.2	5.9	6.7	6.1	4.1	0.4	12.8	20.5	10.9	21.8	21.2	1.2

Table 7S Bond distances (Å), angles and dihedral angles (degrees) of the structures (minima and transition states (ts)) of Fig. 6S.

R = H	**$4E_1$**	**4E2**	**ts_{4E2-13}**	**13**	**ts_{13-24}**	**24**	**ts_{24-14}**	**14**
C5-N	3.323	2.960	1.973	1.522	1.490	1.491	1.432	1.392
C5-O2	2.813	4.131	2.868	2.427	2.459	2.423	2.554	2.452
O2-N	1.216	1.224	1.225	1.257	1.273	1.370	1.505	1.382
N-C3	1.407	1.408	1.348	1.333	1.419	1.496	1.427	1.373
C3-C2	1.369	1.362	1.409	1.442	1.379	1.343	1.360	1.386
C3-R	1.084	1.087	1.083	1.078	1.078	1.078	1.078	1.078
C4-C2	1.463	1.469	1.390	1.362	1.409	1.450	1.438	1.419
C4-C5	1.405	1.404	1.441	1.477	1.402	1.375	1.385	1.399
C5-H1	1.078	1.080	1.088	1.103	1.394	2.060	2.214	2.872
O2-H1	2.126	3.338	2.708	2.697	2.187	1.983	1.366	0.968
H1-C5-N	56.2	43.3	81.2	100.7	53.9	28.6	25.1	34.2
C5-H1-N	105.6	117.9	68.1	47.2	66.8	43.5	33.5	24.5
O2-H1-N	22.5	13.3	25.8	26.4	31.7	40.4	74.4	44.7
N-O2-H1	115.5	25.6	48.3	46.1	32.7	29.3	44.7	105.7
N-C3-R	110.7	116.7	119.2	120.3	117.4	115.9	118.6	120.4
C5-O2-N-C3	29.4	138.6	142.6	172.0	162.8	117.9	140.1	167.6
C5-N-C3-R	177.6	172.7	171.6	175.6	179.8	176.8	176.2	177.5
C5-N-C3-C2	23.2	10.2	19.5	9.0	2.5	0.9	4.4	2.6
N-C3-C2-C4	16.2	3.8	10.2	2.7	1.6	1.2	2.8	1.5
C3-C2-C4-C5	31.2	18.0	10.7	5.1	0.1	1.1	0.2	0.0
R = Me	**$4E_1$**	**4E2**	**ts_{4E2-13}**	**13**	**ts_{13-24}**	**24**	**ts_{24-14}**	**14**
C5-N	3.217	2.797	3.045	1.510	1.489	1.487	1.431	1.394
C5-O2	2.674	3.843	3.049	2.428	2.463	2.415	2.551	2.449
O2-N	1.210	1.218	1.203	1.265	1.275	1.361	1.505	1.383
N-C3	1.426	1.442	1.460	1.337	1.428	1.529	1.441	1.382
C3-C2	1.382	1.376	1.358	1.450	1.388	1.350	1.368	1.393
C3-R	1.501	1.497	1.501	1.486	1.480	1.472	1.478	1.486
C4-C2	1.463	1.468	1.481	1.363	1.408	1.448	1.436	1.418
C4-C5	1.404	1.403	1.402	1.477	1.403	1.375	1.385	1.398
C5-H1	1.078	1.080	1.080	1.103	1.377	2.048	2.217	2.879
O2-H1	2.267	3.183	2.270	2.704	2.195	1.974	1.350	0.968
H1-C5-N	64.8	55.7	58.5	101.3	54.6	29.0	25.2	34.1
C5-H1-N	95.7	102.1	101.2	46.6	67.1	44.0	33.5	24.4
O2-H1-N	22.7	18.9	27.0	26.5	31.6	40.3	74.9	44.7
N-O2-H1	110.9	38.9	94.2	45.9	32.7	29.6	45.1	105.9
N-C3-R	109.5	118.3	107.5	120.8	118.4	116.6	119.7	122.3
C5-O2-N-C3	25.4	122.8	71.9	171.6	163.7	120.1	140.2	165.8
C5-N-C3-R	165.1	162.7	170.3	174.6	179.2	176.0	174.3	177.4
C5-N-C3-C2	32.0	22.5	19.9	8.8	2.4	1.2	5.0	3.0
N-C3-C2-C4	24.3	11.3	7.9	2.4	1.4	0.6	3.2	1.8
C3-C2-C4-C5	39.0	30.9	36.8	5.2	0.2	0.3	0.3	0.1
R = Et	**$4E_1$**	**4E2**	**ts_{4E2-13}**	**13**	**ts_{13-24}**	**24**	**ts_{24-14}**	**14**
C5-N	3.217	2.773	3.060	1.510	1.489	1.487	1.431	1.394
C5-O2	2.688	3.802	3.031	2.423	2.460	2.418	2.549	2.445
O2-N	1.210	1.218	1.205	1.266	1.276	1.360	1.504	1.383
N-C3	1.428	1.444	1.455	1.338	1.430	1.530	1.443	1.383
C3-C2	1.381	1.375	1.359	1.452	1.388	1.350	1.369	1.394
C3-R	1.507	1.502	1.509	1.491	1.485	1.476	1.483	1.491
C4-C2	1.467	1.467	1.481	1.363	1.408	1.448	1.436	1.417
C4-C5	1.404	1.403	1.402	1.477	1.403	1.375	1.385	1.398
C5-H1	1.078	1.080	1.080	1.103	1.376	2.043	2.214	2.880
O2-H1	2.261	3.164	2.257	2.699	2.196	1.973	1.349	0.968
H1-C5-N	65.4	57.4	58.6	101.2	54.6	29.1	25.3	34.0
C5-H1-N	95.1	100.1	101.1	46.7	67.1	44.2	33.6	24.3
O2-H1-N	22.5	19.4	26.8	26.6	31.6	40.4	74.9	44.7
N-O2-H1	112.0	40.4	95.8	46.1	32.7	29.6	45.2	105.8
N-C3-R	109.4	117.1	107.3	121.3	118.6	116.8	120.0	122.6
C5-O2-N-C3	30.5	118.9	70.2	172.1	163.4	120.5	140.4	165.5
C5-N-C3-R	164.6	161.5	169.7	174.2	179.9	175.3	174.6	178.1
C5-N-C3-C2	30.8	25.2	20.4	8.4	2.2	1.8	5.2	3.2
N-C3-C2-C4	22.0	14.2	8.5	2.1	1.2	1.0	3.4	2.0
C3-C2-C4-C5	40.9	30.8	37.1	5.3	0.4	0.2	0.4	0.2
R = Ph	**$4E_1$**	**4E2**	**ts_{4E2-13}**	**13**	**ts_{13-24}**	**24**	**ts_{24-14}**	**14**
C5-N	3.185	2.788	3.010	1.499	1.479	1.473	1.423	1.386
C5-O2	2.655	3.806	3.086	2.394	2.426	2.368	2.501	2.423
O2-N	1.208	1.214	1.201	1.265	1.276	1.369	1.503	1.381
N-C3	1.421	1.453	1.480	1.349	1.443	1.539	1.456	1.390

C3-C2	1.393	1.379	1.358	1.471	1.407	1.375	1.388	1.408
C3-R	1.471	1.475	1.478	1.465	1.461	1.448	1.460	1.466
C4-C2	1.454	1.464	1.479	1.364	1.409	1.451	1.437	1.419
C4-C5	1.406	1.403	1.402	1.474	1.402	1.374	1.383	1.397
C5-H1	1.080	1.081	1.080	1.104	1.369	2.051	2.201	2.870
O2-H1	2.370	3.199	2.334	2.683	2.179	1.984	1.339	0.969
H1-C5-N	64.5	59.1	60.0	101.6	54.8	28.6	25.9	34.3
C5-H1-N	95.8	98.3	99.3	46.3	66.8	43.0	34.0	24.4
O2-H1-N	24.0	19.3	27.0	26.9	32.2	40.3	75.0	44.5
N-O2-H1	102.8	41.1	90.8	46.5	33.3	29.3	45.6	106.0
N-C3-R	110.2	118.3	107.5	122.0	119.7	115.7	120.8	122.1
C5-O2-N-C3	10.1	116.3	74.3	171.2	164.7	119.5	143.5	178.9
C5-N-C3-R	156.8	157.7	168.7	171.4	177.6	174.8	177.2	178.6
C5-N-C3-C2	39.5	27.8	22.0	10.1	2.6	2.8	5.6	0.8
N-C3-C2-C4	35.1	16.5	9.5	3.0	1.3	2.0	4.2	1.0
C3-C2-C4-C5	35.0	32.8	38.5	5.5	0.6	0.3	1.4	0.9

$3E_1$

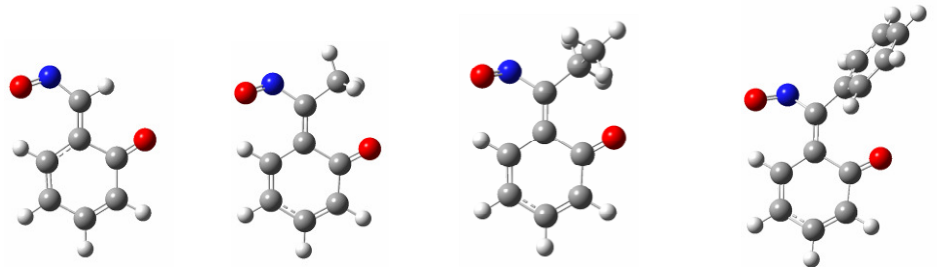

$ts_{3E1\text{-}3E2}$

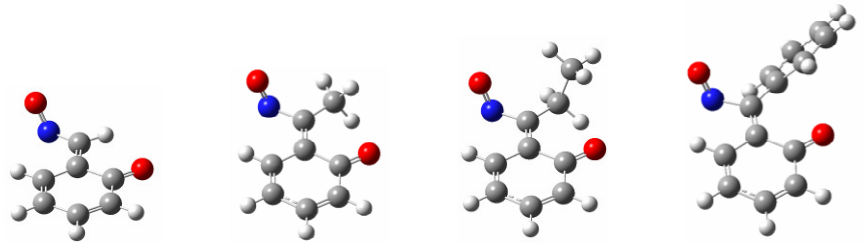

$3E_2$

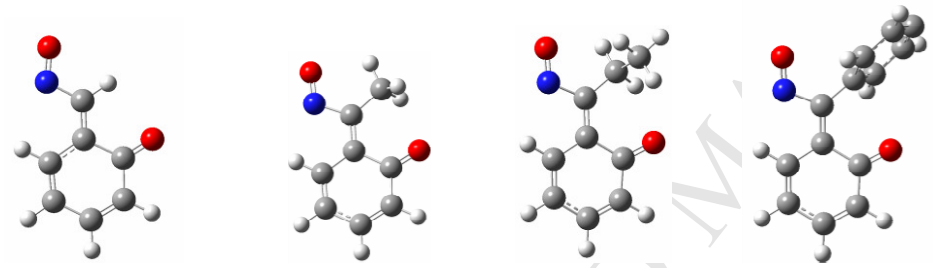

$ts_{3E2\text{-}3Z}$

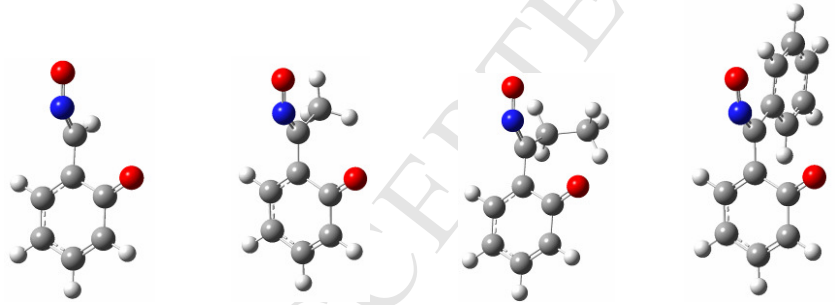

3Z

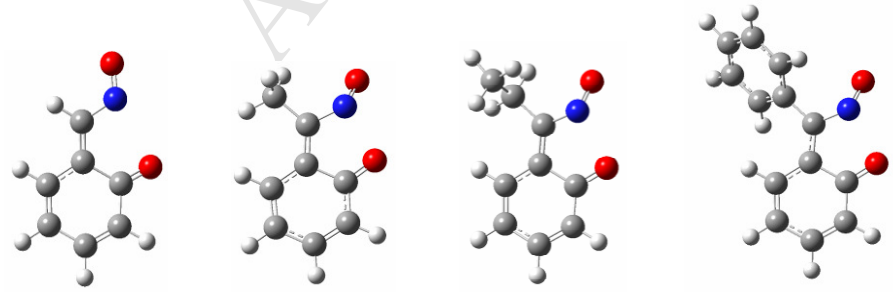

$ts_{3Z\text{-}9}$

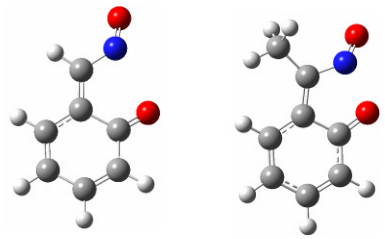

9

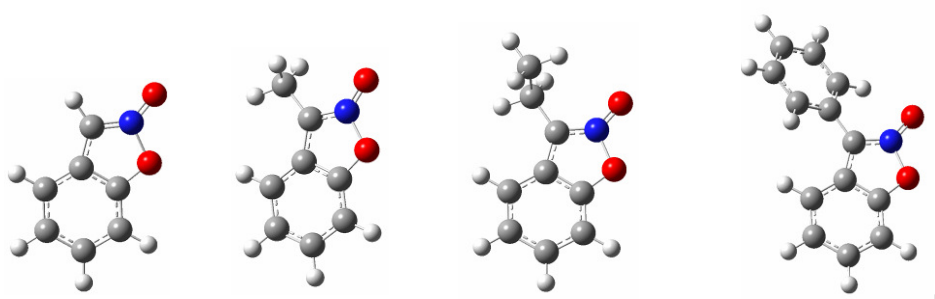

$4E_1$

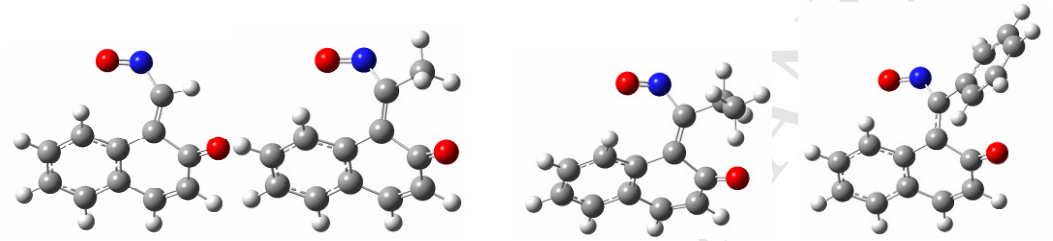

$ts_{4E1\text{-}4E2}$

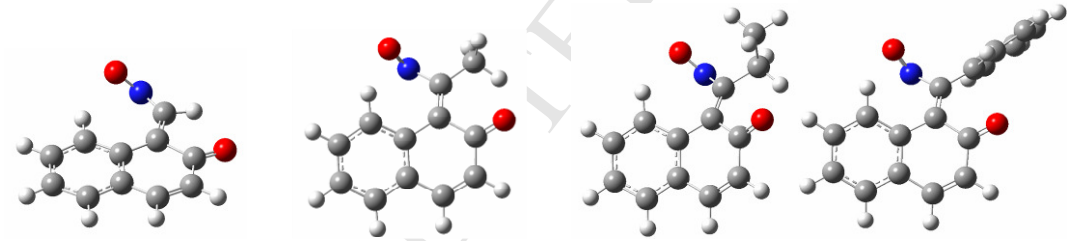

$4E_2$

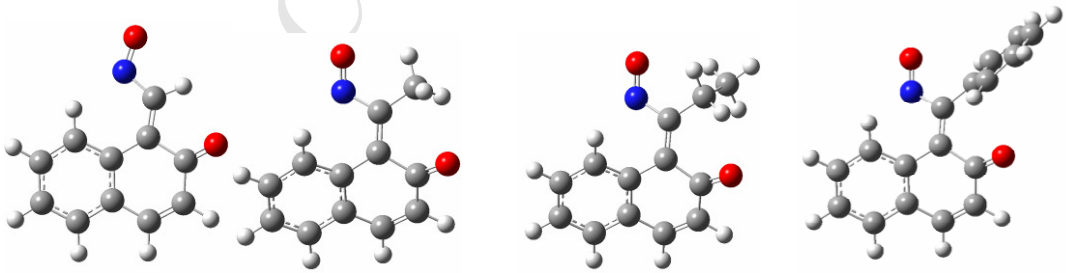

$ts_{4Z\text{-}10}$

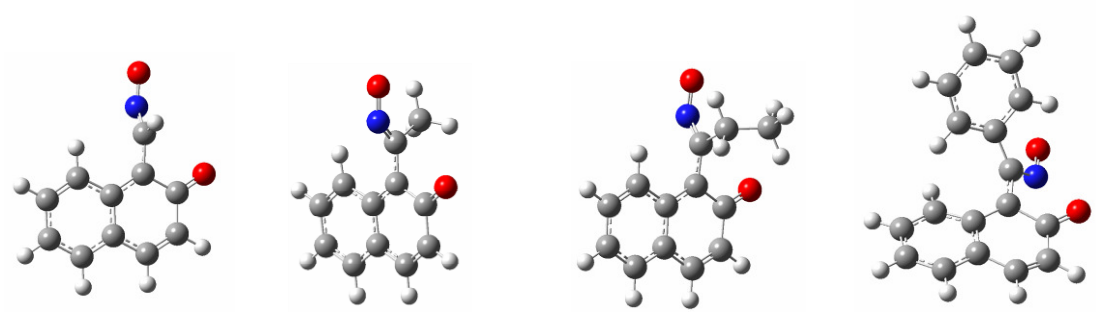

4Z

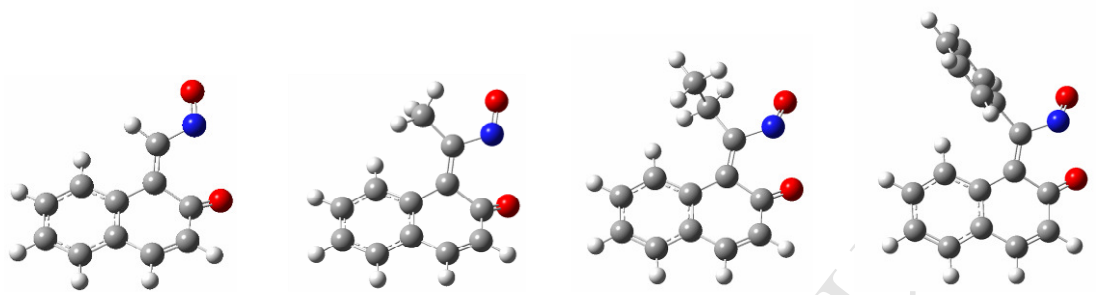

$ts_{4Z\text{-}10}$

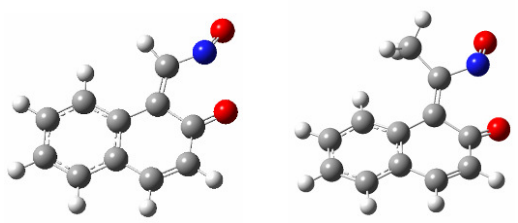

10

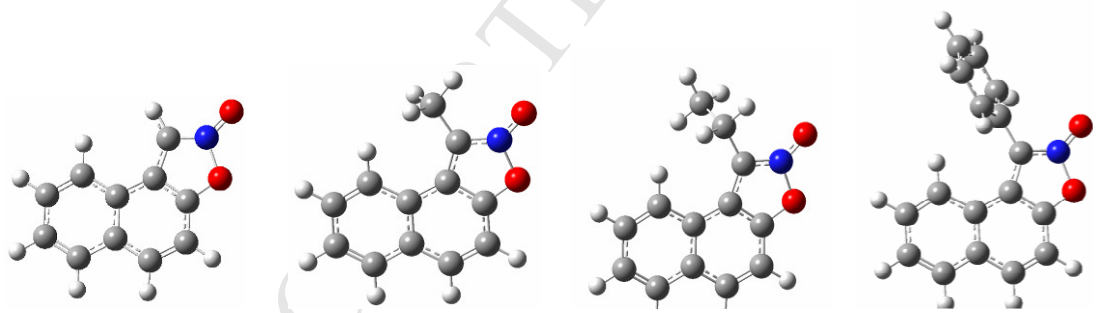

$ts_{4E1\text{-}11}$

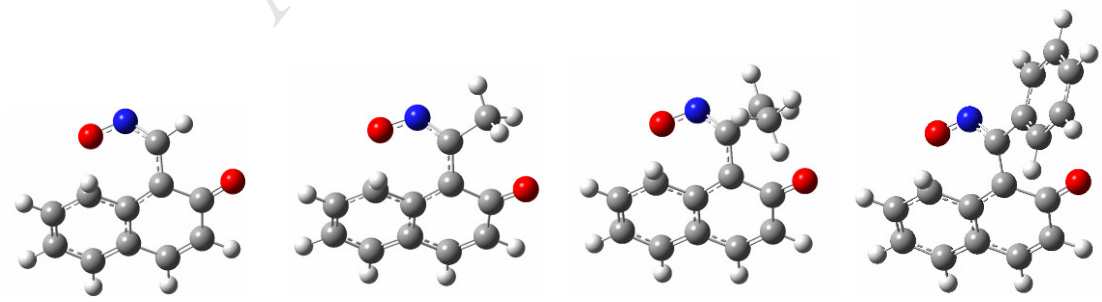

11

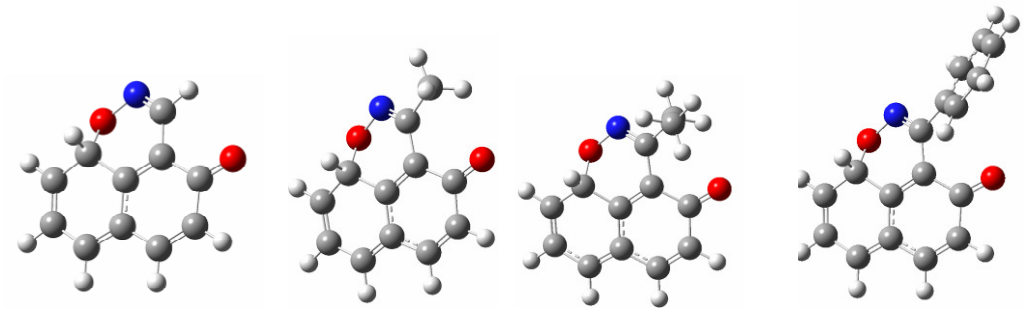

$ts_{11\text{-}16}$

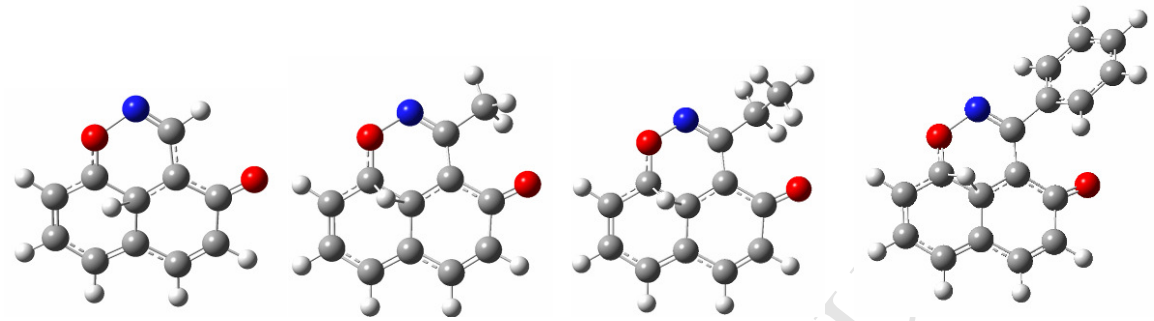

16

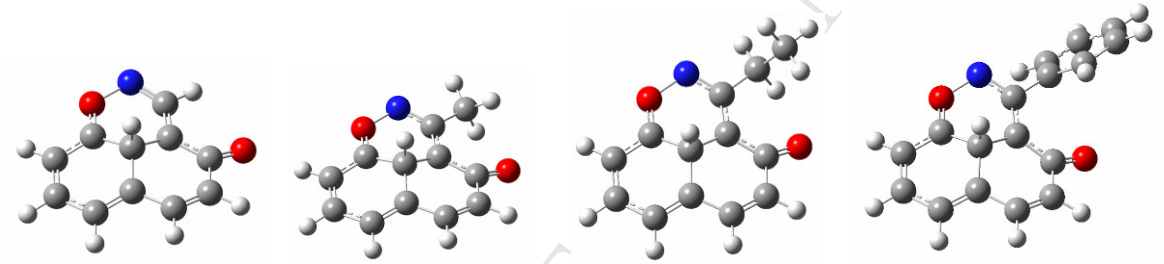

$ts_{16\text{-}17}$

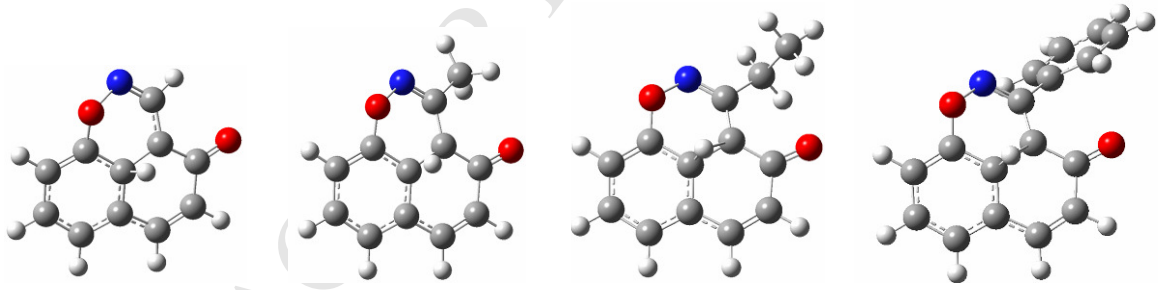

17

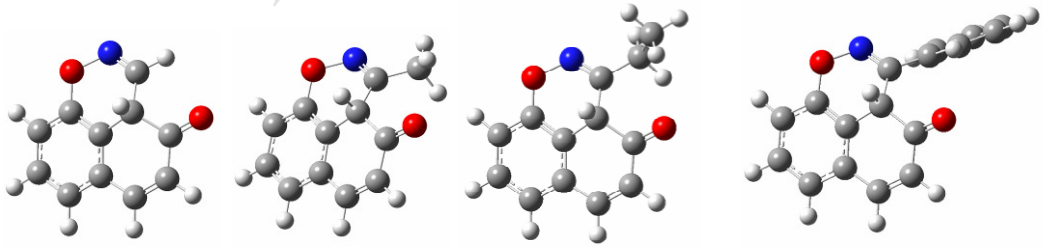

$ts_{17\text{-}12}$

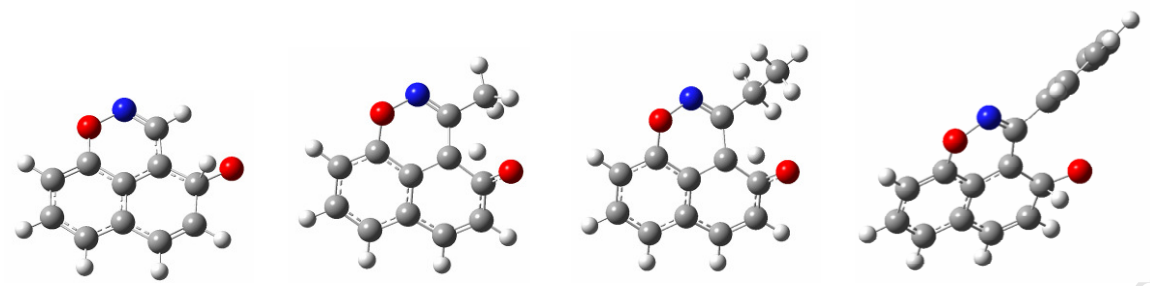

12

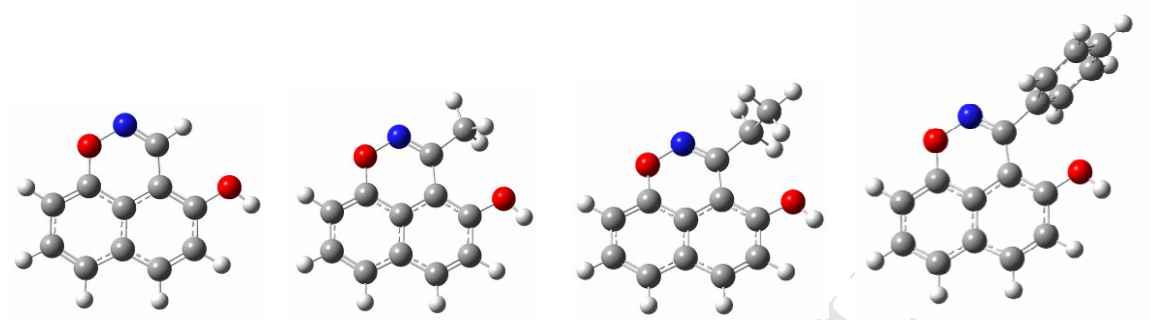

$ts_{11\text{-}18}$

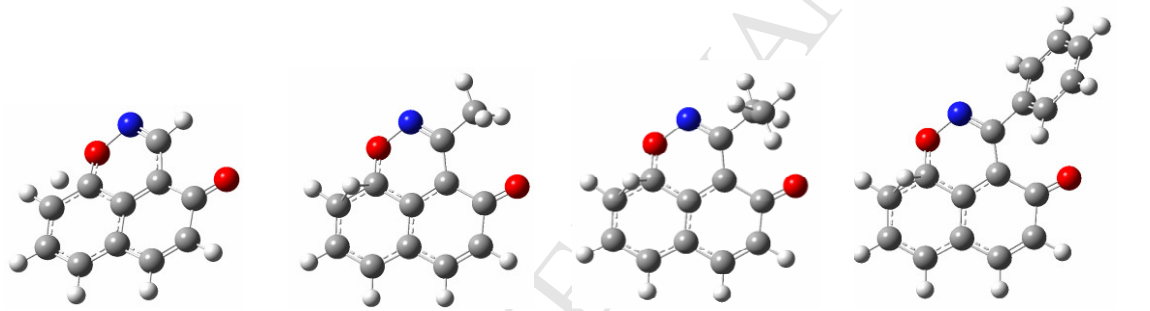

18

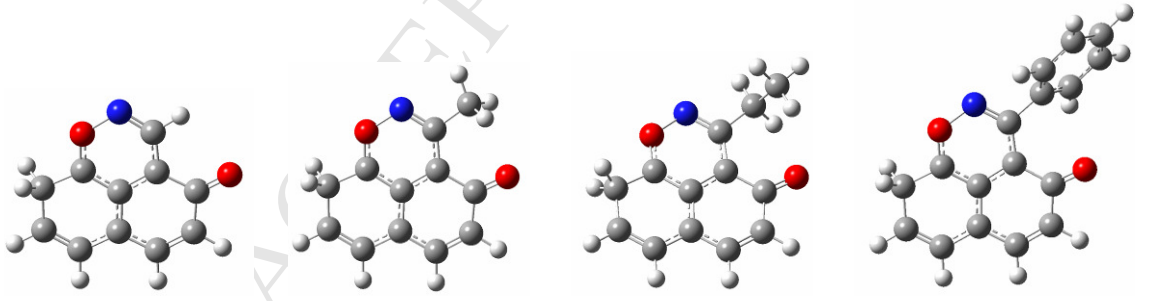

$ts_{18\text{-}19}$

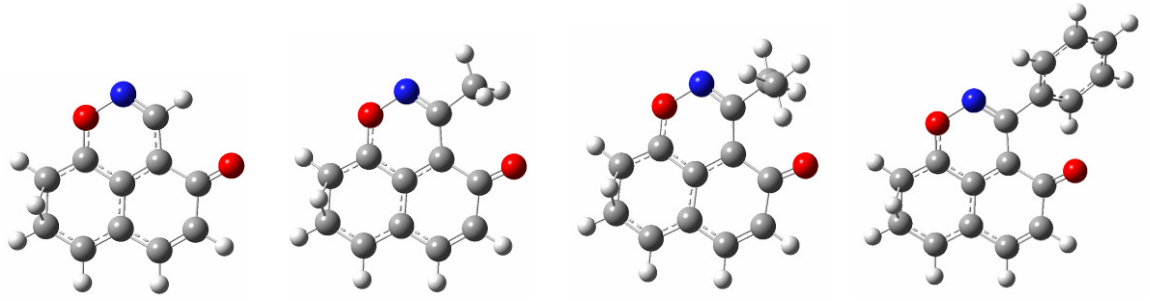

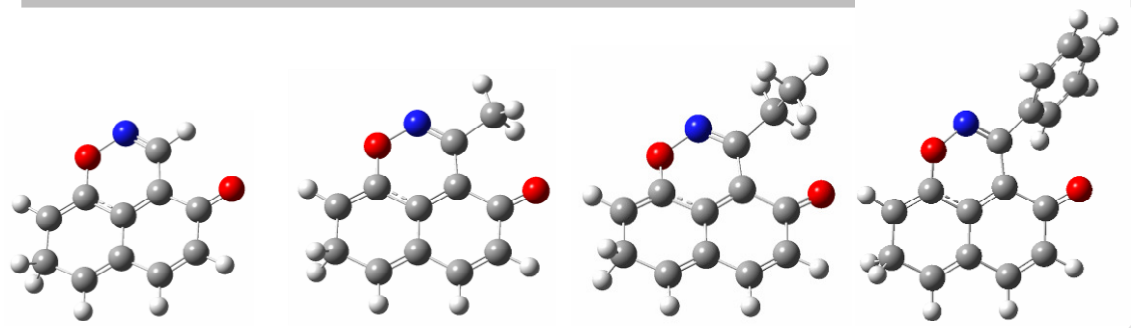

$ts_{19\text{-}20}$

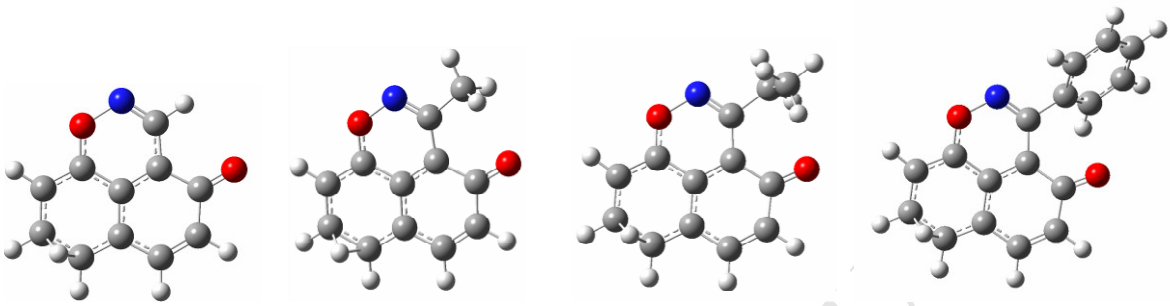

20

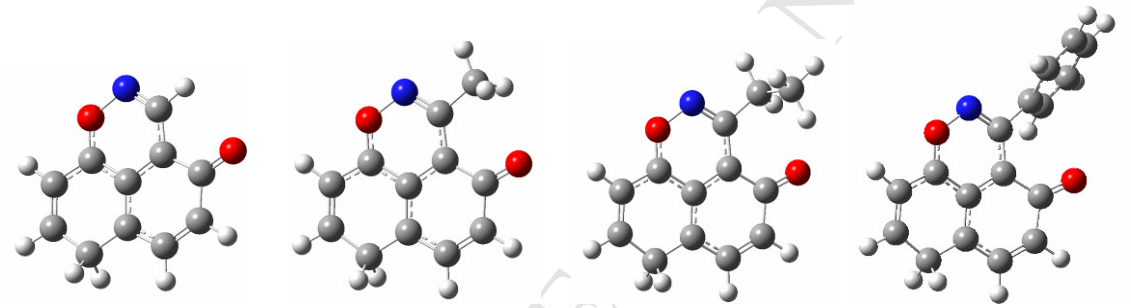

$ts_{20\text{-}21}$

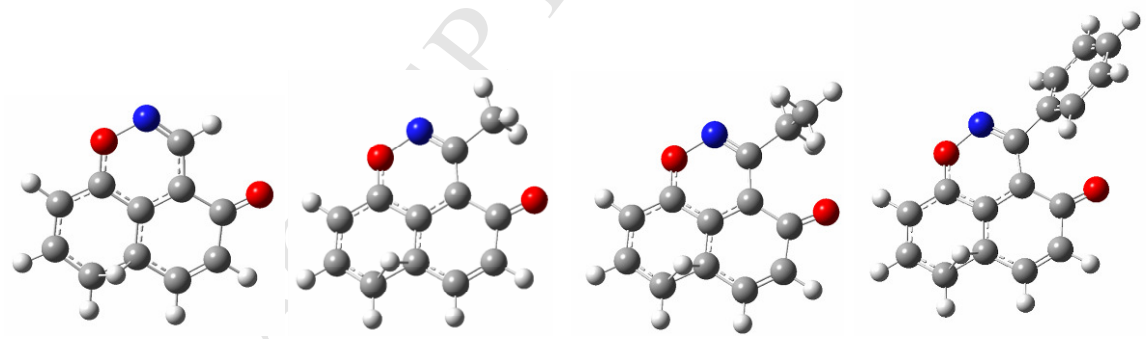

21

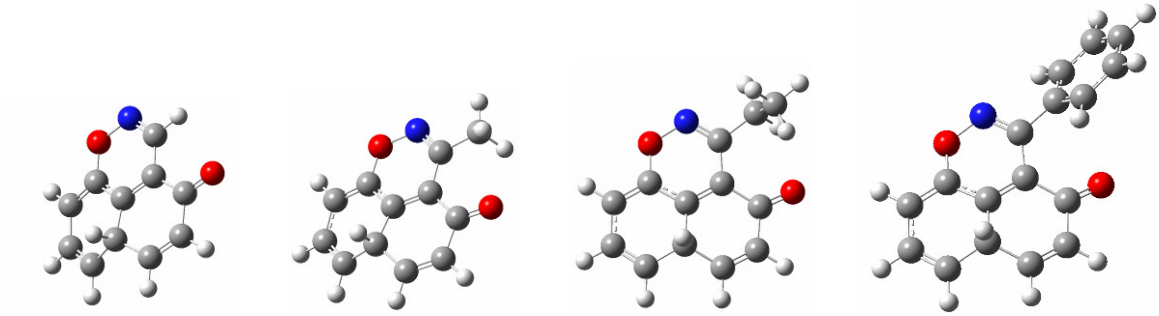

$ts_{21\text{-}22}$

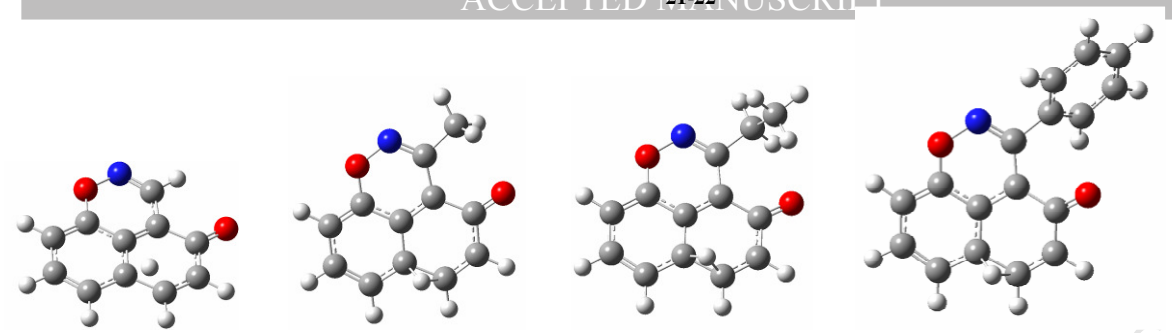

22

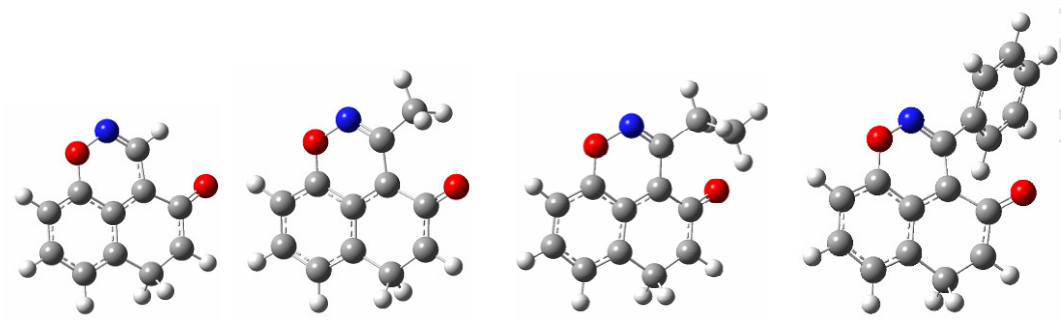

$ts_{22\text{-}23}$

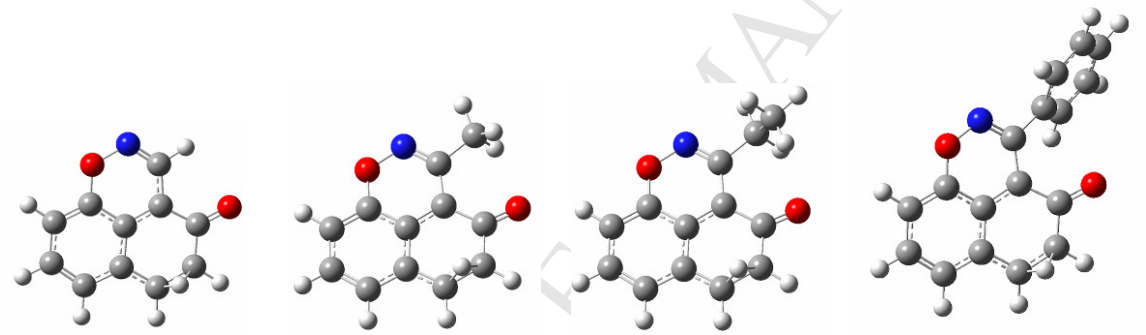

23

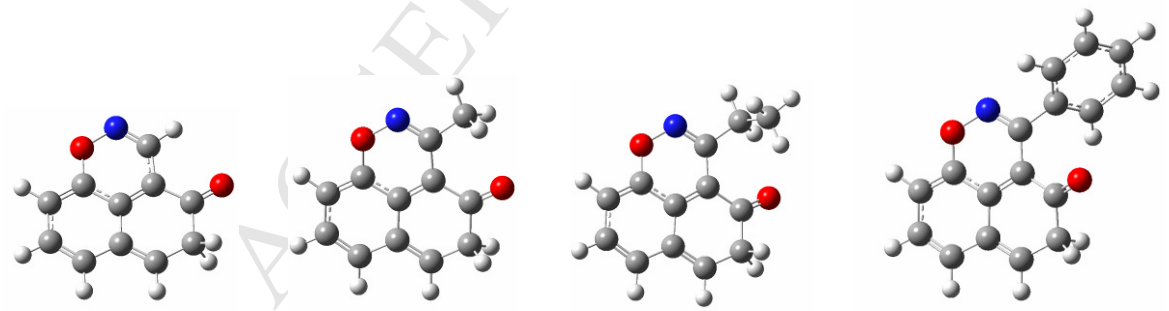

$ts_{23\text{-}12}$

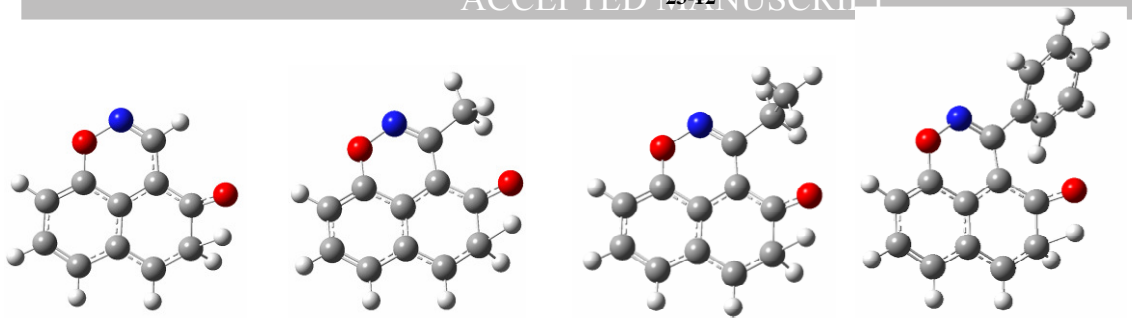

$ts_{4E1\text{-}13}$

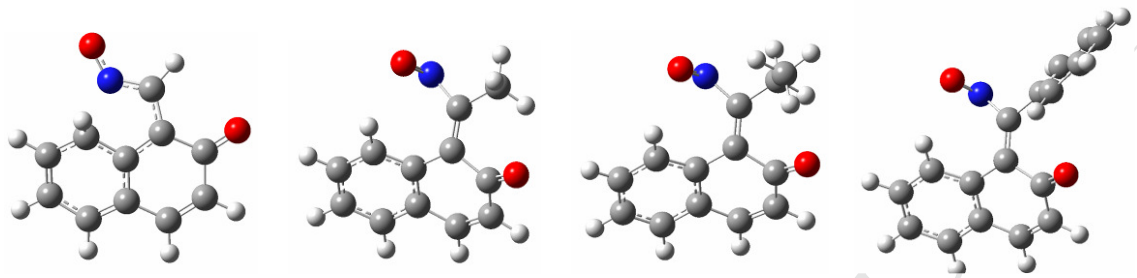

13

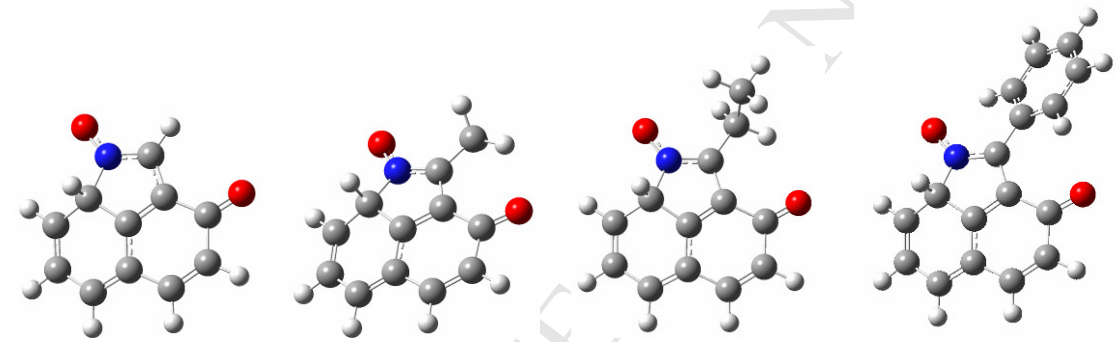

$ts_{13\text{-}24}$

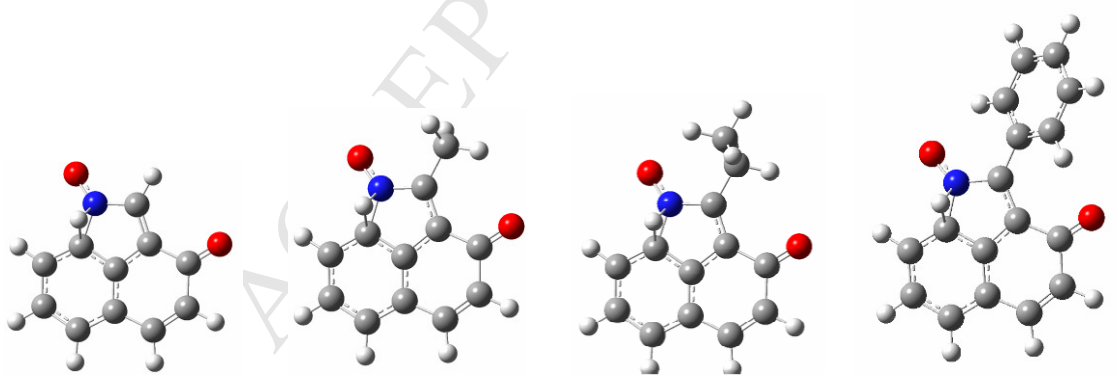

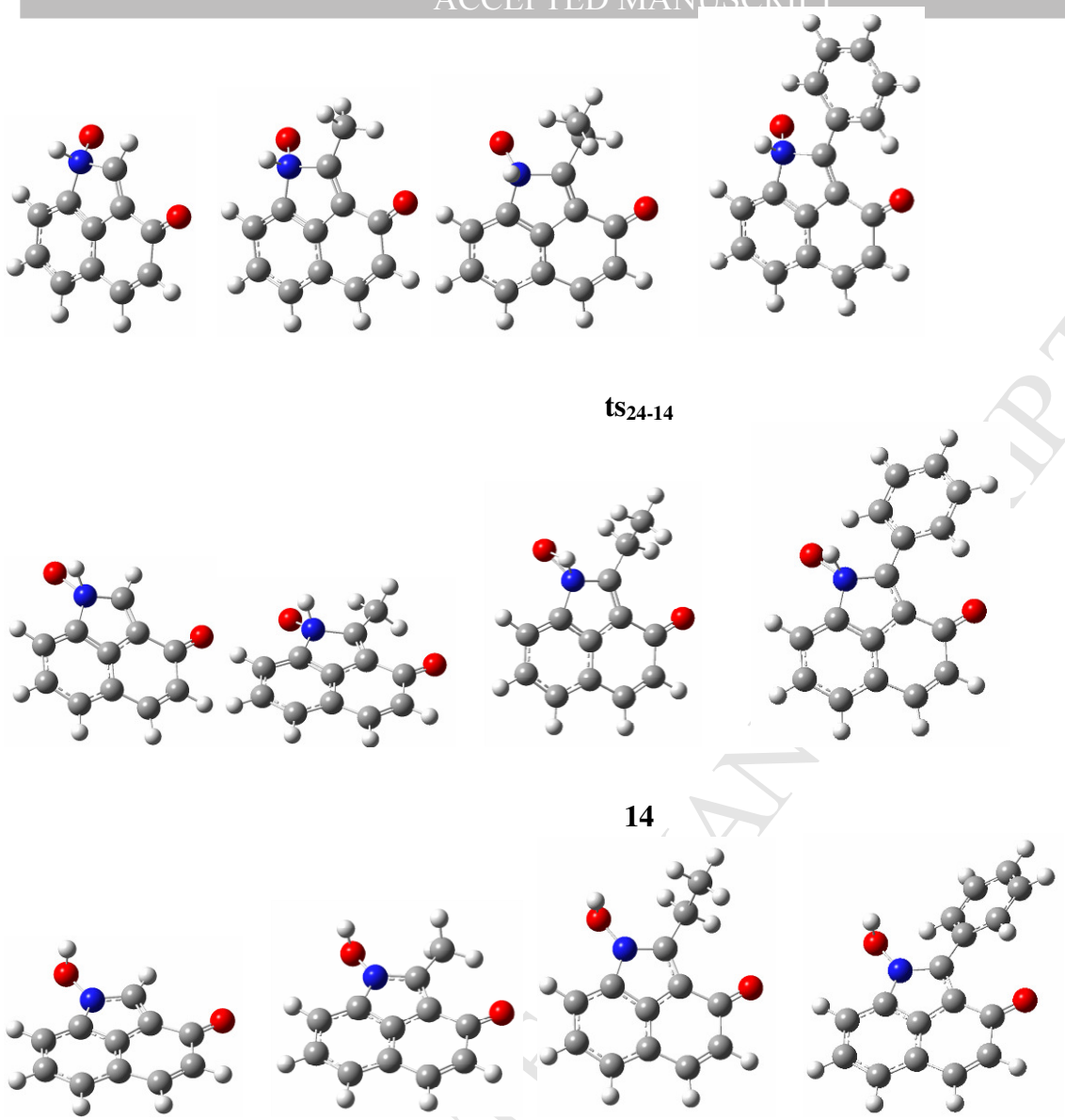

Fig.1S Minima and transitions structures involved in the o- and peri-cyclization modes of the *β*-nitroso-o-quinone methides **3** and **4.**

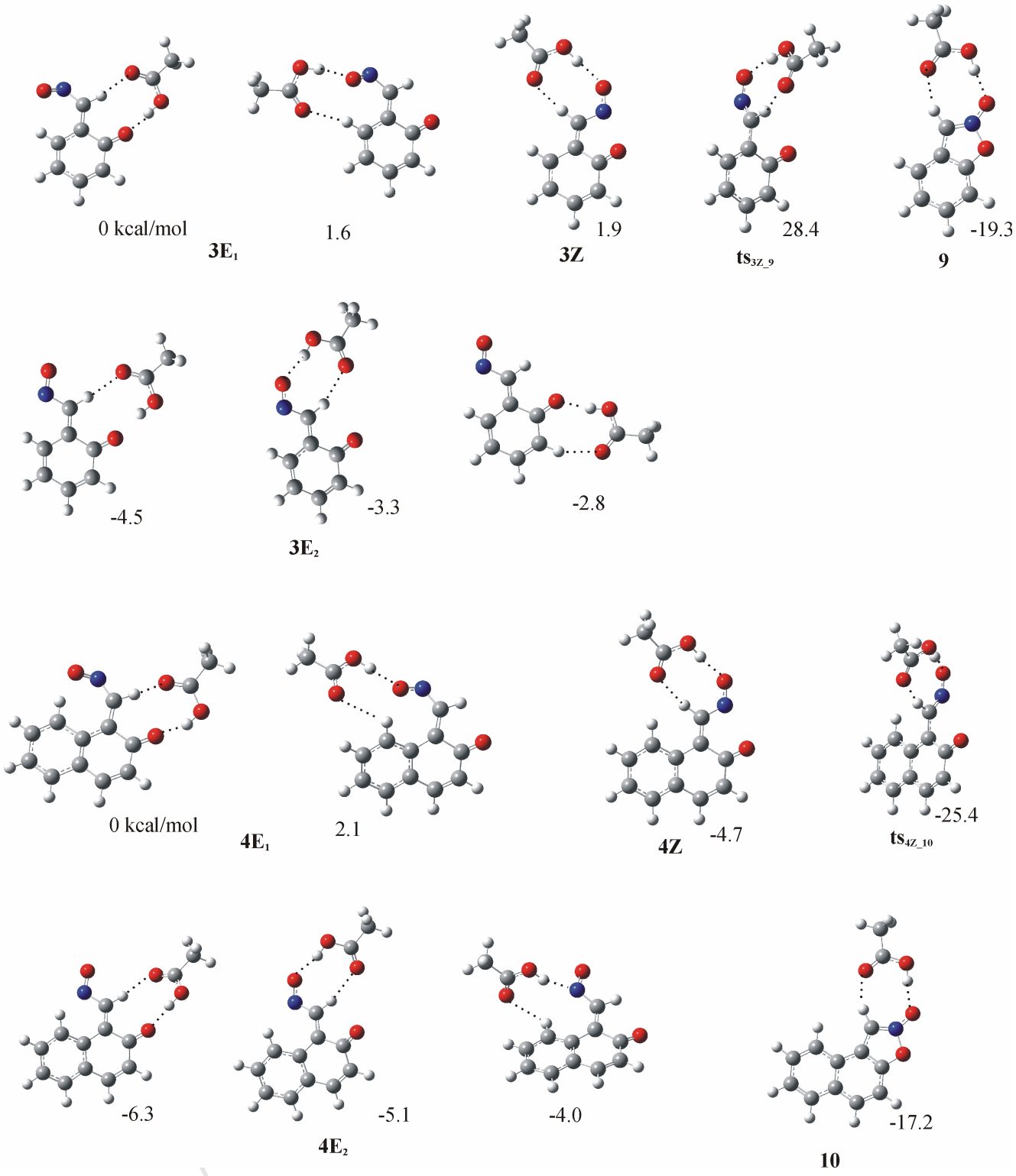

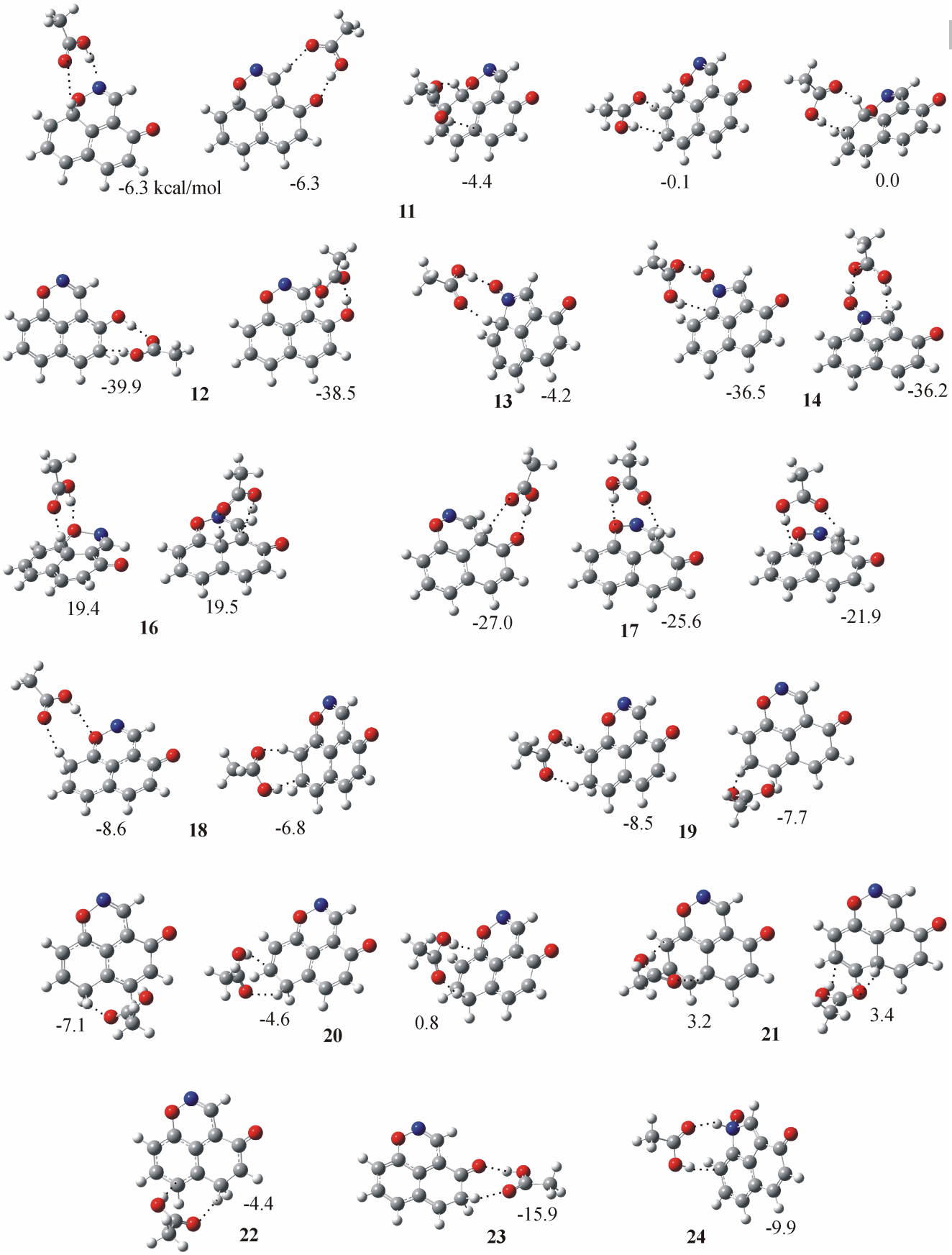
-6.3 kcal/mol
-6.3
-4.4
-0.1
0.0
11
-39.9
12
-38.5
13
-4.2
-36.5
14
-36.2
19.4
19.5
16
-27.0
17
-25.6
-21.9
-8.6
18
-6.8
-8.5
19
-7.7
-7.1
-4.6
20
0.8
3.2
21
3.4
-4.4
22
-15.9
23
-9.9
24

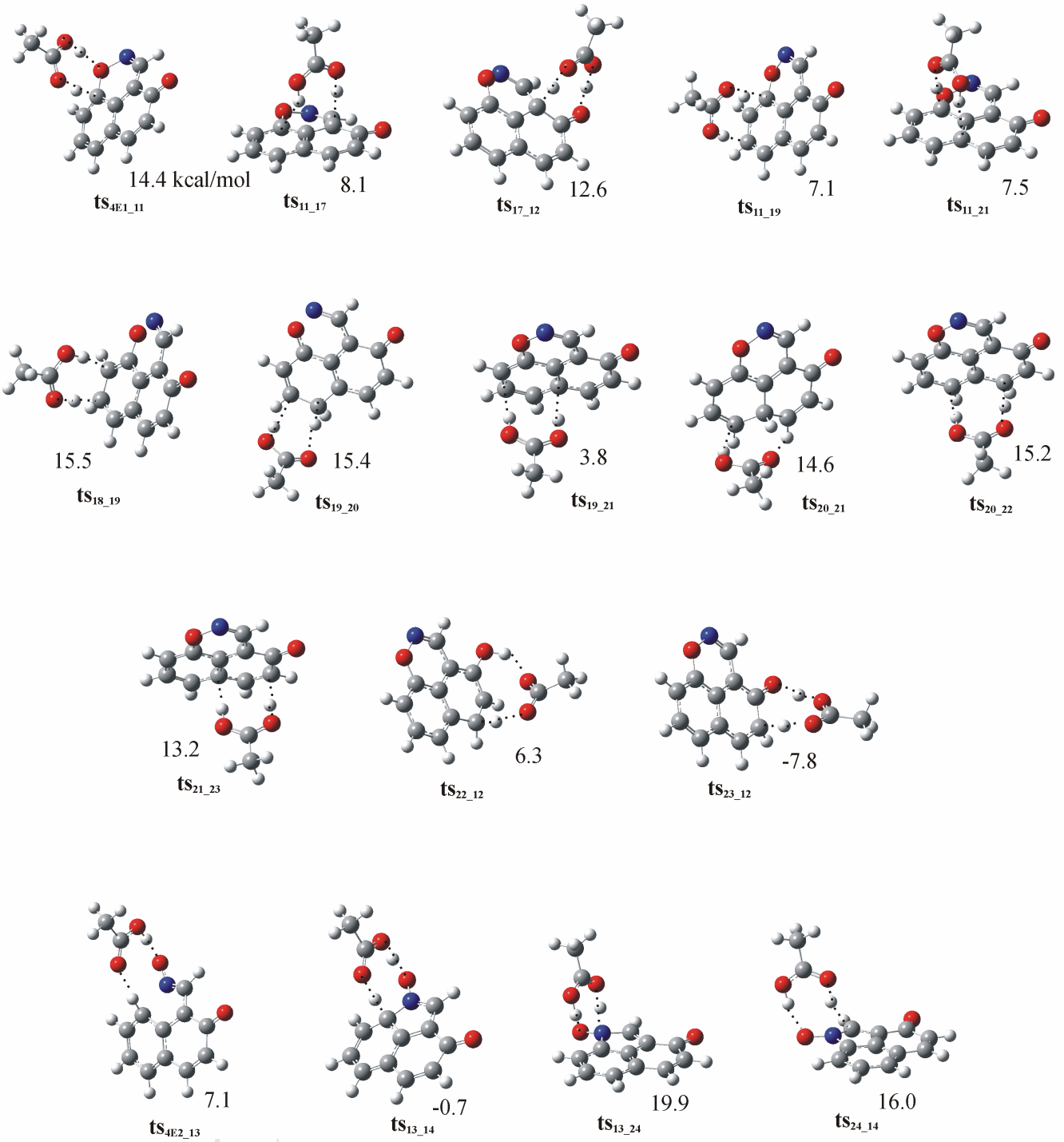

Fig.2S Minima and transitions structures the involved in the o- and peri-cyclization modes of the *β*-nitroso-o-quinone methides **3** and **4** interacting with a AcOH molecule; relative energies in kcal/mol with respect to the $\mathbf{3E_1}$ and $\mathbf{4E_2}$ minimum structures, respectively.

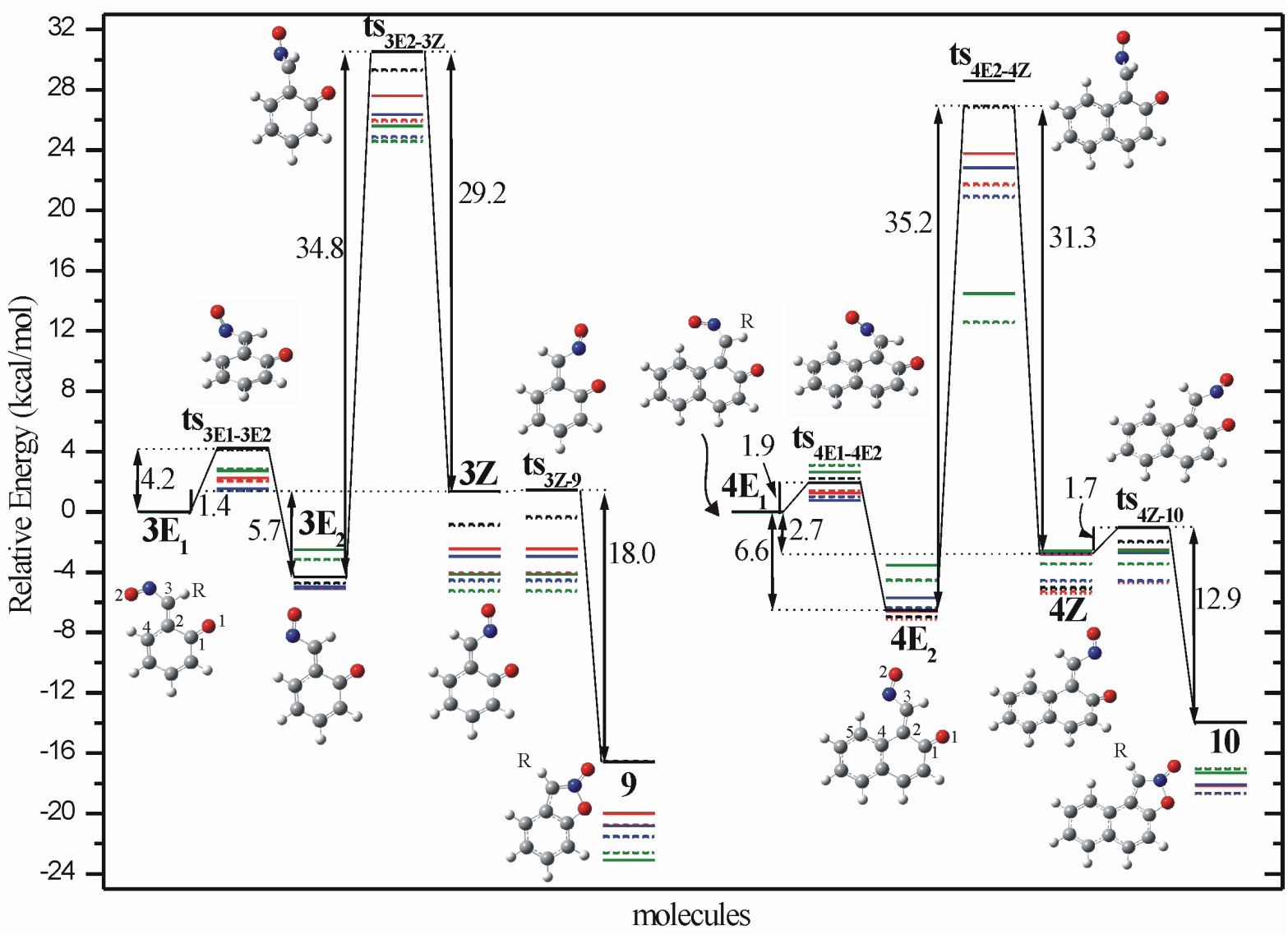

Fig 3S Relative electronic energy levels of the o-(1,5)-cyclization of **3** and **4** minima to **9** and **10** in the gas phase (solid line), in THF solvent (dashed line) and in CH_2Cl_2 solvent (dotted line). R = H (black lines), Me (red), Et (blue), and Ph (green). (C atoms = gray spheres, H = white, O = red, and N = blue).

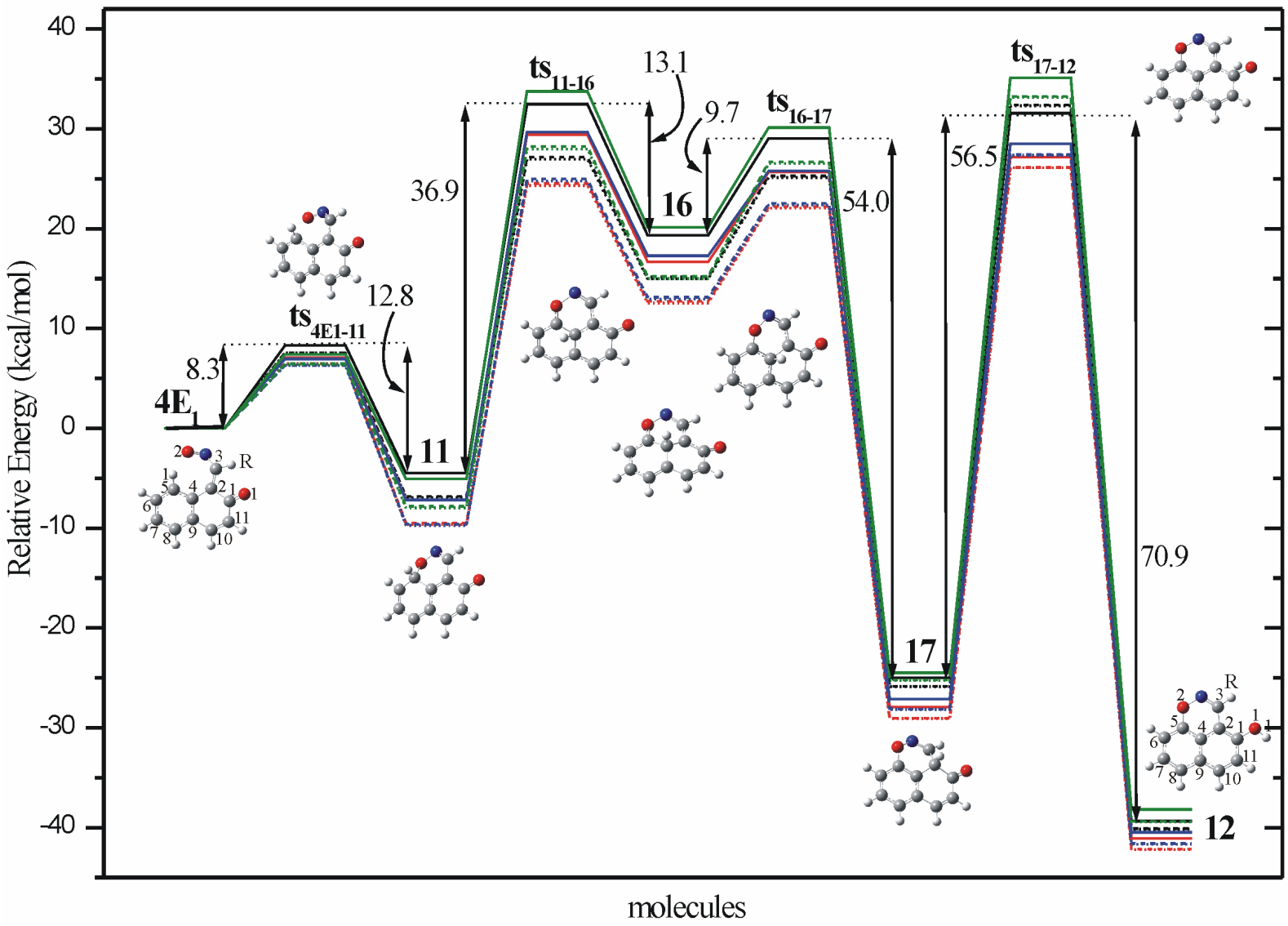

Fig 4S Relative electronic energy levels of the peri-(1,6)-electrocyclization of **4** minimum to **12** in the gas phase (solid line), in THF solvent (dashed line) and in CH_2Cl_2 solvent (dotted line) via first route. R = H (black lines), Me (red), Et (blue), and Ph (green). (C atoms = gray spheres, H = white, O = red, and N = blue).

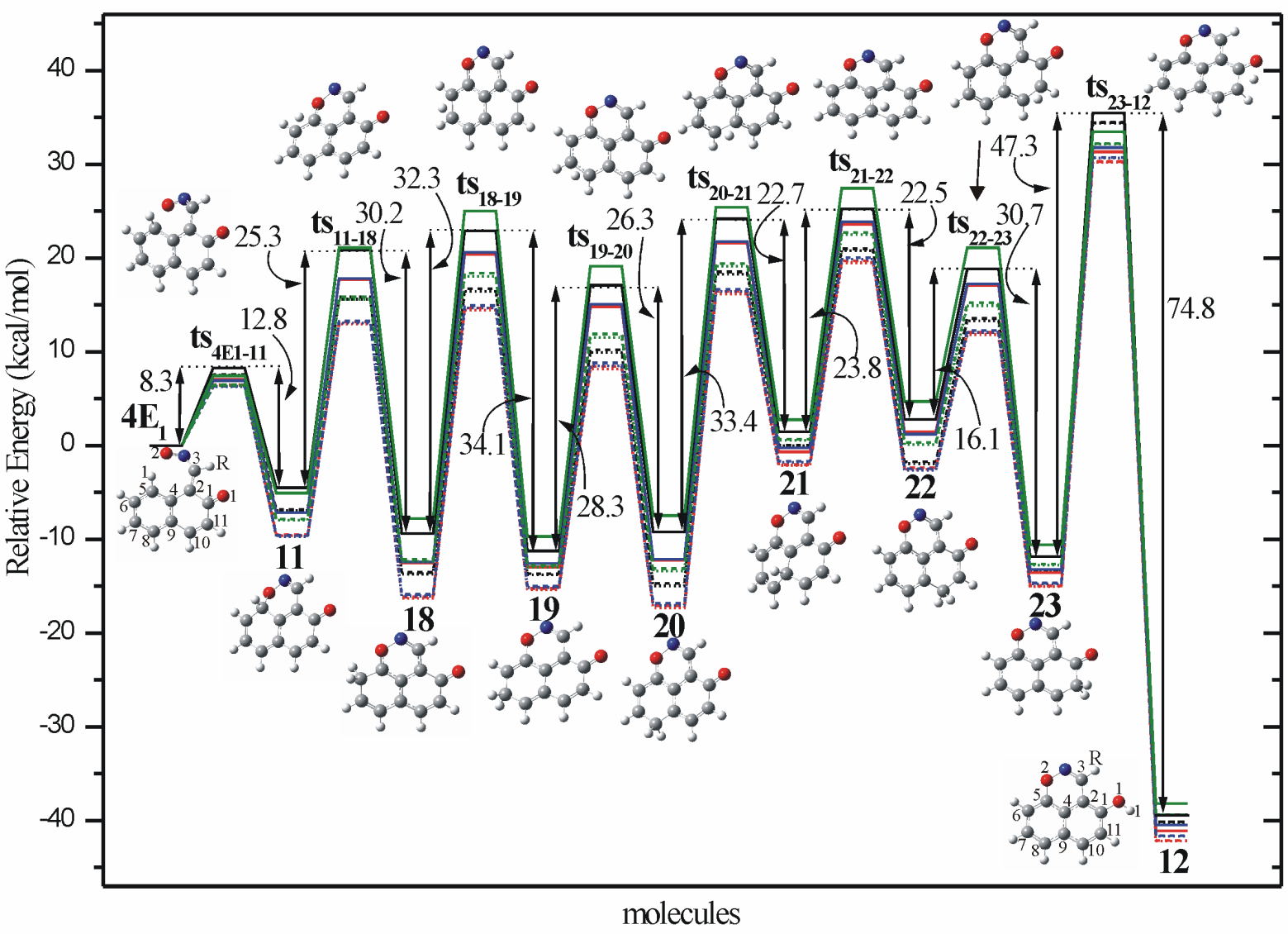

Fig 5S Relative electronic energy levels of the peri-(1,6)-electrocyclization of **4** minimum to **12** in the gas phase (solid line), in THF solvent (dashed line) and in CH_2Cl_2 solvent (dotted line) via second route. R = H (black lines), Me (red), Et (blue), and Ph (green). (C atoms = gray spheres, H = white, O = red, and N = blue).

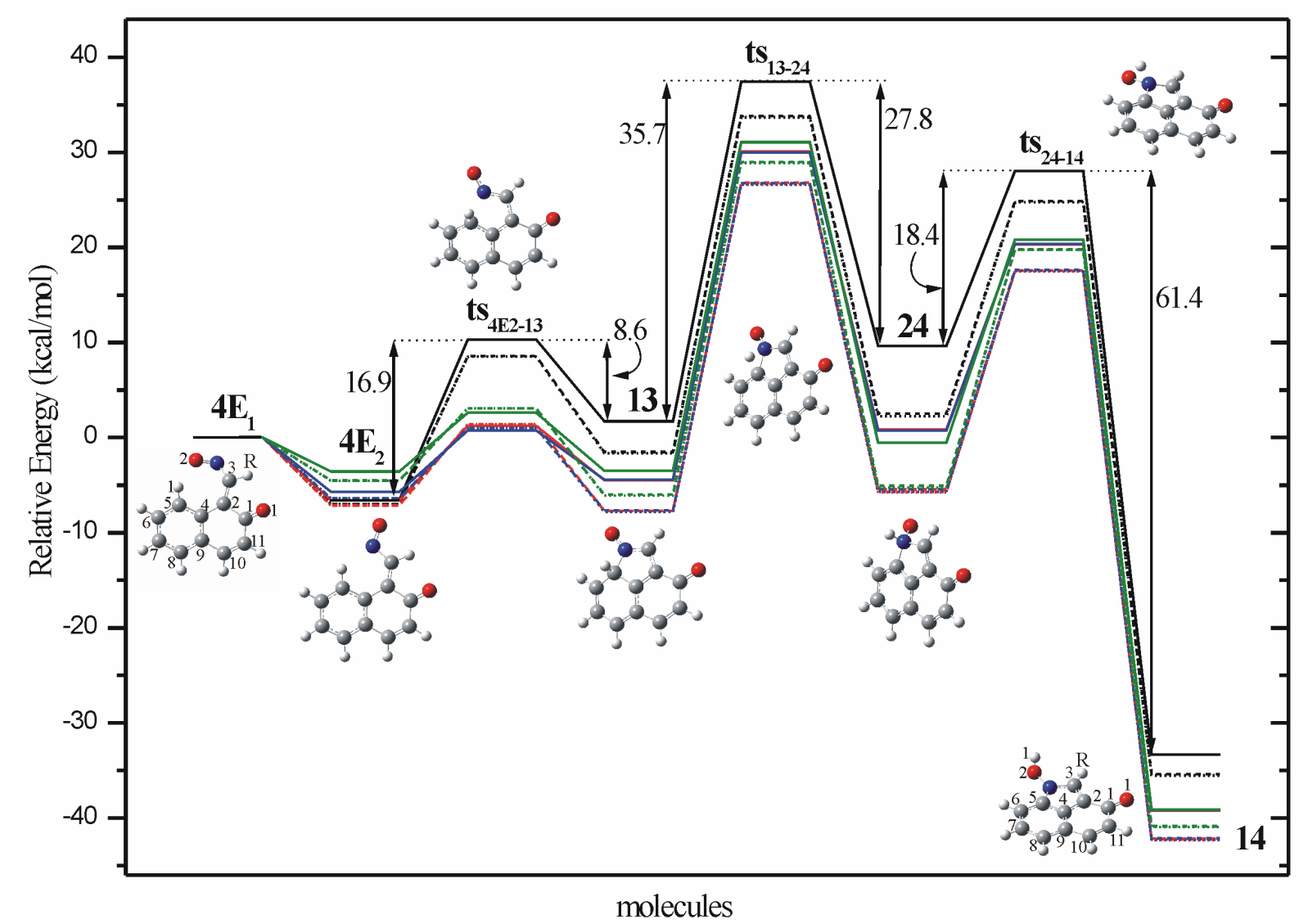

Fig 6S Relative electronic energy levels of the peri-(1,5)-electrocyclization of **4** minima to **14** in the gas phase (solid line), in THF solvent (dashed line) and in CH_2Cl_2 solvent (dotted line) via second route. R = H (black lines), Me (red), Et (blue), and Ph (green). (C atoms = gray spheres, H = white, O = red, and N = blue).